RELAXATION STUDIES AND INTERMOLECULAR INTERACTIONS IN SOME COMPLEX MOLECULES

By

ARPITA DAS

Department of Physics

A thesis submitted in partial
fulfilment of the requirement of the degree of

DOCTOR OF PHILOSOPHY

in

PHYSICS

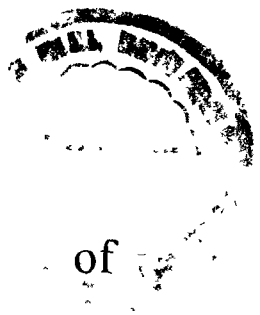

of

North Eastern Hill University
Shillong
INDIA

The North-Eastern Hill University

October 1999

DECLARATION

*I **ARPITA DAS** hereby declare that the subject matter of this thesis is the record of work done by me, that the contents of this thesis did not form basis of the award of any previous degree to me or to the best of my knowledge to anybody else, and that the thesis has not been submitted by me for any research degree in any other university/institute.*

This is being submitted to the North-Eastern Hill University for the degree of Doctor of Philosophy in School of Physical Sciences.

Arpita Das.
(ARPITA DAS)

(Dr.C. S. Shastry) 6/10/99
Professor and Head,
Department of Physics

K Kumar 6/10/99
(Dr. Kamal Kumar)
Professor
Department of Physics

ACKNOWLEDGEMENT

It gives me immense pleasure and satisfaction in bringing forth my research work under the supervision of Dr. Kamal Kumar, Professor, Department of Physics, NEHU. I take the opportunity to express my deep sense of gratitude to him for his guidance and constant encouragement throughout the entire course of my research work.

I also take the opportunity to thank Prof. C. S. Shastry, Head, Department of Physics, NEHU, Prof. A. L. Verma and other faculty members for their encouragement during the course of my work.

I am privileged to thank Mr. A. K. Rathore for helping me in doing experiments. My sincere thanks go to all of my friends for their helpful cooperation in my research work. My thanks also go to Dr. Anusree Ghosh and Dr. Radhendu Das for their wishes of success in this regard.

I owe my regards to my parents for their blessings and moral support throughout my life. My best regards also goes to other family members who stood by me for completing this work .

Arpita Das 6.10.99

(ARPITA DAS)

CONTENTS

CHAPTER 1

Chapter 1

INTRODUCTION

Considerable interest has been shown for the study of molecular dynamics in liquids, liquid crystals, polymers (in bulk and solution) and biopolymers all of which exhibit relaxation phenomena at different frequencies.The relaxation, scattering and absorption spectroscopy provide useful information about the molecular motion in liquids. The molecular motion may be illustrated by the study of vibrational relaxation, orientational relaxation, dielectric relaxation, quasielastic scattering and others. The study of vibrational relaxation in condensed phase has been considered a way of investigating dynamic processes[1–12].

The vibrations of a molecule are sensitive probes of local structure and dynamics in molecular liquids and therefore provide microscopic

information about a state of matter which is relatively poorly understood. The basic idea of research in molecular liquids consists in a careful analysis of the bandshape of the isotropic (I_{iso}) and anisotropic (I_{aniso}) components of the Raman band of the molecule[1-5,13-15]. The sensitivity of Raman peak position and band width (fwhm) on the environment has been demonstrated by the solvent dependent studies which have been useful in obtaining the information on the dynamics of liquids.

Theoretical models for bandshape may often be applied to data obtained by different techniques such as **NMR, ESR** and **vibrational spectroscopy.** Each model has adjustable parameters and could be used to fit the data. In these cases the electromagnetic field causes a change of state in a reference system of nuclear spin or electronic spin states or the vibrational modes (vibrational energy levels) of molecules. The reference system (molecule) immersed in a liquid will have many degrees of freedom of the bath (rotational and translational). Thus the states of the reference system will have a finite lifetime and energy width. This amounts to a decay of the time correlation function corresponding to the reference transition[9].

The bandshape may give valuable information about the interactions of the reference molecule with its environment. In addition, it may provide information about the dynamics of the bath.

The vibrational and rotational frequencies of molecules can be studied by **Raman spectroscopy** as well as by **IR spectroscopy.** It is, however, **the laser Raman scattering experiment** which provides a detailed information about a specific dynamic process in the liquid. In order to understand the vibrational relaxation, one has to study the well isolated vibrational modes. The vibrational relaxation can be understood from the analysis of **Raman band profiles** of **polarized** and **depolarized** configurations, by calculating the intensity of the isotropic component[12]. Only vibrational processes contribute to I_{iso} whereas both vibrational and reorientational processes contribute to I_{aniso}.

For any given system the isotropic Raman band is broadened and the broadening may be influenced by several mechanisms[9]. The two dominant ones are **energy relaxation** and **phase relaxation.** The energy relaxation involves vibrationally inelastic processes and corresponds to what is called T_1 relaxation for spin system, while phase

relaxation involves only quasielastic interactions of the molecules with their surroundings leading to perturbation of the phase of the vibrational wavefunctions without changing their quantum states. Vibrational phase and energy relaxation times can be as short as a few pico seconds and may thus be comparable to the bath relaxation times. This has important consequences for the dynamics of the coupled system. However, phase relaxation (dephasing) in liquids normally occurs much faster than energy relaxation.

Experimental measurements of vibrational phase and energy relaxation may be carried out in either the time or frequency domain. Population (energy) relaxation measurements in the time domain involve pulsed excitation (by stimulated Raman scattering or IR absorption) followed by detection of level populations after a time delay t. In this way relaxation times have been measured ranging from seconds to picoseconds. Picosecond spectroscopy may be used to measure phase relaxation. Frequency domain studies of vibrational energy relaxation involves either ultrasonic absorption or Brillouin line width measurements. Frequency domain measurements of phase relaxation are quite extensive.

Different theoretical models[13–25] on vibrational dephasing have been developed, examples of which are **isolated binary collision (IBC) model**[13,14] **, the hydrodynamic model**[15–17]**, the cell model** and the model based on **resonant energy transfer**[18–25]. In the IBC model the transition rate is assumed to be the product of the collision rate in the liquid and the transition probability per collision in the gas phase. Litovitz[26] approximated the time between collisions to be an Enskog time for the rate of binary collision of hard spheres using cell model. Oxtoby[14,15] has shown that the relaxation time of the random force is responsible for the viscosity dependence of the diffusion coefficient. Fluctuations with wavelengths longer than a molecular diameter decay hydrodynamically with rates characterized by the liquid viscosity but for shorter wavelengths the simple nature is lost.

One of the most important mechanism that may contribute significantly to dephasing processes in liquids is the coupling between the similar modes of identical molecules that results in resonant energy transfer[5]. In some theoretical models long range forces are involved, the collisional events that are considered are those which have too short a time of action to influence cosiderably the dephasing time.

The molecular harmonic oscillator couples to the heat bath through translational diffusion; effects of coupling of rotations to vibrations or translations are neglected. When dipole-dipole interactions and dispersion forces are included there are three contributions to the line broadening[24]: the first is indicated as 'self term' ; the second is named the 'exchange term' and a 'cross self exchange term' is also present. The 'exchange term' is due to the transfer of vibrational quantum states between two identical molecules through corresponding normal modes. This mechanism is normally referred to as resonant energy transfer. It is possible to single out this particular kind of dephasing by performing dilution measurements.

An important coupling mechanism is **transition dipole - transition dipole (TD-TD)** type[5] which is possible when strong IR active transitions are present. The resonant transfer mechanism is identified by dilution experiments with solvents which reduces the coupling. Such experiments may exhibit band narrowing when dilution studies are carried out[24].

The basis of the detailed study of vibrational dephasing is band-shape and solvent induced frequency shift as a result of a competetion

between slowly varying attractive forces and rapid collisional forces in a weak coupling regime. It has been observed in cases of many molecules that the peak frequencies of the Raman bands corresponding to the isotropic and anisotropic components do not coincide in liquid state[23–35]. The difference in peak positions may sometimes be about 15 cm^{-1} or even more. This non-coincidence in Raman spectrum has been observed for many IR active modes. The solvent dependent studies have shown that the magnitude of the splitting decreases with increasing concentration of the solvent and tends to vanish in the limit of infinite dilution. The effect is widely observed for example in the CO stretches in carbonyls[29–31], SO stretches in sulphones[1], CN in nitriles[21], CH stretch of chloroform[35] and several others. The non-coincidence effect has been attributed to the resonant transfer of vibrational excitation in the presence of local order due to strong interactions between permanent dipole moments. The most common source of resonant transfer relevant to the effect is due to transition dipole - transition dipole (TD-TD) coupling.

The non-coincidence effect can arise simply from an angular dependent interaction potential which preferentially weights the relative

alignment of a pair of molecules between which resonant excitonic transfer can occur. This concept does not contradict the dynamic nature of the liquid phase, since it is only necessary that the lifetime of the quasicrystalline regions (local ordering) be long compared to the vibrational period.

Although the vibrational resonance coupling due to the TD-TD interaction may be important in some polar modes, it has been pointed out earlier by Wang and McHale[4] that the vibrational resonance coupling Hamiltonian may originate from quadrupole-quadrupole interaction or any other type of intermolecular interactions. The Hamiltonian which determines the time evolution of the dynamic variables is written as

$$H = H_{osc} + H_B + H'$$

Where H_{osc} is the sum of harmonic oscillator Hamiltonian, H_B is the bath Hamiltonian and H' is the part of the Hamiltonian which couples the internal vibrational coordinates of the bath molecules.

In order to understand the nature of the intermolecular interactions and molecular dynamics, there is a definite need for additional systematic studies on vibrational relaxation, reorientational motion,

frequency shifts and band shapes in various liquids. The information content of the solvent effects on frequency shifts and shapes of various vibrational bands has not yet been fully explored. In particular the anisotropy shift and variation of band width in dipolar liquids may offer new information about strong inter- and intra-molecular interactions. The study of the influence of the solvents on the band shape parameters is of permanent importance not only in connection with molecular structure and liquid dynamics, but also with solution kinetics. For analyzing the anisotropy shift and dephasing results we have chosen C=O symmetric stretching mode. Its normal mode presents particular characteristics that make its study of great importance:

(i) It lies at high frequencies, so the condition $\hbar\omega >> k_B$T is always true.

(ii) Usually it is little mixed and/or coupled with other vibrations, which means that its normal coordinate can be considered as a pure one.

(iii) It is a well separated mode in all the molecules under study. Therefore it is particularly suitable for probing the molecular environment.

A simple theoretical approach[24,25] to the behaviour of various bandshape parameters in terms of dipole-dipole interactions has been worked out in the frequency domain. The structural effect seems to play an important role in influencing the bandshape of polar Raman bands in liquids with dipole-dipole interaction energies of the order of kT. The asymmetry of the I_{VV} component of the band was explained on the basis of the change in the orientation probability distribution into the direction of energeticallly favourable orientations. However, the theoretical approach is too simple to allow more than a qualitative interpretation of the experimental data. Moreover, when the dipole sizes are comparable with those of solvent molecules, the fundamental problem lies in the determination of an effective electric permittivity of the medium. The explanation for vibrational relaxation and non-coincidence for complex molecular systems, sometimes cannot be given on the basis of a macroscopic perception of the solute-solvent system. The two interacting situations, in the pure solute and when dissolved in a solvent differ markedly especially at high dilution. The solvent electric field influences the bandshape of a reference mode significantly. In the present work we have studied the

Raman bandshape of several molecules and tried to explain the experimental results by taking into consideration the concept of microenvironment, the role of various multipolar interactions and the concept of effective van der Waals' volume. The non-coincidence effect has been studied in p-methylacetophenone and benzaldehyde molecules by taking into account the screening factor related to permanent and transition dipoles. The isotropic band width of Raman band and the dephasing process have also been studied for the two molecules to develop a microscopic picture of the processes involved in liquids. The anisotropic component of the Raman band gives information about the angular dependence of intermolecular potentials. Therefore the anisotropic band width has been studied for the molecules p-methylacetophenone (PMA), benzaldehyde (BH), cyclohexanone (CH), N,N-dimethylacetamide (DMA), N,N- dimethylformamide (DMF) using different solvents by considering the van der Waals' volume of the sphere of influence in solution. The study of the spectral properties of Raman bands has contributed in a major way to our understanding of the processes involved.

REFERENCES

1. G. Fini and P. Mirone, *J. Chem. Soc., Faraday Trans.2,* **70,** 1776 (1974).

2. E. W. Knapp and S. F. Fischer. *J. Chem. Phys.,* **76,** 4730(1982)

3. W. Schindler, P.T. Sherko and J. Jonas, *J. Chem. Phys.* **76,** 3439(1982).

4. C. H. Wang and J. McHale, *J. Chem. Phys.,* **72,** 4039(1980)

5. J. McHale, *J. Chem. Phys.* **75,** 30(1981).

6. W. Schindler and J. Jonas, *J. Chem. Phys.,* **72,** 5019(1980).

7. J. Schroeder and J. Jonas, *J. Chem. Phys.,* **34,** 11(1978)

8. T. W. Zerda, S. Perry and J. Jonas, *Chem. Phys. Lett.,* **83** , 600(1981)

9. D. W. Oxtoby, *J. Phys. Chem.,* **87,** 3028(1983).

10. W. Schindler. T. W. Zerda and J. Jonas, *J. Chem. Phys.,* **81,** 4306(1984).

11. J. Jonas, *Acc. Chem. Res.,* **17,** 74(1984).

12. L. A. Nafie and W. L. Peticolas, *J. Chem. Phys.,* **57,** 3145(1972).

13. S. F. Fischer and A. Lauberau, *Chem. Phys. Lett.,* **35,** 6(1975).

14. D. W. Oxtoby and S. A. Rice, *Chem. Phys. Lett,* **42,** 1(1976).

15. D. W. Oxtoby, *J. Chem. Phys.*, **70,** 2605(1979).

16. R. Ouillon, V. Sergiescu and R. J. D'Leon, *Mol. Phys.*, **49,** 151(1983).

17. P. S. Dardiaw, R. I. Culier, *J. Chem. Phys.*, **89,** 4415(1988).

18. W. Rothschild, *J. Chem. Phys.*, **62,** 1253(1975).

19. W. Rothschild, *J. Chem. Phys.*, **65,** 455(1976).

20. G. Döge, Z. Nabrforsch, *Jeil, A,* **28,** 419(1973).

21. G. Fini and P. Mirone, *Spectrochim. Acta.* **32A,** 625 (1976).

22. P. Mirone and G. Fini, *J. Chem. Phys.*, **71,** 2241 (1979).

23. M. G. Giorgini, G. Fini and P. Mirone, *J. Chem. Phys.*, **79,** 639 (1983).

24. D. Schiebe and G. Döge, *Ber. Bunsenges. Phys. Chem.*,**85,** 520 (1981).

25. D. Scheibe, *J. Raman Spectrosc.*, **13,** 103 (1982).

26. F. J. Bartoli and T. A. Litovitz, *J. Chem. Phys.*, **56,** 404(1972).

27. G. Fini, P. Mirone and B. Fortunato, *J. Chem. Soc., Faraday Trans 2.*,**69,** 1243 (1973).

28. W. Schindler, T. W. Zerda and J. Jonas, *J. Chem. Phys.*,**81,**

4306 (1984).

29. A. Purkayastha and K. Kumar, *Spectrochim. Acta,* **42A,** 1379 (1986).

30. A. Purkayastha and K. Kumar, *Spectrochim. Acta,* **43A,** 1269 (1987).

31. A. Purkayastha and K. Kumar, *J. Raman Spectrosc.,* **19,** 249 (1988).

32. V. M. Shelly, A. Talintyr, J. Yarwood and R. Buchner, *Faraday Dissc. Chem. Soc.,***85** 211 (1988).

33. J. Dybal and B. Schneider, *Spectrochim. Acta,* **41A,** 691 (1985).

34. T. F. Sun, J. B. Chan, S. N. Walen and J. Jonas, *J. Chem. Phys.,* **94,** 7486 (1991).

35. G. Döge, D. Schneider and A. Morresi, *Mol. Phys.,***80,** 525 (1993).

CHAPTER 2

Chapter 2

THEORETICAL ASPECTS

INTRODUCTION

The vibrational relaxation has been considered a way of investigating dynamic processes in liquids. Vibrational relaxation time can be of the order of picoseconds. This has important consequences for the dynamics of the coupled systems[1–5]. In small molecules reorientation provides the primary relaxation mechanism for allowed transitions (energy relaxation). For larger molecules, vibrational relaxation plays an increasingly important role. Measurements of vibrational band-shape and the corresponding relaxation studies can potentially reveal a great deal of information about dynamics of molecules in liquid phase. In particular, studies of vibrational ralaxation processes lead to an understanding of the interactions between a vibrating molecule

and its surroundings.

Considering the molecule as an isolated active oscillator, we can characterize its vibrational wavefunction by a quantum state and a phase. When the oscillator is perturbed by the external environment, its wavefunction can be modified in two ways: (i) The quantum state changes; in this case the energy difference between the vibrational excited state and the ground state is dissipated to the bath (rotations and translations); and we have a vibrational energy relaxation (also named population relaxation). This is the analouge of a T_1 process in NMR. (ii) The perturbation conserves the vibrational energy of the considered oscillator causing only a shift in its phase, which is called vibrational dephasing process. This is the analouge of T_2 in NMR. In the liquid phase, population relaxation events usually need relatively long lifetime in comparison with phase relaxation events. Sometimes both processes contribute to the whole vibrational relaxation. However, in most cases vibrational bandshapes are mainly determined by dephasing process.

The key idea of the general approach[2–5] to the vibrational dephasing process is the partitioning of the degrees of freedom of the

molecule and the surroundings into two groups, the exchanging group and the reservoir. In most cases a clear distinction may be made between vibrational degrees of freedom in liquids, on the one hand and rotational and translational degrees of freedom on the other. Vibrational frequencies are typically in much larger range of frequencies (500 - 4000 cm^{-1}) whereas at room temperature, the thermal energy k_BT corresponds to 200 cm^{-1}. As a result only a few states are thermally populated. On the other hand, rotational and translational modes have lower frequencies so that more states are thermally populated and it is not very meaningful to describe them as discrete levels. Vibrational dephasing then occurs through the coupling of a quantum vibrational system to a classical heat bath of rotational and translational degrees of freedom. The microscopic Hamiltonian of a dephasing system can generally be written as

$$H = H_0 + H_B + H_{coup} \qquad 2.1.1$$

where H_0 is the Hamiltonian for the isolated active oscillator, H_B includes the translational and rotational degrees of freedom of the bath and H_{coup} describes the coupling of the vibrations to the bath.

2.1 ORIGIN OF VIBRATIONAL RELAXATION PROCESSES IN MOLECULAR LIQUIDS:

Vibrational dephasing originates from a variety of mechanisms, which include inhomogeneous line broadening, vibrational energy relaxation and redistribution as well as pure homogeneous dephasing process. Vibrational phase relaxation leads to broadening of the isotropic Raman band. Gordon[1] showed that this decay is given by an autocorrelation function which is the fourier transform of the Raman bandshape.

For a well separated vibrational transition there are three primary sources of line broadening and thus of phase relaxation:(i) Lifetime broadening which arises due to the uncertainity principle. This uncertainity broadening generally makes small contribution to the band width. (ii) Environmental broadening which arises from the fact that the vibrational frequency of a molecule i is perturbed by its interaction with other molecules and therefore has a component $\Delta\omega_i(t)$ which fluctuates with time[2–5]. The isotropic Raman bandshape is given by the Fourier transform of the vibrational co-ordinate autocorrelation function$\langle Q_i(t)Q_i(0)\rangle$ where the angular brackets define an ensemble

average vibrational co-ordinate Q_i at time t and differs from $Q_i(0)$ by a phase factor $exp[\phi_i(t) - \phi_i(0)]$. The phase difference is given by

$$\langle \phi_i(t) - \phi_i(o) \rangle = \bar{\omega} t + \int dt' \Delta\omega_i(t') \qquad 2.1.2$$

where $\bar{\omega}$ is the average vibrational transition frequency in the liquid and $\Delta\omega_i(t)$ gives the fluctuation in frequency due to the environment. The vibrational phase relaxation is then given by[3,4],

$$\langle Q_i(t) Q_i(0) \rangle = \left\langle exp[i \int_0^t dt' \Delta\omega_i(t')] \right\rangle \qquad 2.1.3$$

and depends on the statistical properties of $\Delta\omega_i(t)$. If we consider the autocorrelation function of $\Delta\omega_i(t)$, *i.e.*, $\langle \Delta\omega_i(t) \Delta\omega_i(0) \rangle$, the bath relaxation time may then be defined[5] through

$$\tau_c = \int_0^\infty dt \frac{\langle \Delta\omega_i(t) \Delta\omega_i(0) \rangle}{\langle \Delta\omega_i^2 \rangle} \qquad 2.1.4$$

The nature of the bandshape depends on the relative magnitude of the two characteristic frequencies $\langle \Delta\omega_i^2 \rangle^{1/2}$ and τ_c^{-1} .We can define a modulation regime depending on the value of $\langle \Delta\omega_i^2 \rangle^{1/2} \tau_c$. When $\langle \Delta\omega_i^2 \rangle^{1/2} \tau_c >> 1$, the active molecule undergoes a perturbation for a

long time. If it were possible to freeze the environment at a particular time, one would observe a distribution of frequency shift; and a broadened vibrational bandshape (Gaussian) is obtained. This is referred to as static limit. While when $\langle \Delta\omega_i^2 \rangle^{1/2} \tau_c << 1$, we have the rapid modulation limit where there is a perturbation for a short time on the active molecule and the band is narrowed to a Lorentzian curve with full width at half maximum (in cm^{-1}) given by

$$fwhm = \langle \Delta\omega_i^2 \rangle \tau_c / \pi c \qquad 2.1.5$$

(iii) The third contribution to vibrational line broadening is resonance transfer, or excitonic broadening which usually appears in pure liquids. If two identical molecules are brought together, the energy levels which were earlier degenerate will now split; with one moving higher and the other lower.If a large number of molecules are brought together this splitting gives rise to a broad excitonic band.

When a molecule is surrounded by isotopically substituted molecules the potential will change slightly while the vibrational frequency may be shifted sufficiently out of resonance to eliminate the excitonic broadening. The resonance energy transfer (RET) and environmental

broadening contributions are not independent. In fact the resonance transfer may even lead to a narrowing of the isotropic Raman band. It has been experimentally verified that for vibrational modes involving RET the position of the peak frequencies for isotropic and anisotropic Raman band components differ from each other.This is termed as anisotropy shift or non-coincidence effect (NCE). It has been found that for pure substance the Raman frequency of the anisotropic profile is blue shifted with respect to the isotropic profile.

The $I_{\text{aniso}}(\tilde{\nu})$ component reflects the angular dependence of the intermolecular potential, while $I_{iso}(\tilde{\nu})$ detects only the spherically symmetric average value of the potential. Because of these different dependences, the $I_{iso}(\tilde{\nu})$ and $I_{\text{aniso}}(\tilde{\nu})$ will not only exhibit different shapes but their positions will also be shifted to a different extent leading to a nonvanishing splitting factor

$$\delta\tilde{\nu} = \tilde{\nu}(aniso) - \tilde{\nu}(iso) \qquad 2.1.6$$

The phase relaxation peocess involves only quasielastic interactions of the molecules with their surroundings leading to perturbation of the

phase of the vibrational wavefunctions without changing their quantum states. Vibrational energy relaxation (population relaxation) involves inelastic processes and transfer of energy between the vibrational degrees of freedom and the bath. The energy transfer may be partial or complete to, or from the bath. Partial energy transfer includes both intra and intermolecular transfer.

In order to explain the mechanism of vibrational relaxation and non-coincidence effect one needs the detailed knowledge about the perturbing coupling potential between the molecules and the bath. A number of approaches have been suggested recently. It has been seen that bandshape cannot be described simply by models of harmonic oscillator in liquids[6]. Computer simulations are much more useful because they allow essentially exact calculations of phase relaxation rates and bandshapes for well defined potentials.

Collisional model

In isolated binary collision (IBC) model proposed by Fischer and Laubereau[7], phase shifts and therefore bandshapes are obtained using a repulsive potential surface which was subsequently modified by

Oxtoby *et al*[4] with the introduction of anharmonicity and by Tanabe and Jonas[8] for use in binary mixtures.

Assuming that the collisions are not correlated, it is possible to describe the general expression of the vibrational relaxation rate as a sum of two contributions

$$\tau^{-1} = \tau_v^{-1} + \tau_E^{-1} \qquad 2.1.7$$

where τ_v^{-1} is the dephasing term due to pure dephasing caused only by quasielastic collisions, and τ_E^{-1} is the energy relaxation time. However this model does not reflect the whole complexity of the liquid environment because of difficulties in estimating some parameters for complex molecules. For complex systems the values of anharmonicity constants and the reduced mass of the molecules are not always available.

The hydrodynamic model

The hydrodynamic calculations presented by Oxtoby[5] which included the anharmonicity effects was essentially an opposite approach to that of Fischer and Laubereau[7]. In hydrodynamic approach a vibrating molecule is modelled as a macroscopic body embedded in a

viscoelastic continuum. In the limit of weak coupling of the vibration to the bath, collective effects are involved producing a viscosity dependent collision frequency. The expression for the dephasing rate for polyatomic system is of the form

$$\tau_v^{-1} \propto \eta T \qquad 2.1.8$$

showing the dependence on viscosity η and temperature T.

The model given by Schweizer and Chandler (SC)[9] illustrates the the importance of a detailed description of the liquid state structure in determining the dephasing process. This model simultaneously examines both the broadening mechanisms and the frequency shifts. The SC model also shows how the potential may be separated into a rapidly varying short range part and a slowly varying long range part. Refinement of SC theory were proposed by Ben Amotz *et al*[10], competitive short range repulsive and long range attractive forces were invoked to reproduce solvent- and pressure- induced frequency shifts. A cavity distribution function was introduced to describe the repulsive frequency shift, while a van der Waals' mean field approximation was used for the attractive contribution.

Resonant energy transfer

The coupling potential V can be expanded in a Taylor series in vibrational coordinates[11]

$$V = V_0 + \left(\frac{\delta V}{\delta Q_i}\right)_0 Q^2 + \frac{1}{2}\left(\frac{\delta^2 V}{\delta Q_i^2}\right)_0 Q^2 + \frac{1}{2}\sum_{ij}\left(\frac{\delta^2 V}{\delta Q_i \delta Q_j}\right)_0 Q_i Q_j + \ldots \qquad 2.1.9$$

The first three terms are similar to the potential of a harmonic oscillator corresponding to a normal coordinate Q_i. By chosing the energy of the equilibrium configuration to be zero, V_0 may be eliminated. The last term is responsible for resonant energy transfer from one oscillator to another and leads to anisotropy shift or non-coincidence effect.

Since $V << H_0$, the first order perturbation calculation for the frequency difference between the ground and the first excited state can be performed leading to the expression

$$\Delta E = \left(\frac{\delta V}{\delta Q}\right)_0 (\langle 1|Q|1\rangle) - (\langle 0|Q|0\rangle) + \frac{1}{2}\left(\frac{\delta^2 V}{\delta Q_i^2}\right)_0 (\langle 1|Q^2|1\rangle) - (\langle 0|Q^2|0\rangle)$$

$$+ \left(\frac{\delta^2 V}{\delta Q_i \delta Q_j}\right)_0 (\langle 1|Q|0\rangle)^2 + \ldots\ldots \qquad 2.1.10$$

Where Q is the normal coordinate of the molecule and$\langle 1|Q|0\rangle$is the expectation value of the normal coordinate in the transition state which is same for molecules i and j as we are considering similar vibrational modes of both molecules.The first two terms in equation (2.1.9) give the main contribution to the lineshift. The term $(\langle 1|Q|1\rangle) - (\langle 0|Q|0\rangle)$ vanishes for a harmonic oscillator, but in real molecule we deal with anharmonic oscillators.

For a diatomic oscillator, the potential governing the vibrational motion can be expressed as

$$V = \frac{1}{2}KQ^2 + K_3Q^3 + K_4Q^4 \qquad 2.1.11$$

where the first term is the harmonic potential and the higher terms represent mechanical anharmonicity. In the harmonic oscillator approximation overtones and combination tones are forbidden. Mechanical anharmonicity is one factor that might give them intensity through violating the $\Delta\nu = \pm 1$ selection rule. There is another possible cause for this, however, which might operate even when the oscillator is perfectly harmonic. It is electrical anharmonicity. The

transition moment R can be written in the form

$$R = \int \psi_{v'} \mu \psi_{v''}, d\tau \qquad 2..12$$

The (instantaneous) dipole moment μ varies during the vibration. It can be expanded in Taylor series at the equilibrium geometry:

$$\mu = \mu_e + \left(\frac{\delta\mu}{\delta Q}\right)_e Q + \left(\frac{\delta^2\mu}{\delta Q^2}\right)_e Q^2 + ... \qquad 2.1.13$$

where the sum of the higher than linear terms is called electrical anharmonicity.

Thus electrical anharmonicity is the nonlinear part of the variation of the dipole moment with normal coordinate. It can give intensity to overtones and combination tones. In the general case both mechanical and electrical anharmonicities contribute to the intensity. Thus in equation (2.1.10) the first term corresponds to mechanical anharmonicity, second term to electrical anharmonicity and the last term corresponds to resonance interaction. The resonance interaction term is given by

$$\Delta E_{res} = (\delta^2 V/\delta Q_i \delta Q_j)(\langle 1|Q|0\rangle)^2 \qquad 2.1.14$$

For Transition dipole-Transition dipole (TD-TD) interaction, equation (2.1.14) takes the form[12]

$$\Delta E_{TD-TD} = \left(\frac{\delta\mu}{\delta Q}\right)^2 \left\langle \frac{K_{ij}}{R_{ij}^3} \right\rangle \langle 1|Q|0\rangle^2 \qquad 2.1.15$$

where R_{ij} is the distance between the molecules and K_{ij} is a factor describing the relative orientation of the two dipole moment vectors. This term is responsible for the splitting factor due to dipole-dipole coupling and V was given by

$$V = \frac{\mu_i \mu_j}{R_{ij}^3} K_{ij} \qquad 2.1.16$$

Almost all the experimental work on RET assumes that the coupling mechanism is due exclusively to TD-TD interactions. At infinite dilution the isotropic and anisotropic Raman components tend to coincide.

It has been shown that for dipole-dipole interaction the splitting factor is given by

$$\delta\tilde{\nu} \propto \langle K_{ij}/R_{ij}^3 \rangle (\delta\mu/\delta Q)^2 \qquad 2.1.17$$

For different relative orientations, the anisotropic component of the band is shifted to various degrees depending upon the values of K_{ij}.

It is usually very difficult to calculate the quantity (K_{ij}/R_{ij}^3) and therefore, one may reduce above relatonship to the proportionality,

$$\delta\tilde{\nu} \propto (\delta\mu/\delta Q)^2 \qquad 2.1.18$$

As mentioned previously, besides the frequency shift, frequency splitting is also observed in most liquids and in some liquids the splitting is quite large. Since the quantity $(\delta\mu/\delta Q)^2$ is proportional to the infrared absorption coefficient for a given vibration, Raman bands corresponding to the strong IR absorption shoud show a large anisotropy shift.

Bratos and Tarjus[13,14] assume that the full difference in the relaxation rate on going from the pure liquid to isotopic dilution is due to the distinct term whereas according to Döge *et al*,[11] it is mainly the self term which is affected via transition dipole interactions.

Logan[15–17] developed the Bratos approach for bringing out the consequences of isotopic dilution on frequency shifts and bandshapes, i.e the first and second frequency moments respectively. In Logan's approach the contributions to the self, distinct and total vibrational

correlation functions arising from a dipolar contribution to the total liquid Hamiltonian is examined explicitly. In addition to TD-TD resonant energy transfer, dipolar interactions also contribute to the bath-vibration coupling terms in the vibrational Hamiltonian, which give rise to environmentally induced frequency fluctuations. Permanent dipolar interactions further contribute to the bath Hamiltonian which determines the liquid structure and in turn strongly influences the vibrational dynamics.

Logan's approach[14,15] considers general binary mixture of polyatomic molecules, diluted in an isotopic or nonisotopic solvent; the microscopic model adopted is that of point dipoles. The non-coincidence effect is assumed to be the result of a resonant excitonic transfer of vibrational excitation between the same normal mode of different solute molecules. Logan's theory is surely the most detailed and satisfactory one for the modelling of the RET process; however, it does not always give good approximations for the dispersion effect. Logan's approach assumes only point dipoles whereas it is necessary to account for the dipoles of a finite length and repulsive interactions should also be considered.

Screening effect

Mirone and coworkers[18–22] hypothesised that the anisotropy shift is the result of microscopic local order in the liquid phase, owing to the strong interaction between permanent dipoles; which permits a vibrational coupling through neighbouring transition dipoles. Macroscopic properties are involved in the equations proposed by Mirone and coworkers to reproduce the behaviour of I_{iso} and I_{aniso} in the pure liquid on dilution:

$$\Delta\nu = \Delta\nu_{neat}\frac{\epsilon_1}{1-\Phi_0}\frac{\Phi-\Phi_0}{\epsilon_1\Phi+\epsilon_2(1-\Phi)}, \Phi > \Phi_0 \qquad 2.1.19$$

$$\Delta\nu = 0, \Phi < \Phi_0 \qquad 2.1.20$$

where ϵ_1 and ϵ_2 are the dielectric constants of the pure solute and the solvent, Φ is the volume fraction

$$\phi_A = n_A v_A/[(n_A v_A + n_B v_B)] \qquad 2.1.21$$

and Φ_0 is a concentration threshold. If $\Phi < \Phi_0$ energy relaxation mechanisms are assumed to be active, whereas if $\Phi > \Phi_0$ there is process of resonance intermolecular vibrational coupling. Wang and Mc Hale[23,24] developed a general expression for a coupling Hamiltonian and concluded that local short range order is not of fundamental

importance for the NCE.Its existence can modify the shift between isotropic and anisotropic maxima. The essential condition for a resonant energy transfer (RET) process is the angular dependence of the interaction potential. It is also demonstrated that $\Delta\nu_{\mathrm{NCE}} = \nu_{\mathrm{aniso}} - \nu_{\mathrm{iso}}$ can take positive or negative values depending on the physical properties involved. In TD-TD interactions $\Delta\nu_{\mathrm{NCE}}$ is always positive. Mc Hale[24] has derived an expression for $\Delta\nu$

$$\Delta\nu_{\mathrm{NCE}} = \frac{2\mu^2 N_0}{25\pi^2 c^2 k_B T d^3 \nu_0 V_m} \left(\frac{\delta\mu}{\delta Q}\right)^2 \Phi S \qquad 2.1.22$$

where Q and ν_0 are the normal coordinate and the wavenumber of the chosen vibrational mode between two molecules of dipole moment μ, coupled through their $\frac{\delta\mu}{\delta Q}$, V_m is the molar volume, c is the velocity of light and N_0 is the Avogadro's number. Φ is the volume fraction of the solute and S is the screening factor of the interacting transition dipoles.

Mc Hale proposed $S = \epsilon^{-2}$, where ϵ is the static dielectric constant of the solution. Mirone[22] corrected Mc Hale's assumption proposing

$$S = \left(\frac{n^2+2}{2\epsilon+n^2}\right)^2 \epsilon \qquad 2.1.23$$

where n is the refractive index of the solute species.

According to Giorgini etal[25], the screening factor S comprises two factors, S_p and S_t, related to the interaction of permanent and transition dipoles.The first term is given by

$$S_p = \left(\frac{n^2+2}{2\epsilon+n^2}\right)^2 \epsilon \qquad 2.1.24$$

and the second term is given by

$$S_t = \left(\frac{\left[n^2+2\right]^2}{9n^2}\right) \qquad 2.1.25$$

which comes after substituting

$$\epsilon = n^2$$

Here ϵ is the dielectric constant of the medium.

Kubo model of correlation function

A general theory of relaxation mechanism as developed by Kubo[26] has also been adapted by several workers to explain vibrational relaxation. Using this theory, the correlation function[27] that involves the process of pure dephasing is given by the expression

$$\phi_p(t) = exp\left[-\langle\Delta\omega_i^2\rangle\left(\tau_c^2\left\{e^{-t/\tau_c}-1\right\}+t\tau_c\right)\right] \qquad 2.1.26$$

$\langle\Delta\omega_i^2\rangle$ is the second frequency moment. It measures the magnitude of the random frequency modulation, i.e., the range of frequency distribution due to the various molecular interactions.

$$\langle\Delta\omega_i^2\rangle = \frac{\int_{\text{band}} I_{\text{iso}}(\omega)\omega^2 d\omega}{\int_{\text{band}} I_{\text{iso}} d\omega} \qquad 2.1.27$$

τ_c is the correlation time related to the time scale of the molecular fluctuations in the medium. It can be identified with the average time between perturbative events. Expression(2.1.34) can be modified in two extreme cases of short and long times.The vibrational relaxation time can then be defined as

$$\tau_v = \int_0^\infty \phi_{\text{p}}(t)dt \qquad 2.1.28$$

for the long time approximation, and for the fast modulation regime

$$\tau_v = (\pi c f w h m)^{-1} \qquad 2.1.29$$

where, $fwhm$ = full width at half height [of $I_{(iso)}$] and c is the speed of light.

For slow modulation limit

$$\tau_v = (\langle \Delta\omega_i^2 \rangle \tau_c)^{-1} \qquad 2.1.30$$

The great advantage of Kubo representation is that it permits us to confront the problem, how is the vibrational dephasing determined. In the case of long range dipolar interactions τ_c is directly proportional to dynamic viscosity. Therefore, τ_v is expected to depend on the viscosity of the medium. So far the bandshapes considered are for simple, well separated transitions. If other transitions are nearby or overlap, there can be further contributions to phase relaxation and spectral broadening[28,29].

Although considerable progress has been made towards the understanding of vibrational relaxation processes, there is clearly a need for further experimental as well as theoretical studies in this direction.

2.2 DIELECTRIC THEORY:

When a material is brought into an external field, every particle of the material is subjected to an internal field E_i proportional to the electric field E. This internal field is defined as the total electric field at the position of the particle minus the field due to the particle itself. Furthermore, the applied field tends to direct the permanent dipoles. In both cases the electric field gives rise to a dipole density; in other words, the electric field polarizes the dielectric. The polarization P and the macroscopic field E are related as[30]

$$P = \epsilon_0 \chi E \qquad 2.2.1$$

If the material contains N dipoles per unit volume, then

$$P = N\alpha E_i \qquad 2.2.2$$

and from equations (2.2.1) and (2.2.2) the relative dielectric susceptibility is given by

$$\chi = \frac{n\alpha}{\epsilon_0}\frac{E_i}{E} \qquad 2.2.3$$

Equation (2.2.2) is valid for liquids and gases in static or low frequency fields of moderate intensity. At moderate intensity the electric field

gives rise to a dipole density by translation and rotation effect. The polarization P may be assumed to be divided into two parts: The induced polarization P_α, caused by the translation effects and the dipole polarization P_μ, caused by the orientation of the permanent dipoles. At higher field intensities, the field tends to direct an anisotropic particle to an orientation such that its axis of highest polarizability coincides with the direction of the external field: and the chemical equilibria with different permanent dipole moments are shifted by the electric field in favour of the component with a high permanent dipole moment[31]. The induced polarization may be written as

$$P_\alpha = \sum_k N_k \alpha_k (E_i)_k \qquad 2.2.4$$

where N is the number of particles per cm^3,

α is the scalar polarizability and

E_i is the average electric field strength acting upon the particle.

The orientation polarization can be written as

$$P_\mu = \sum_k N_k \bar{\mu_k} (E_i)_k \qquad 2.2.5$$

where $\bar{\mu_k}$ is the value of the permanent dipole vector averaged over

all orientations.

The average moment per dipole in the direction of the applied field is given by

$$\bar{\mu} = \frac{\mu^2}{3k_B T} E_d \qquad 2.2.6$$

Hence equation (2.2.5) can be written as

$$P_\mu = \sum_k \frac{\mu_k^2}{3k_B T} (E_d)_k \qquad 2.2.7$$

For $\mu E_d >> k_B T$, orientational saturations are appreciable.

Now using equations (2.2.4) and (2.2.7) we have,

$$\frac{\epsilon - 1}{4\pi} = P_\alpha + P_\mu$$

$$\frac{\epsilon - 1}{4\pi} E = \sum_k N_k \left[\alpha_k (E_i)_k + \frac{\mu_k^2}{3k_B T} (E_d)_k \right] \qquad 2.2.8$$

Equation (2.2.8) is the fundamental equation for the dielectric constant for various polar and nonpolar dielectrics.

The homogeneous field of the permanent dipole of a molecule polarizes its environment. When a molecule with a permanent dipole strength μ is surrounded by other particles, moments proportional

to the polarizability are induced in the surrounding particles and if these particles have a permanent dipole moment their orientation is influenced.

The resulting inhomogeneous polarization of the environment will give rise to a field R and R will be proportional to μ so long as no saturation effects occur[31]. Thus

$$R = f\mu \qquad 2.2.9$$

The factor f is called the factor of the reaction field. R will have the same direction as μ.

Using Onsager approximation,

$$\frac{4}{3}\pi N a^3 = 1 \qquad 2.2.10$$

where N is the number of particles per cm^3 and a is the radius of the spherical cavity where the ideal dipole moment μ is placed. The value of a is generally considered to be approximately equal to the molecular radius.

The reaction field for a nonpolarizable point dipole is then given by

$$R = \frac{1}{a^3}\frac{2\epsilon - 1}{2\epsilon + 1}\mu \qquad 2.2.11$$

Comparing this equation with (2.2.9) we see that

$$f = \frac{1}{a^3}\frac{2\epsilon - 1}{2\epsilon + 1}$$

The field in the dielecric can be described as the field of a virtual dipole μ_e at the centre of the cavity, which was called by Onsager as the external moment of the immersed dipole and is given by

$$\mu_e = \frac{3\epsilon}{2\epsilon + 1}\mu \qquad 2.2.12$$

In the case of polarizable permanent dipole, having an average polarizability α the reaction field R induces a dipole αR and satisfies the equation

$$R = f(\mu + \alpha R) \qquad 2.2.13$$

where μ is the permanent dipole moment. Therefore

$$R = \frac{f}{1 - f\alpha}\mu \qquad 2.2.14$$

Eliminating f and substituting Onsager approximation (2.2.10) and using the relation

$$\frac{\alpha}{a^3} = \frac{n_D^2 + 1}{n_D^2 + 2} \qquad 2.2.15$$

where n_D is the index of refraction, in equation (2.2.14) we have

$$R = \frac{4\pi}{3} N \frac{2(\epsilon - 1)}{2\epsilon + n_D^2} \frac{n_D^2 + 2}{3} \mu \qquad 2.2.16$$

N is the number of particles per cm^3 and can be computed from

$$N = \frac{\alpha}{M} N_A$$

where M is the molecular weight of the substance, d is the density and N_α is the Avogadro's number.

Under the influence of the reaction field the dipole moment increases considerably; the increased moment is

$$\mu^* = \mu + \alpha R \qquad 2.2.17$$

Comparing equations (2.2.17) and (2.2.14) we have

$$\mu^* = \frac{\mu}{1 - f\alpha} \qquad 2.2.18$$

Using the value of f in the above equation

$$\mu^* = \frac{\mu}{1 - \frac{\alpha}{a^3} \frac{2(\epsilon - 1)}{2\epsilon + 1}} \qquad 2.2.19$$

Again substituting $\frac{\alpha}{a^3}$ from equation (2.2.15) in the above equation we obtain

$$\frac{\mu^*}{\mu} = \frac{2\epsilon + 1}{2\epsilon + n_D^2} \frac{n_D^2 + 2}{3} \qquad 2.2.20$$

When the dipole is not surrounded by the molecules of the same kind, the reaction field and the ratio $\frac{\mu^*}{\mu}$ are changed. The changes in R and in $\frac{\mu^*}{\mu}$, when the environment of the dipole is changed, results in a change of the factor $\frac{2(\epsilon-1)}{2\epsilon+n_D^2}$ in equation (2.2.15) and a change of the factor $\frac{2\epsilon+1}{2\epsilon+n_D^2}$ in equation (2.2.20) respectively.

2.3 THE INTERNAL AND DIRECTING FIELDS FOR NON POLAR AND POLAR DIELECTRICS - ONSAGER EQUATION:

For a nonpolar system the fundamental equation (2.2.8) for dielectric constant simplifies to[35]

$$\frac{\epsilon - 1}{4\pi} E = \sum_k N_k \alpha_k (E_i)_k \qquad 2.3.1$$

The internal field for nonpolar dielectric can be taken as the sum of the spherical cavity field E_c and the reaction field R of the induced

dipole given by

$$E_i = E_c + R \tag{2.3.2}$$

where

$$E_c = \frac{3\epsilon}{2\epsilon + 1} E \tag{2.3.3}$$

For polar molecules the internal field can also be built up from the cavity field and the reaction field. The reaction field in this case is the total dipole moment of the molecule. The reaction field R does not influence the direction of the dipole moment of the molecule under consideration as in a spherical cavity the permanent dipole moment and the reaction field caused by it will also have the same direction. Thus the reaction field contributes to the internal field E_i, because it polarizes the molecules and does not contribute to the directing field E_d. As a result there is a difference between the internal field E_i and the directing field E_d and is given by the value of the reaction field averaged over all orientations of the polar molecules.

$$E_i - E_d = \bar{R} \tag{2.3.4}$$

The directing field E_d can be obtained by eliminating the contribution of R to E_i by removing the permanent dipole of the molecule and is

given by the equation

$$E_d = E_c + f\alpha E_d \qquad 2.3.5$$

where E_c is the cavity field given by the equation (2.3.3), f is the reaction field factor and α is the polarizability. Thus combining equations (2.3.3) and (2.3.5) we find

$$E_d = \frac{1}{1 - f\alpha}\frac{3\epsilon}{2\epsilon + 1}E \qquad 2.3.6$$

In the case of a dielectric consisting of different kinds of molecules we have, for the kth kind of molecule, the directing field as

$$(E_d)_k = \frac{1}{1 - f_k\alpha_k}\frac{3\epsilon}{2\epsilon + 1}E \qquad 2.3.7$$

with

$$f_k = \frac{1}{a^3}\frac{2(\epsilon - 1)}{2\epsilon + 1} \qquad 2.3.8$$

where ϵ is now the dielectric constant of the mixture and a_k the radius of the cavity belonging to the particle of the kth kind. The internal field is now found from equation (2.3.4)

$$E_i = E_d + \bar{R} \qquad 2.3.9$$

where

$$\bar{R} = \frac{f}{1 - f\alpha}\bar{\mu} \qquad 2.3.10$$

in which $\bar{\mu}$ is the value of μ averaged over all orientations.

$$\bar{\mu} = \frac{\mu^2}{3k_BT}E_d$$

Hence for a mixture of different kinds of molecules the internal field for kth kind of molecule

$$= \left(1 + \frac{f_k}{1 - f_k\alpha_k}\frac{\mu_k^2}{3k_BT}\right)\frac{1}{1 - f_k\alpha_k}\frac{3\epsilon}{2\epsilon + 1}E \qquad 2.3.11$$

Now substituting equation (2.3.7) and (2.3.11) in the fundamental equation (2.3.1) we then find

$$\frac{[\epsilon - 1][2\epsilon + 1]}{12\pi\epsilon} = \sum_k N_k \frac{1}{1 - f_k\alpha_k}\left[\alpha_k + \frac{1}{3k_BT}\frac{\mu_k^2}{1 - f_k\alpha_k}\right] \qquad 2.3.12$$

Taking Onsager approximation for the radius of cavity

$$\frac{4\pi}{3}N_k a_k^3 = 1 \qquad 2.3.13$$

and the polarizability given by

$$\frac{(\epsilon_\infty)_k - 1}{(\epsilon_\infty)_k + 2} = \frac{4\pi}{3}N_k\alpha_k \qquad 2.3.14$$

where ϵ_∞ is the dielectric constant characteristic for the induced polarization, we obtain

$$\frac{\alpha_k}{a_k^3} = \frac{(\epsilon_\infty)_k - 1}{(\epsilon_\infty)_k + 2} \qquad 2.3.15$$

From this we find

$$\frac{1}{1 - f_k \alpha_K} = \frac{[(\epsilon_\infty)_k + 2][2\epsilon + 1]}{3[2\epsilon + (\epsilon_\infty)_k]} \qquad 2.3.16$$

Hence equation (2.3.12) can be written as

$$\frac{\epsilon - 1}{4\pi\epsilon} = \sum_k N_k \frac{(\epsilon_\infty)_k + 2}{2\epsilon + (\epsilon_\infty)_k} \left[\alpha_k + \frac{[(\epsilon_\infty)_k + 2][2\epsilon + 1]}{3[2\epsilon + (\epsilon_\infty)_k]} \frac{\mu_k^2}{3k_B T}\right] \qquad 2.3.17$$

For pure dipole liquids we find,

$$\frac{\epsilon - 1}{4\pi} = \frac{3\epsilon}{4\pi} \frac{\epsilon_\infty - 1}{2\epsilon + \epsilon_\infty} + \frac{(\epsilon_\infty + 2)^2 (2\epsilon + 1)\epsilon}{2\epsilon + \epsilon_\infty)^2} \frac{N_\mu^2}{9kT} \qquad 2.3.18$$

which after simplifying and rearranging gives

$$\mu^2 = \frac{9kT}{4\pi N} \frac{(\epsilon - \epsilon_\infty)(2\epsilon + \epsilon_\infty)}{\epsilon(\epsilon_\infty + 2)^2} \qquad 2.3.19$$

Equation (2.3.19) is the Onsager equation.

Following Maxwell's relation, for most dielectrics the dielectric constant will be equal to the square of the index of refraction n, so that

$$\epsilon_\infty = n^2 \qquad 2.3.20$$

In dilute solutions of a dipolar solute in a non-polar solvent, the polar molecules are far apart so that the interactions between them can be neglected. There will, however, be an interaction between the polar molecules and the molecules of the solvent, and this interaction can be taken into account approximately by using the form of Lorentz local field.

2.4.KIRKWOOD-FRÖHLICH DIELECTRIC MODEL:

For the representation of a dielectric with dielectric constant ϵ, consisting of polarizable molecules with a permanent dipole moment, Fröhlich introduced[35] a continuum with dielectric constant ϵ_∞ in which point dipoles with a moment μ_d are embeded. In this model each molecule is replaced by a point dipole μ_d having the same non-electrostatic interactions with the other point dipoles, while the polarizability of the molecules can be imagined to form a continuum with dielectric constant ϵ_∞; the polarization P will now split into two parts, the

induced polarization

$$P_{ind} = \frac{\epsilon_\infty - 1}{4\pi} E \qquad 2.4.1$$

and the orientation polarization

$$P_{or} = \frac{1}{V} \langle M_d.e \rangle \qquad 2.4.2$$

where

$$M_d = \sum_{i=1}^{N'} (\mu_d)_i \qquad 2.4.3$$

and

$$\langle M_d.e \rangle = \frac{\int dx^{N'} M_d.e.exp\left(\frac{-U}{kT}\right)}{\int dx^{N'} exp\left(\frac{-U}{kT}\right)} \qquad 2.4.4$$

is the average component of the moment due to the dipoles in the sphere. U is the energy of the dipoles in the sphere consisting of

(i) the energy of the dipoles in the external field

(ii) the electrostatic interaction energy of the dipoles

(iii) the non-electrostatic interaction energy between the molecules which is responsible for the short range correlation between orientations and positions of the molecules.

In this model the spherical cavity is situated in a dielectric with dielectric constant ϵ. The cavity field with a continuum dielectric constant ϵ_∞ will be equal to the external field, which will be called Fröhlich field E_F and is given by

$$E_\mathrm{F} = \frac{3\epsilon}{2\epsilon + \epsilon_\infty} E \qquad 2.4.5$$

The general expression for the dielectric constant in this case can be written as

$$\frac{\epsilon - 1}{4\pi} = \left(\frac{\delta}{\delta E} (P_{ind} + P_{or}) \right)_{\mathrm{E}=0}$$

After substitution of (2.4.18) and (2.4.19) and rearrangement

$$\epsilon - \epsilon_\infty = \frac{4\pi}{V} \left(\frac{\delta}{\delta E} \langle M_d . e \rangle \right)_{\mathrm{E}=0}$$

Rewriting with E_F instead of E as the independent variable

$$\epsilon - \epsilon_\infty = \frac{4\pi}{V} \left(\frac{\delta E_\mathrm{F}}{\delta E} \right)_{\mathrm{E}=0} \left(\frac{\delta}{\delta E_\mathrm{F}} \langle M_d . e \rangle \right)_{E_\mathrm{F}=0} \qquad 2.4.6$$

Since in this case,

$$\frac{\delta U}{\delta E_F} = -M_d . e$$

we obtain

$$\epsilon - \epsilon_\infty = \frac{4\pi}{V}\left(\frac{\delta E_F}{\delta E}\right)_{E=0}\frac{\langle M_d^2\rangle_0}{3kT} \qquad 2.4.7$$

Equation (2.4.7) is the expression for the dielectric constant in Frohlich model. Using equation (2.4.5) we can write

$$\epsilon - \epsilon_\infty = \frac{4\pi}{V}\frac{3\epsilon}{2\epsilon+\epsilon_\infty}\frac{\langle M_d^2\rangle_0}{3kT} \qquad 2.4.8$$

$$\langle M_d^2\rangle_0 = \frac{kTV}{4\pi}\frac{(\epsilon-\epsilon_\infty)(2\epsilon+\epsilon_\infty)}{\epsilon} \qquad 2.4.9$$

Evaluating the average of $\langle M_d^2\rangle_0$ we now obtain

$$\frac{(\epsilon-\epsilon_\infty)(2\epsilon+\epsilon_\infty)}{12\pi\epsilon} = \frac{N}{3kT}g\mu_d^2 \qquad 2.4.10$$

g is the correlation factor introduced by Kirkwood which takes into account the correlation between the orientation due to the short range order.

$$\mu_d = \frac{\epsilon_\infty+2}{3}\mu \qquad 2.4.11$$

where μ is the moment of the molecules in the gas phase. Substituting equation (2.4.11) into equation (2.4.10) and after rearrangement we

obtain

$$g\mu^2 = \frac{9kT}{4\pi N}\frac{(\epsilon - \epsilon_\infty)(2\epsilon + \epsilon_\infty)}{\epsilon(\epsilon_\infty + 2)^2} \qquad 2.4.12$$

Equation (2.4.12) is called Kirkwood-Fröhlich equation which can be seen as the generalization of the Onsager equation. Equation (2.4.29) gives the relation between ϵ, the dielectric constant ϵ_∞, the dielectric constant of induced polarization, the temperature, the density, and the permanent dipole moment.

Dielectric constant measurements yield the Kirkwood correlation factor g for polar liquids. This factor is a measure of the short range effects which tend to orient a molecule with respect to its neighbours. If the correlations are not negligible detailed information about the molecular interactions is required for the calculation of g.For systems in which intermolecular forces orient neighbouring dipoles in a parallel fashion, g is greater than unity; for an antiparallel configuration of dipoles g is less than unity. If there are no specific correlations one has $g = 1$. g can be formally defined by the relation

$$g = 1 + \frac{N_A}{V_M}\int_{V_0} cos\gamma exp\left(\frac{-W}{k_B T}\right) dW dV \qquad 2.4.13$$

where N_A is the Avogadro's number, V_M is the molar volume and γ is the angle between the dipole moments of an arbitrary pair of molecules, W is the potential average force and the integration extends over all relative orientations and positions of the centre of gravity of the pair within a sphere of volume V_0, outside of which the local dielectric constant equals the macroscopic dielectric constant. Now, if dipolar forces only are acting, it is possible even in the presence of a certain degree of order, that some positions give a positive and others a negative contribution to the integral, thus leading to a g value close to unity. This would be the case of compounds containing C=O stretching region. For associating compounds, where the association between the molecules makes relevant the assumption that only certain specific angles between the dipoles of neighbouring molecules are possible, the molecular interactions may be represented by simplified models.

2.5. INTERMOLECULAR INTERACTIONS IN LIQUIDS:

The interactions of two molecules or atoms may be represented[32,33] by treating the molecules as rigid and perfectly elastic spheres and

taking into account the fact that molecules attract each other at longer distances and repel each other at shorter distances. The functional form of the intermolecular potential is given by[32-34]

$$V = 4\epsilon \left[\left(\frac{\sigma}{r}\right)^{12} - \left(\frac{\sigma}{r}\right)^{6} \right] \qquad 2.5.1$$

where ϵ is the well depth and σ is the distance between atoms or molecules at which $V = 0$. r is the distance between atoms or molecules. This is called the Lennard-Jones (L-J) potential. It is also referred as 6 - 12 potential being a number of the family given as

$$V = A \left[\left(\frac{\sigma}{r}\right)^{m} - \left(\frac{\sigma}{r}\right)^{n} \right], m > n \qquad 2.5.2$$

m and n being the integers. The potentials are zero at $r = \infty$ and $r = \sigma$ and have a minimum at

$$\sigma_{min} = r \left(\frac{m}{n}\right)^{\frac{1}{(m-n)}} \qquad 2.5.3$$

For larger values of r the L-J potential is asymptotic to an r^{-6} curve and therefore it has the correct form to reproduce the long range dispersion energy between closed shell atoms and molecules.

A most commonly employed potential contains the exponential term and is given by the following relation

$$V = -\frac{A}{r^6} + Bexp(-\alpha r) \qquad 2.5.4.$$

which is usually called the exp-6 potential. A, B and α are constants. The merit of this function is that the long range attraction and short range repulsion are supported by theoretical analysis.

When two molecules are sufficiently far apart that the overlap of their charge clouds is negligible, a part of the interaction energy can be integrated as being electrostatic and due to Coulomb forces between the two charge clouds. This contribution to the interaction energy arises even for rigid (non-polarizable) molecules, and can be evaluated classically by calculating the field acting on one molecule due to the other. This field is usually approximated by a multipole series, which is valid if the distance r between the two molecular centres is greater then dimension of the molecular charge clouds. The multipole interactions can be attractive or repulsive depending on the relative orientations of the two molecules.

For molecules with no internal rotations, and which are in their

ground electronic and ground vibrational states, the pair potential can be assumed to depend only on the intermolecular separation and on the molecular orientations. At long range the interaction energy can be classified as multipolar (electrostatic), dispersion and induction energy and at short range as overlap (electrostatic and exchange) energy.

The total multipolar (electrostatic) interaction energy of two rigid charge clouds is given by[35]

$$V = \sum_{ij} \frac{q_i q_j}{r_{ij}} \qquad 2.5.5$$

where i and j run over the charge distribution 1 and 2 respectively and r_{ij} is the separation between q_i and q_j . If the two charge distributions do not overlap, we can resolve equation (2.5.5) into multipole-multipole constituents V_{l_1,l_2}, in which the multipole of order l_1 of distribution 1 interacts with the multipole of order l_2 of distribution 2.

Using spherical tensor expansions, the total interaction energy between the charge distributions is thus given by

$$V = \sum_{l_1,l_2} V_{l_1.l_2} \qquad 2.5.6$$

where

$$V_{l_1,l_2} = \left(A_{l_1,l_2}/r^{l+1}\right) \sum_{m_1,m_2,m} C(l_1 l_2 l_3; m_1 m_2 m) X Q_{l_1 m_1} Q_{l_2 m_2} Y^*_{lm}(\omega) \qquad 2.5.7$$

Q_{lm} are the space-fixed multipole moments. V_{l_1,l_2} is the electrostatic interaction energy between the multipoles of orders l_1 and l_2 of charge distributuins 1 and 2., respectively; V_{11} being the dipole-dipole interaction, V_{12} being the dipole-quadrupole interaction, and so on.

The potential function can be expressed in different ways so far as the charge distribution of the molecules do not overlap. The alignment theory of Keesom considers molecular attractions as a direct interaction between static multipoles within the molecule. The Keesom interaction is important whenever the molecules have permanent dipole moments. The alignment effect in its simplest form can be

expressed by

$$V = -\frac{\mu_1\mu_2}{r^3}\left[2cos\theta_1\theta_2 + sin\theta_1 sin\theta_2 cos(\phi_1 - \phi_2)\right]$$

$$+\frac{3}{2r^4}\{\left[Q_1\mu_2(cos\theta_2 + 2cos\theta_1 sin\theta_1 sin\theta_2 cos(\phi_1 - \phi_2) - 3cos^2\theta_1 cos\theta_2)\right]$$

$$-\mu_1 Q_2\left[cos\theta_1 + 2cos\theta_2 sin\theta_2 sin\theta_1 cos(\phi_1 - \phi_2) - 3cos^2\theta_2 cos\theta_1\right]\}$$

$$+\frac{3}{4r^5}\{Q_1Q_2[1 - 5cos^2\theta_1 - 5cos^2\theta_2 - 15cos^2\theta_1 cos^2\theta_2$$

$$+2(4cos\theta_1 cos\theta_2 - sin\theta_1 sin\theta_2)cos(\phi_1 - \phi_2)]\}$$

$$+\frac{1}{2r^5}\{O_1\mu_2[(12 - 20cos^2\theta_1)cos\theta_1 cos\theta_2$$

$$+(15cos^2\theta_1 - 3)sin\theta_1 sin\theta_2 cos(\phi_1 - \phi_2)]$$

$$+\mu_1 O_2\left[(12 - 20cos^2\theta_2)cos\theta_1 cos\theta_2 + (15cos^2\theta_1 - 3)sin\theta_2 sin\theta_1 cos(\phi_1 - \phi_2)\right]\}$$

$$+\text{terms of order } r^{-6} etc. \qquad 2.5.8$$

where μ_1, Q_1 and O_1 denote the dipole moment , quadrupole moment and octupole moment respectively of molecules 1 and μ_2, Q_2 and O_2 are respectively the corresponding moments of molecule 2.The mean value of V is zero if and only if all orientations of molecules are equally probable.

The interaction potential between two molecules of dipole moment μ_i and μ_j at positions r_i and r_j which tend to align both molecules is given by

$$V_{or}(r_{ij}) = \mu_i.\nabla_i.\nabla_j \left|r_i - r_j\right|^{-1}.\mu_j \qquad 2.5.9$$

This orientation is the parallel alignment of the two molecules[35]. The interaction energy for such a system can be written as

$$V_{or} = -\frac{2\mu_i\mu_j}{r_{ij}^3}, for\ k_BT << \frac{\mu_i\mu_j}{r_{ij}^3} \qquad 2.5.10$$

and

$$V_{or} = -\frac{2\mu_i\mu_j^2}{3k_BTr_{ij}^6}, for\ k_BT >> \frac{\mu_i\mu_j}{r_{ij}^3} \qquad 2.5.11$$

where the orientation effect of both the dipoles have been considered leading to the doubling of the interaction energy(Fig.2.1). The orientation effect vanishes for molecules which donot possess permanent dipoles. Due to the thermal motion any alignment vanishes at high temperature.

In space-fixed axes the dipole-dipole term V_{11} is

$$V_{11} = (-\mu_1\mu_2/r^3)(3C_1C_2 - C_{12}) \qquad 2.5.12$$

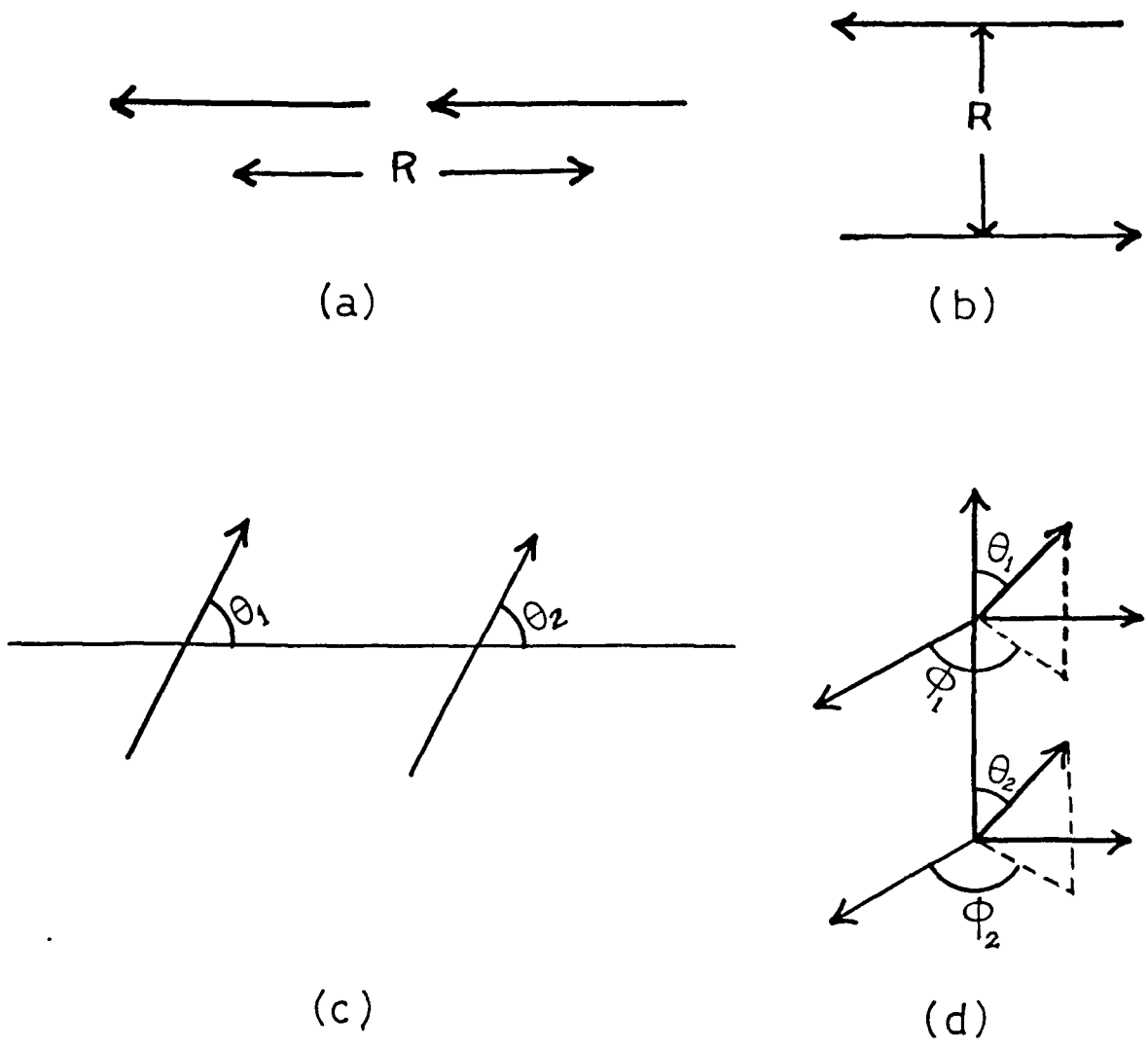

Figure 2.1 The orientational configuration of two dipoles

where C_i is the cosine of the angle between μ_i and r and C_{12} is the cosine of the angle between μ_1 and μ_2. The direction of r is chosen from molecule 1 and 2 in the intermolecular frame with polar axis along r. For axially symmetric molecules (for molecules with atleast threefold symmetry axes), the dipole-quadrupole term V_{12} in the space-fixed axes the result is

$$V_{12} = \frac{3}{2}(\mu_1 Q_2/r^4)\left(C_1(5C_2^2 - 1) - 2C_{12}C_2\right) \qquad 2.5.13$$

The quadrupole-quadrupole interaction energy can be derived similarly in space-fixed axes as

$$V_{22} = \frac{3}{4}\left(Q_1 Q_2/r^5\right)\left(1 - 5C_1^2 - 5C_2^2 + 2C_{12}^2 + 35C_1^2C_2^2 - 20C_1C_2C_{12}\right)$$

2.5.14

The minimum energy orientations for the three interactions V_{11}, V_{12} and V_{22} are shown in Fig.(2.2).

For dispersion interactions the preferred orientation[35] at fixed r is end-to-end, as opposed to the **T** orientation for quadrupole-quadrupole interactions. The induction energy is often small for isolated molecular pairs, and therefore for low density gases. For liquids it turns out that induction interaction can make a significant contribution to the

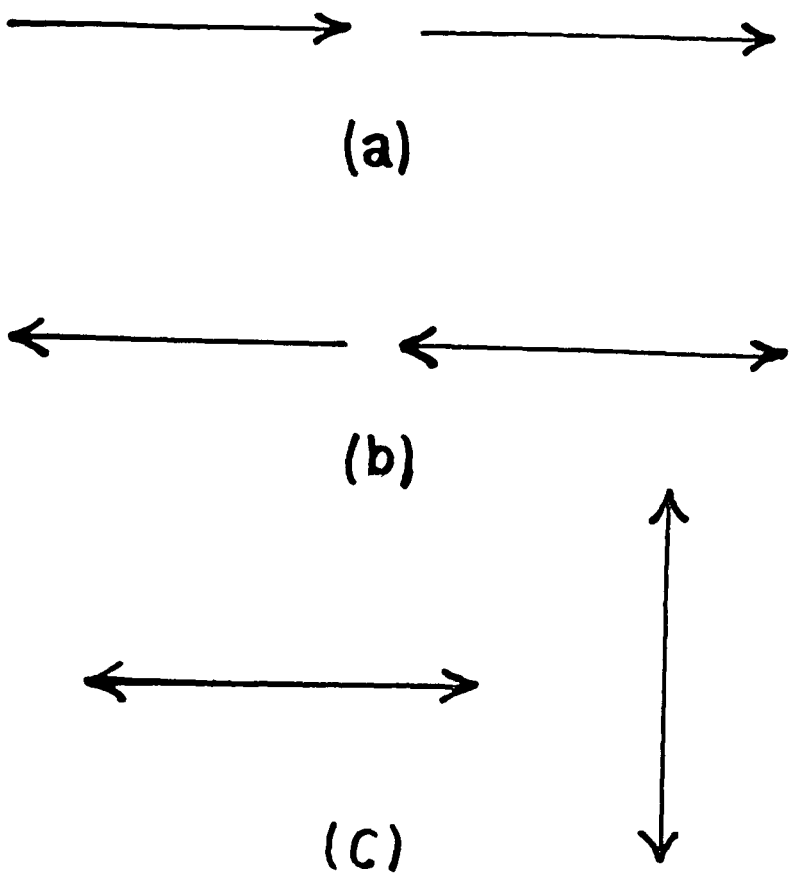

Figure 2.2 Minimum energy orientation for
(a) dipole - dipole
(b) dipole - quadrupole
(c) quadrupole - quadrupole

the free energy and pressure even when the contribution to internal energy is small. Multibody induction interactions are also important in liquids and can enhance these effects.

The molecular shape influences the preferred orientations by controlling the distance of closest approach. For specific molecules there are often additional competing interactions, such as dispersion which may lead to preferred orientations different from those favoured purely electrostatically.

Another very important type of potential which has to be taken into consideration is H - bonding type. The main contribution to the binding energy of H atom to the electronegative atoms comes from the electrostatic energy between the dipolar A-H bond and a partial negative charge on the electronegative atom B. For the stronger complexes, however, there is a significant contribution arising from the overlap of orbitals of A-H bond with those of B. This interaction leads to a partial transfer of electrons from B to the A-H bond.

2.6 RAMAN ACTIVITY:

The Raman effect is an inelastic scattering phenomenon in which the illuminated sample absorbs a photon and simultaneously emits another photon of different frequency. When the emitted photon is of lower frequency than the absorbed photon, the process is termed as Stokes Raman scattering, while if the emitted photon is of higher frequency than the absorbed photon, the process is termed as Anti-Stokes Raman scattering (Fig.2.3). The dashed line in the diagram indicates the virtual electronic states of the molecule and states o and p represent lowest lying excited electronic levels of the molecule. The levels m and n are most often molecular vibrational levels for which the transition frequencies are much smaller than the optical excitation frequencies. The resonance Raman effect arises when the excitation frequencies are equal to the frequencies of one photon allowed transition between the states n or m and states o or p as shown in the Fig.2.3(B). The process depicted in Fig.2.3(A) is often referred to as spontaneous Raman scattering.

The phenomenon of Raman effect arises because molecular vibrations modulate the frequency of the dipole induced in a molecule by

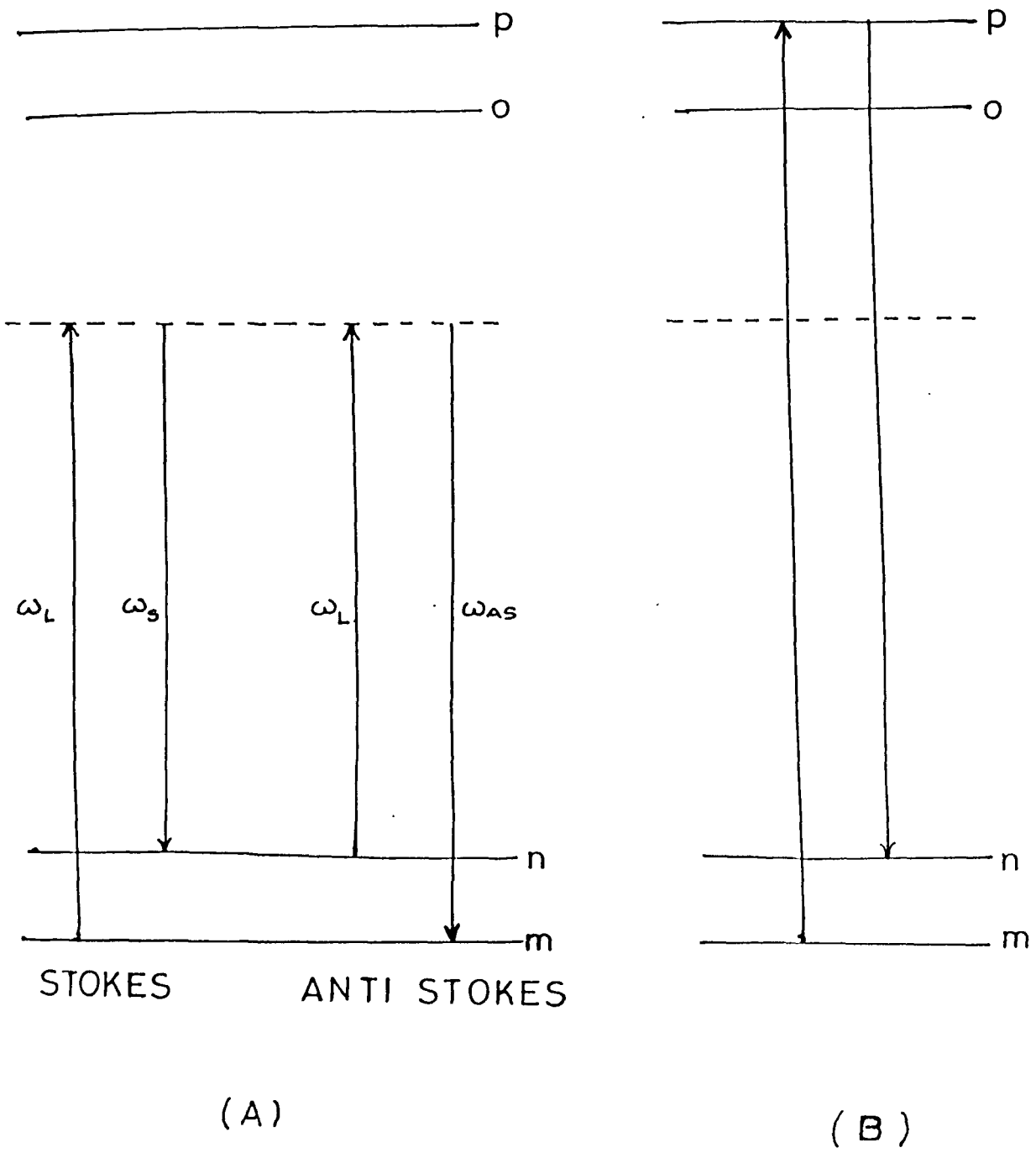

Figure 2.3 Energy level diagram for

(A) Spontaneous Raman scattering
(B) Resonance Raman effect

an incident field. The electric dipolemoment induced in a molecule by the electric field E can be expanded in a power series[36]

$$\mu = \alpha E + \beta E^2 + \gamma E^3 \qquad 2.6.1$$

α is the polarizability tensor of rank 2, while β, γ, etc. are the hyperpolarizabilities of rank 3, 4, etc. Spontaneous Raman scattering arises due to the linear term in equation (2.6.1).

Although a quantum mechanical treatment is necessary for a complete explanation of Raman scattering, many aspects of the phenomenon can be described reasonably well by the classical electromagnetics of the induced dipole and the molecular vibration. The classical electromagnetism also reveals the principal selection rule for Raman scattering. Following the treatment of Placzek, the polarizability can be expanded in a Taylor series as a function of the vibrational normal coordinate q as[37]

$$\alpha = \alpha_0 + \left(\frac{\delta\alpha}{\delta q}\right)_0 q + \frac{1}{2}\left(\frac{\delta^2\alpha}{\delta q^2}\right)_0 q^2 + \ldots \qquad 2.6.2$$

For a particular vibrational mode to be Raman active, the derivative of the polarizability with respect to the normal coordinate evaluated at the equilibrium position must be non-zero (i.e., $\alpha'_{ij} \neq 0$, where $i, j = x, y,$ or z). The polarizability tensor is a symmetric one for normal Raman effect and therefore only six components have to be taken into account.

REFERENCES

1. R. G. Gordon, *J. Chem. Phys.*, **40,** 1973 (1964).

2. D. W. Oxtoby, *Adv. Chem. Phys.*,**40,** 1078 (1971).

3. D. W. Oxtoby, *Chem. Phys. Lett.*, **52,** 224 (1977).

4. D. W. Oxtoby, D. Levesque and J. -J. Weis, *J. Chem. Phys.*, **68,** 5528 (1978).

5. D. W. Oxtoby, *J. Phys. Chem.*,**87,** 3028 (1983).

6. D. Levesque, J.-J. Weis and D. W. Oxtoby, *J. Chem. Phys.*, **77,** 2153 (1982).

7. S. F. Fischer and A. Laubereau, *Chem. Phys. Lett,* **35,** 6 (1975).

8. K. Tanabe and J. Jonas, *Chem. Phys. Lett.*, **53,** 278 (1978).

9. K. S. Schweizer and D. Chandler, *J. Chem. Phys.*, **76,** 2296 (1982).

10. D. Ben Amotz, M. R. Lee, S. Y. Cho and D. J. List, *J. Chem. Phys.*, **96,** 8781 (1992).

11. G. Döge, R. Arndt and J. Yarwood, *Mol. Phys.*, **52,** 399 (1984).

12. W. Schindler, T. W. Zerda and J. Jonas, *J. Chem. Phys.*, **79,** 639 (1983).

13. Bratos. S. and Tarjus. G, *Phys. RevA,* **24,** 1591 (1981).

14. Tarjus. G and Bratos. S, *Mol. Phys.*, **33,** 907 (1981).

15. D. E. Logan, *Mol. Phys.*, **58(1),** 79 (1986).

16. D. E. Logan, *J. Chem. Phys.*, **103,** 215 (1986).

17. D. E. Logan, *J. Chem. Phys.*, **131,** 199 (1989).

18. G. Fini and P. Mirone, *J. Chem. Soc., Faraday Trans.*, **270,** 1776 (1970).

19. G. Fini, P. Mirone and B. Fortunato, *J. Chem. Soc., Faraday Trans.*, **1169,** 1243 (1973).

20. G. Fini and P. Mirone, *Spectrochim. Acta,* **32A,** 625 (1976).

21. P. Mirone and G. Fini, *.J. Chem. Phys.*, **71,** 2241 (1979).

22. P. mirone, *J. Chem. Phys.*, **77,** 2704 (1982).

23. C. H. Wang and J. McHale, *J. Chem. Phys.*, **72,** 4039 (1980).

24. J. McHale, *J. Chem. Phys.*, **75,** 30 (1981).

25. M. G. Giorgini, G. Fini and P. Mirone, *J. Chem. Phys.*, **79,** 639 (1983).

26. R. Kubo, *in Fluctuations, Relaxation and Resonance in Magnetic systems,* edited by D. ter Haar, **pp.,** 23, Oliver and Boyd, Edinburgh (1962).

27. J. Yarwood and R. Arndt, *in Molecular Association,* edited by R. Forster, **Vol2, pp.** 287-300, Academic press, London.

28. C. B. Harris, R. M. Shelby and P. A. Cornelus, *Chem. Phys. Lett.,* **57**, 8 (1978).

29. R. M. Shelby, C. B. Harris, and P. A. Cornelus, *J. Chem. Phys.*, **70,** 34 (1979).

30. S. Bone, J. Eden, P. R. C. Gasloyne and R. Pethig, *J. Chem. Soc., Faraday Trans. 1,* **77,** 1729 (1981).

31. C. J. F. Bottcher, *Theory of Electric Polarization,* **Vol1,** Elsevier, Amsterdam (1973).

32. H. Margenau and N. R. Kestner, *Theory of Intermolecular Forces,* Pergamon Press, Oxford (1979).

33. F. Daniels and R. A. Alberty, *Physical Chemistry,* John Wiley and Sons., Newyork (1975).

34. M. Karplus and R. N. Porter, *Atoms and Molecules, An Introduction for Students of Physical Chrmistry,* **pp.** 262-267, The Benjamin/Cummings Publishing Company, California (1970).

35. C. G. Gray and K. E. Gubbins, *Theory of Molecular Fluids,*

Vol1: *Fundamentals,* International Series of Monographs on Chemistry , Clarendon Press, Oxford, (1984).

36. L. J. Radziemski, R. W. Solarz and J. A. Paisner, *Laser Spectroscopy and its Applications,* Edited by, Marcel Dekker, **pp** 514, New York, (1987).

37. H. A. Szymanski (Ed.), *Raman Spectroscopy,* **Vol1**,Plenum, New York (1967).

CHAPTER 3

Chapter 3

EXPERIMENTAL ASPECTS

Introduction

The Raman scattering is a very weak phenomenon compared to Rayleigh scattering ($\approx 10^{-6}$ of the intensity of Rayleigh light) and only a small fraction of photons are scattered by Raman scattering. The majority of the scattered light is similar to the original incident light in terms of photon energy. In a standard Raman experiment, an intense monochromatic radiation is focussed onto the sample. The scattered light is gathered by the collecting optics and is directed to a dispersive system (usually a double monochromator) which selects the scattered light of particular frequency range. The signals are detected by a photomultiplier tube and are recorded by the DATAMATE (Fig. 3.1).

3.1 Source of Excitation:

The Spectra Physics model 165 Ar^+ laser and the Liconix model 4240 He-Cd laser are the laser sources used for recording the Raman spectra.

3.2.1 Spectra Physics Model 165 Ar^+ Laser:

The Spectra Physics model 165-09 Ar^+ laser is a continuous wave (CW) laser. It essentially consists of a laser head and an exciter (Spectra Physics model 265). The laser head consists of a Berrylium oxide plasma tube closed at each end by the brewster angle windows, a solenoid and an optical resonator. The optical resonator is formed by a reflector (spherical) at the output end together with a prism assisted by a flat reflecting mirror at the back end. The prism is placed in the optical path of the resonator in such a way that it selects the correct wavelength. The plasma tube is positioned exactly along the central line of the mirror. External thumb wheel controls are provided for the selection of wavelength of the emitted radiation and for changing the intra-cavity aperture. The emitted light from this laser source is

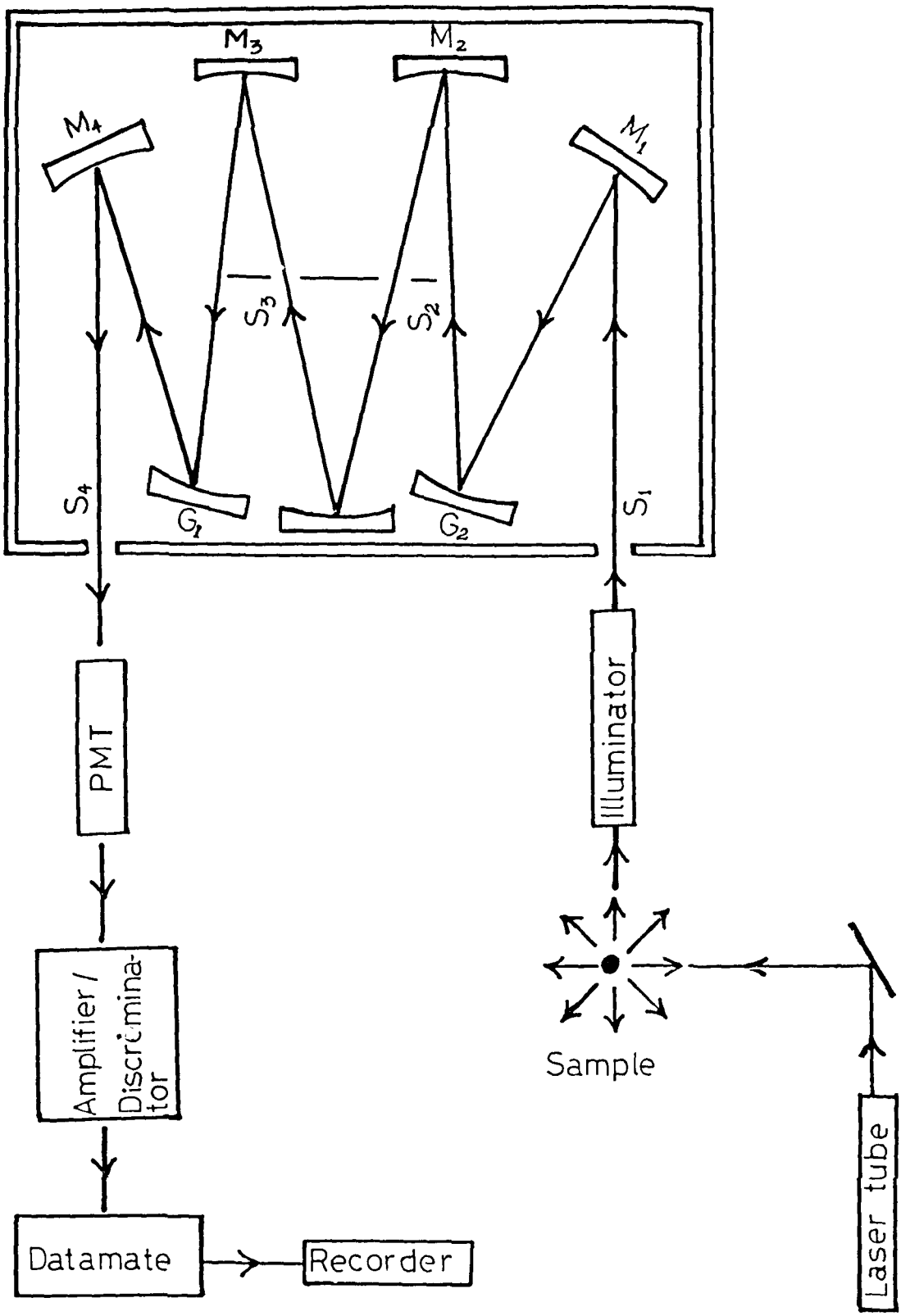

Fig. 3.1

Block diagram of a Raman instrument

polarized and the plane of polarization can be changed to any desired plane by using the $\lambda/2$ plate.

The Spectra Physics model 265 Exciter contains the necessary electric and electronic circuitries in order to create, sustain and monitor the ionic discharge in the plasma tube. It also monitors and controls the output power and regulates the solenoid current of the 165 Ar^+ laser head. The 265 exciter runs on a 230 volts three phase power line which is provided by a power transformer supplied with a three phase 400 volts stabilized power from the main line. The input power stabilization was achieved with the help of three single phase 8.3 KVA (each) Nelco voltage stabilizers connected in the star (Y) configuration. Both the 165 Ar^+ laser head and the 265 exciter are continuously cooled by flowing chilled deionised distilled water at a constant temperature of 15^{o}C and at a pressure of 40 PSIG from the Neslab HX-500 (air cooled) water chiller plant.

3.2.2 Liconix model 4240 He-Cd Laser

Liconix model 4240 He-Cd laser[1] essentially consists of a laser head and a power supply, The optical section of the laser head is formed

by two mirrors mounted on adjustable plates and held at a precise separation by three invar rods that run along the length of the laser tube made of pyrex glass. the mirrors are adjusted to reflect the laser light down the bore of the laser tube and to allow the emission of a precise amount of light as an output beam. The laser head is an air cooled system and requires no external cooling device. The output power at 4416 Åis about 40 mW.

In order to maintain the photon producing conditions the helium pressure and the cadmium vapour pressure must be maintained within a certain limit. Cadmium vapour pressure is maintained by electronically controlling the temperature of a heater surrounding the cadmium reservoir. Helium is consumed by entrapment in the cathode and under cadmium deposits inside the laser tube. The cleaned up helium is replaced and pressure is maintained by use of a heat controlled leak between a small (higher pressure) bottle and the helium ballast. The helium gas heater is electronically controlled, using the voltage drop across the tube as pressure indicator.

The power supply model 4240 PS utilizes AC power from the primary source and converts it into different DC levels for maintaining

a constant output power by controlling the gas pressure.

3.3 Optics around the sample

A laser filter or the lasermate is kept in the light path before it enters the focussing system. The laser filter is a small grating monochromator which allows the excitation wavelength to pass through but blocks weaker nonlasing lines from the laser plasma. It is therefore able to provide a clean Raman spectrum uncluttered by the laser-plasma lines, especially for a strong scattering sample[2].

The filtered laser beam is deflected upward through 90^o by a mirror and is focussed onto the sample to a spot of diameter of around 10 μm by the fused silicon condensing lens. Scattered radiation from the sample passes through a polarization analyzer, a device based on birefringence and total reflection or on dichroism. The polarization analyzer transmits light of a particular polarization depending on the orientation of the polarizer. Use of polarization analyzer therefore provides direct information regarding the state of polarization of the observed plasma band. The scattered radiation is collected by an elliptical mirror which ascertains a large solid angle about the focal

volume and hence collects the optimum amount of scattered light. Fig.3.2 shows the optical diagram of the light scattering system.

3.4 The Spectrometer: SPEX Ramalog model 1403 Double Monochromator:

The function of the spectrometer is to separate the spatially scattered photons from the sample on the basis of their frequency. The light dispersing process is repeated by linking two single monochromators to form a double monochromator. The double monochromator also separates the Raman photons from the overwhelming number of Rayleigh photons.

All the Raman spectra in the present study have been recorded with the help of SPEX Ramalog 1403 double monochromator[2] coupled with a water cooled photomultiplier tube RCA C-31034-02.

The SPEX Ramalog 1403 double monochromator is f/7.8 instrument with a spectral coverage from $3.1X10^4$ cm^{-1} to $1.1X10^4$ cm^{-1}. An accuracy of $\pm 1 cm^{-1}$ in the 10,000 cm^{-1} range, a resolution of 0.15 cm^{-1} and a spectral repeatability of ± 0.2 cm^{-1} can be achieved by this instrument. The 1800 grooves/mm holographic gratings are

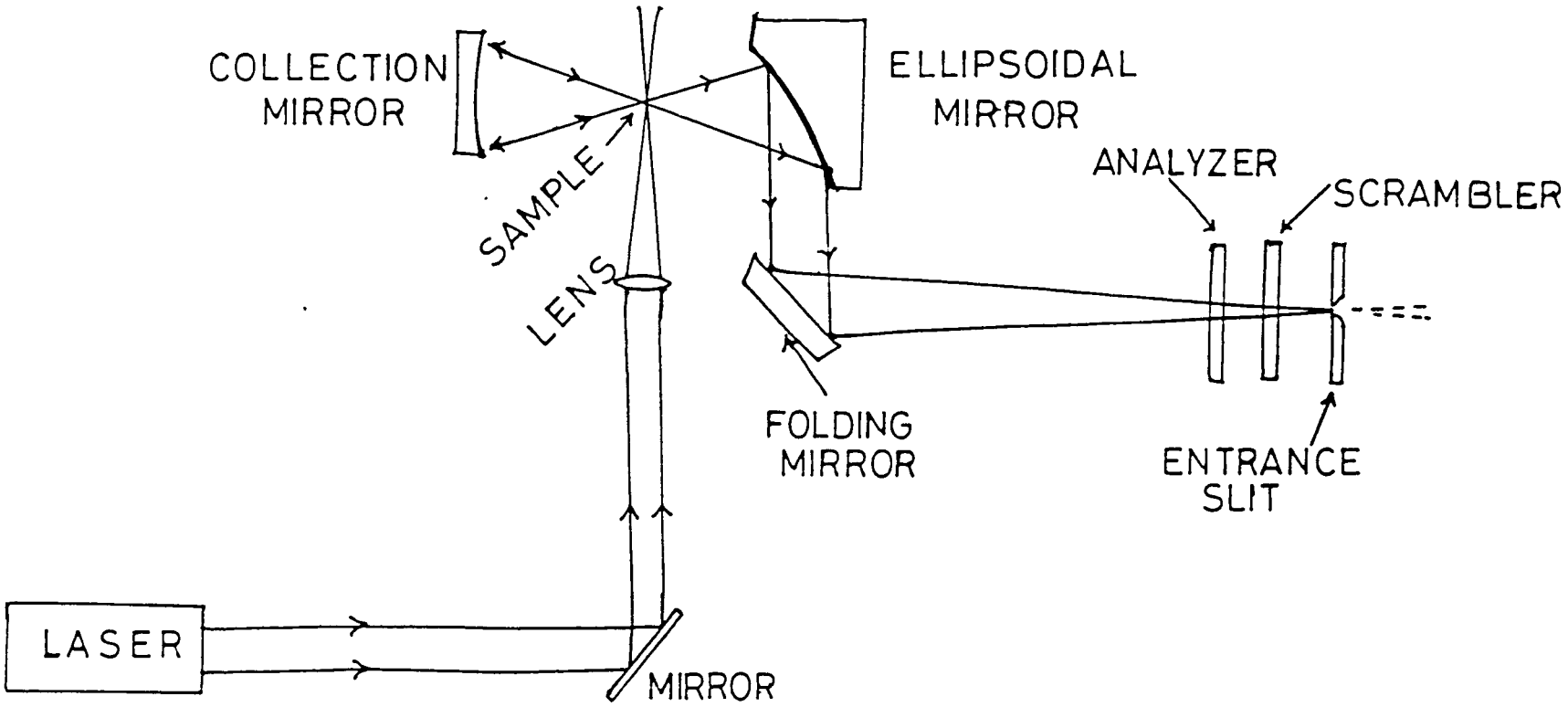

Fig. 3.2

Optical diagram of the light-collecting system of a Raman instrument

used in this instrument. The gratings are mounted on a modified Czerny-Turner mount as shown in Fig.3.3.

The fundamental grating equation[3] as applied to Czerny-Turner mount is

$$d(sin\alpha + sin\beta) = m\lambda \qquad 3.4.1$$

where m = order, λ = wavelength, d = grating spacing, α = angle of incidence and β = angle of diffraction. In case of 1403 instrument this formula may be expressed as

$$2dsin\theta cos\phi = n\lambda \qquad 3.4.2$$

where $\phi = 10^o$: hence $cos\phi = 0.984$.

Equation (3.4.2) was obtained by substituting

$$\alpha = \theta + \phi$$

and

$$\beta = \theta - \phi$$

Here θ denotes the angle of rotation of the grating from zero as illustrated in the Fig.3.3 and ϕ represents the constant angle which depends on the design of the instrument.

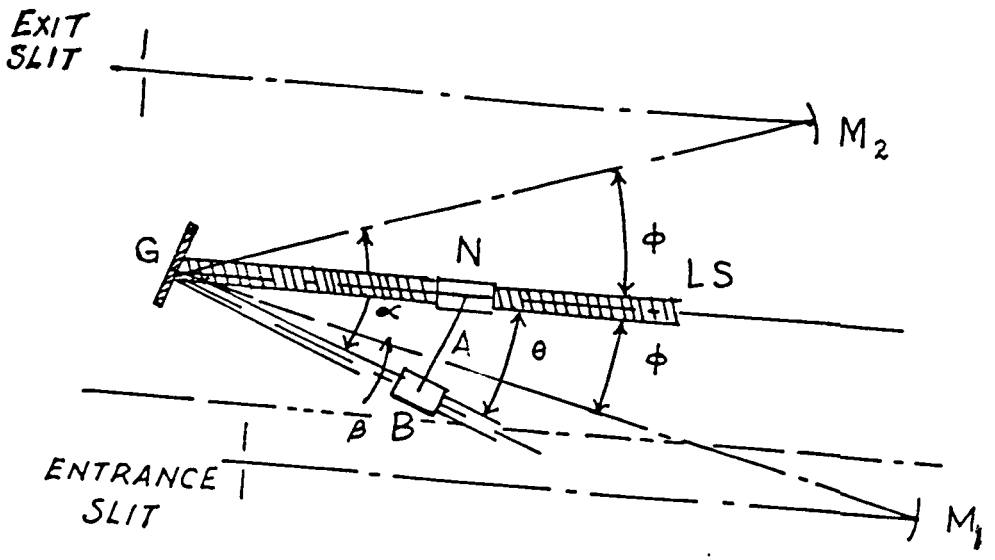

Fig. 3.3

Czerny Turner mount of gratings for the SPEX model 1403 Ramalog

The scattered radiation focussed onto the entrance slit of the spectrometer gets dispersed by the 1800 grooves/mm holographic gratings. Nearly monochromatic radiation of frequency ν for a particular tuning of the spectrometer reaches the exit slit of the double monochromator by the grating mirror combination.

The theoretical resolving power R_T is given by

$$R_T = \frac{\lambda}{\Delta\lambda} = \frac{\nu}{\Delta\nu} = 2sin\theta cos\phi W/\lambda = mN \qquad 3.4.3$$

where

λ = wavelength.

ν = wavenumber

N = total number of grating grooves

W = width of grating ruling and

m = order of diffraction.

Factors influencing resolution:

Source: From equation (3.4.1), since resolution depends linearly on the grating width (i.e. optical path difference), resolution deteriorates if the source illuminates less than the full width of the grating. As a

result, the source or condensing lens should fully illuminate the collimating mirror. This can usually be checked visually by opening the spectrometer or, in the case of energy outside the visible spectrum, by making certain that throughput is reached when the edges of the collimating mirror are obstructed.

Slit width: Spectral bandpass is a function of the reciprocal linear dispersion which, in turn, depends on the wavelength, the grating constant, the focal length of the instrument and the spectral order.

Slit height: Increase in the heights of straight slits reduces the instrumental resolution. As the height of the slits is increased the ends of the exit slit begin to pass portions of adjoining wavelengths.

3.5 Collection of scattered radiation:

A standered sampling platform is supplied with the SPEX 1459 illuminator. The 14318 liquid cell of 1 ml. capacity with 1431 N holder was used for holding the sample.The sample is illuminated with laser radiation and then the laser focus control is adjusted until the brightest image is observed at the sample. The image of the

sample scattered radiation is deflected on the target. The imaging of the scattered radiation on the entrance slit of the spectrometer is done by an elliptical collection mirror (f/1.4). The image is centred on the cross wires with the lateral adjustments and focus adjustment is turned until the sharpest image is achieved. By rotating the swing away mirror counter clockwise the sample scattered radiation is allowed to pass into the spectrometer. The signal is now peaked photoelectrically between the focus and lateral adjustments until the signal from the detector is maximum. In order to increase the scattering and collection efficiency spherical mirrors may be mounted above and behind the sample in the 1459 illuminator. Both mirrors increase the amount of scattered radiation that reaches the spectrometer entrance slit and therefore also increase the signal from the detector.

Two optical elements may be interposed in the beam, an analyzer and a scrambler, before it reaches the entrance slit. The scrambler is a wedge of birefringent material. The two components of polarized light passing through it will be thrown out of phase as with a $\lambda/2$ plate. The retardation will vary from place to place and is not

exactly $\lambda/2$; hence the emerging radiation will be depolarized. It cancels variation in spectrometer response that results from polarization dependent efficiencies.

The laser output is polarized perpendicularly, whereas the Raman radiation from the sample is depolarized. The analyzer interposed in pathway may transmit the light either perpendicularly polarized or parallel polarized, depending on the orientation of the analyzer. In both the cases the same scrambler is employed in front of the entrance slit of the monochromator to depolarize the radiation.

3.6 Photon counting detection

The detection system consists of a RCA C31034-02, II-stage QUANTACON type photomultiplier tube (PMT) with S-20 response in the photon counting mode. The C31034-02 is designed specifically for use at reduced temperatures, e.g., -30°C. Cooling reduces the dark count caused by the thermionic emission to $\approx$ 10 cps. Spex DATAMATE-DM1 and DM3000 software were used for recording the spectra and also for the acquisition of the data. The central processing unit (CPU) of the DATAMATE is a 8-bit microprocessor based ROM. The data

can be processed in real time to subtract away background, take ratios, integrate or convert to logerithm for absorption states. DATAMATE photon counting results are expressed as and normalized to counts/sec. The DATAMATE also supplies high voltage (0-2000 volts D.C. -ve) to PMT. The high voltage is CPU selectable in 10 volts increment. The output current is variable from 0-2 mA. The linearity is better than 0.01% over full range. The noise level is 0.015% peak to peak at full load. the input in photon counting - DAM mode is -ve going pulse 0.1 mV amplitude or greater. The gain of the amplifier is 400 and the rise time is 10 ns. The pulse pair resolution is less than 25 ns. The discreminator is internally adjustable from 5 mV to 200 mV. The maximum count rate for photon counting is 25 X 10^6 Hz. The linearity and accuracy of the output data (Y-axis) is 0.3% full scale and resolution is one part in 4000.

3.7 The photomultiplier tube:

RCA C-31034-02 photomultiplier tube, cooled to -30^{o}C by a thermoelectric cooling device was used for obtaining the Raman spectral

data. The photomultiplier tube having an almost linear absolute responsivity 3000 Åwavelength range was operated for a current gain of 10^6 with a maximum dark pulse summation of 12 cps. The RCA C-31034-02 photomultiplier tube consists of a gallium arsenide chip placed at its photocathode, an ultraviolet transmitting glass window and an inline copper beryllium dynode structure consisting of eleven dynodes.

The raw data is obtained from the output of the preamplifier (pc Dam) of gain 400. The anode of the PMT is the input of the pc Dam. The high voltage of 1750 volts required for operating the PMT is supplied by the datamate with a stability of +0.002% after 30 minutes of warm up.

3.8 Sampling techniques:

A laser beam, being a narrow and unidirectional, entity, can be manipulated in a variety of sample cell configurations thus providing considerable ingenuity in exercising the design and use of sample cells. A substantial advantange stemming from the geometric simplicity of

the Raman experiment, is that samples may be examined in any physical states. For liquid samples, which we have used more frequently a cell consisting of around 1 cm path length is adequate, provided the cell bottom is transparent. In order to minimise the amount of scattered light from the interface reaching the spectrometer, the cell should be toped around the meniscus.

3.9 The polarized and depolarized components of scattered light:

In order to measure the depolarzation ratio accurately, the polarization of the exciting laser beam is kept constant and the analyzer is placed after the sample[4]. Suppose the polarization of the laser beam is parallel to the Z axis (Fig.3.4) and the direct transmission of the analyzer is turned from Y to Z direction to measure I_{VH} and I_{VV} respectively. The intensity of the I_{VH} component is proportional to

$$I_{VH} \propto 3\gamma'^2 \qquad 3.9.1$$

and that of I_{VV} component is proportional to

$$I_{VV} \propto \left(45\bar{\alpha}'^2 + 4\gamma'^2\right) \qquad 3.9.2$$

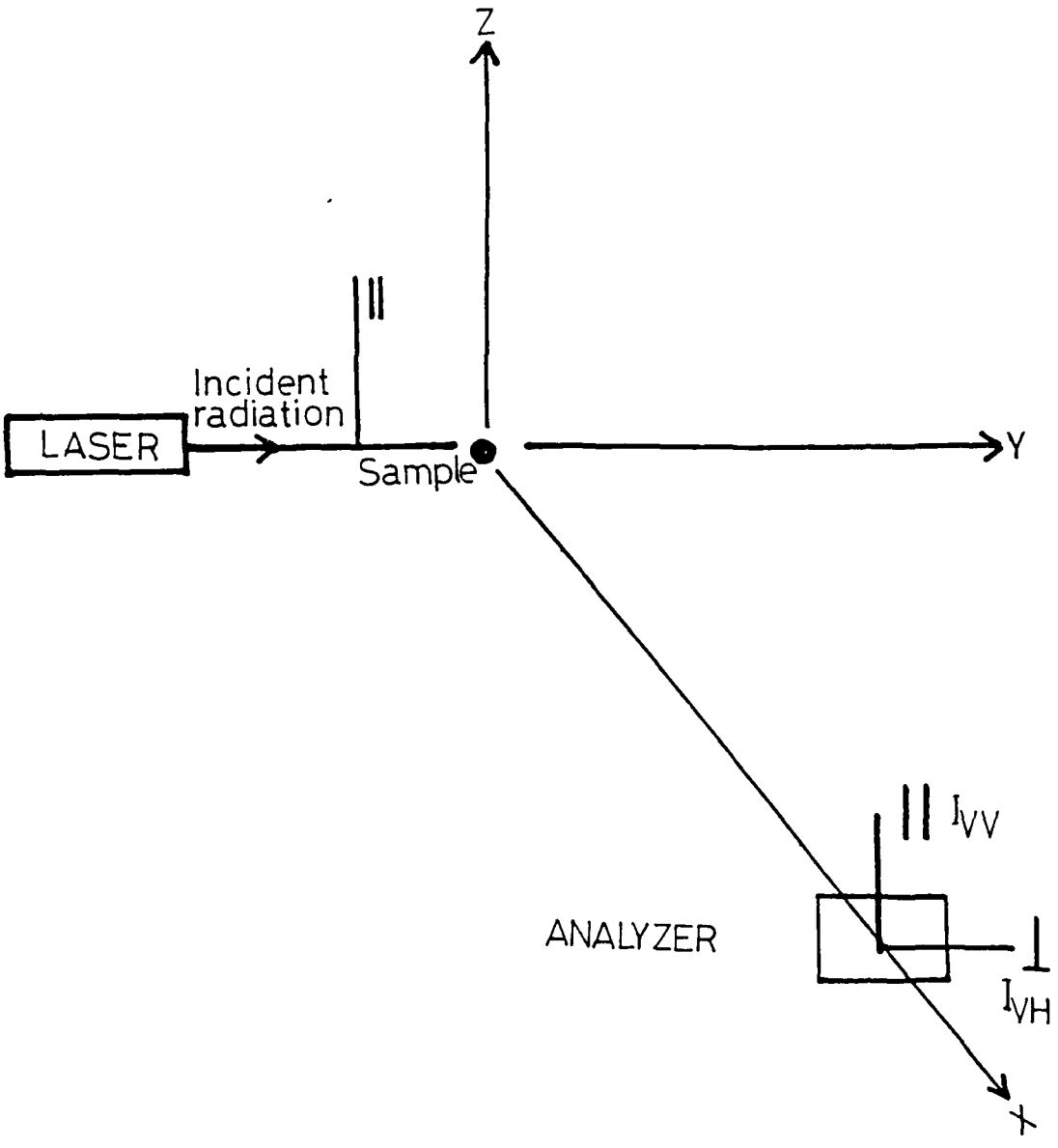

Fig. 3.4

Optical diagram showing the two components of scattered intensity.

where the factors $\bar{\alpha}'^2$ and γ'^2 are defined by the derivatives of the polarizabilities as,

$$\bar{\alpha}' = \frac{1}{3}(\alpha'_{XX} + \alpha'_{YY} + \alpha'_{ZZ}) \qquad 3.9.3$$

$$\gamma'^2 = \frac{1}{2}\left[(\alpha'_{XX} - \alpha'_{YY})^2 + (\alpha'_{YY} - \alpha'_{ZZ})^2 + (\alpha'_{ZZ} - \alpha'_{XX})^2\right]$$

$$+6\left(\alpha'^2_{XY} + \alpha'^2_{YZ} + \alpha'^2_{ZX}\right) \qquad 3.9.4$$

Since the constant factor is same for the fixed experimental conditions, the depolarzation ratio is

$$\rho = \frac{I_{VV}}{I_{VH}} = \frac{3\gamma'^2}{45\bar{\alpha}'^2 + 4\gamma'^2} \qquad 3.9.5$$

If the Raman scatter is known for the directions X and Y, its intensity in any direction ϕ of the X-Z plane may be calculated from

$$I(\phi) = I_X cos^2\phi + I_Z sin^2\phi \qquad 3.9.6$$

The angle dependent intensities after the anlyzer are

$$I_{VH}(\phi) \propto 3\gamma'^2 \qquad 3.9.7$$

$$I_{VV}(\phi) \propto \left(45\bar{\alpha}'^2 + 4\gamma'^2\right) cos^2\phi + 3\gamma'^2 sin^2\phi$$

$$= \left(45\bar{\alpha}'^2 + \gamma'^2\right) cos^2\phi + 3\gamma'^2 \qquad 3.9.8$$

The observed depolarization ratio is

$$\rho_{\text{obs}} = \rho + \rho(1-\rho)\frac{\phi^2}{3} \qquad 3.7.9$$

For $\rho << 0.75$, $\rho(1-\rho)\frac{\phi^2}{3}$ is of the order of magnitude of ϕ. Thus the measured depolarization ratio ρ_{obs} will be larger thal the true depolarization ratio, ρ.

If an angle $\phi = 10^o$ (=0.175 rad) is needed to measure a depolarization ratio of $\rho = 0.01$, in the case of highly polarized band, this method will produce a systematic error of

$$\left(1-\rho^2\right)\frac{\phi^2}{3} \approx 10^{-4} or 1\%$$

However, if a completely depolarized band is to be measured for which the depolarization ratio is $\rho = 0.75$, the systematic error by using the same collecting angle $\phi = 10^o$ will be

$$0.19X10^{-2} or 0.3\%$$

Therefore we see that measured depolarization ratio is always larger than the theoretically expected value.

The intensity of isotropic and anisotropic components of Raman band can be calculated by using the standered relationship

$$I_{iso}(\tilde{\nu}) = I_{VV}(\tilde{\nu}) - \frac{4}{3} I_{VH}(\tilde{\nu}) \qquad 3.9.10$$

$$I_{aniso}(\tilde{\nu}) = I_{VH}(\tilde{\nu}) \qquad 3.9.11$$

REFERENCES

1. Instruction manual for Liconix Model 4240 He-Cd Laser (1982).

2. Operation and maintainance instruction manual for SPEX Model 1403 Spectrometer (1982).

3. H. A. Strobel, *Chemical Instrumentation, pp. 320-327* Addison - Wesley, Mass, (1973).

4. C. D. Allemand, *Applied Spectrsc.*, **24,** 348 (1970).

CHAPTER 4

Chapter 4

SOLVENT DEPENDENT ANISOTROPY SHIFT IN p-METHYLACETOPHENONE AND BENZALDEHYDE: ROLE OF REPULSIVE FORCES

INTRODUCTION

Raman bandshape analysis is relevant to understanding in detail the solute-solvent system especially at the microscopic level. The dependence of band width and frequency of Raman vibrational bands on environment provides useful information regarding the solute solvent interactions and intermolecular forces. The analysis of the Raman spectra of several molecular liquids indicates that the peak frequencies of the isotropic and anisotropic components of totally symmetric

mode do not coincide (non-coincidence effect)[1-10]. This anisotropy shift has been found in some liquids, to be as large as 10 cm^{-1} or even more. Several theoretical models have been proposed for the explanation of non-coincidence effect, notably by Wang and McHale[11,12], Fini and Mirone [13-15], Döge etal[16,17] and Logan[18-20]. The theory proposed by Wang and McHale has taken into account several mechanisms which contribute to the non-coincidence effect, such as hydrogen bonding, quadrupole-quadrupole coupling, dipole-dipole coupling and transition dipole-transition dipole $(\delta\mu/\delta Q)$[17,18,21,22] interactions. Logan's approach assumes non-coincidence effect to be the result of a resonant excitonic transfer of vibrational excitation between the same normal mode of different solute molecules. Mirone and coworkers hypothesised that the anisotropy shift is the result of microscopic local order in the liquid phase, owing to the strong interaction between permanent dipoles; which permits a vibrational coupling through neighbouring transition dipoles. The neighbouring molecules are oriented and form aggregates with a lifetime longer than the vibrational period. The difference between the peak frequencies are expected to give information on the intermolecular forces and liquid structure.

In the theory proposed by Mirone and coworkers macroscopic properties are involved to reproduce the behaviour of isotropic (I_{iso}) and

anisotropic (I_{aniso}) components on dilution of liquid under study. However, it is sometimes not possible to understand clearly the complicated nature of the processes involved in complex molecular systems on the basis of macroscopic perception of the solute-solvent system, as it is progressively diluted. In an attempt to have a detailed information about the processes involved in complex molecular systems, p-methyl acetophenone (PMA) and benzaldehyde (BH) molecules have been chosen by taking the C=O stretching vibration as the reference mode. The C=O stretching vibration of both PMA and BH is well isolated from other modes of vibration and the dipole moment is also concentrated on the C=O bond of the molecule.

2.EXPERIMENTAL:

The sample of PMA and BH and the solvents were obtained commercially and were used without further purification. Raman spectra of PMA and BH in different solvents were recorded in 90^o scattering geometry with a SPEX Ramalog 1403 double monochromator equipped with a cooled RCA 31034 photomultiplier and a photon counting arrangement. The spectrometer control and data processing were achieved with the help of DM-3000 software. Excitation wavelength of 4416 Åprovided by a liconix model 4240 He-Cd laser was

used for BH and that of 4880 Åprovided by Spectra Physics model 165 Ar^+ laser was used for PMA. The liquid sample was taken in a quartz cell [(2-3)ml] and the laser beam was made to strike at the bottom of the cell very near to its perimeter. The reported Raman spectral measurements are accurate to $\pm 0.5\ cm^{-1}$. Other spectral conditions were adjusted to get the best possible spectra. The isotropic component was obtained by using the formula

$$I_{iso}(\tilde{\nu}) = I_{VV}(\tilde{\nu}) - \frac{4}{3} I_{VH}(\tilde{\nu}) \qquad 4.2.1$$

and

$$I_{aniso}(\tilde{\nu}) = I_{VH}(\tilde{\nu}) \qquad 4.2.2$$

where $I_{VV}(\tilde{\nu})$ and $I_{VH}(\tilde{\nu})$ represent the polarized and depolarized Raman spectra respectively. $\tilde{\nu}$ is the frequency in wave number.

The dielectric constant of PMA and BH were obtained experimentally using DM01 (WTW GmbH, Germany) dipolemeter equipped with a cylindrical gold plated condenser cell (Type DFL2). The neat liquid was placed in the cell and the instrument was operated on a superposition (beat) method with a measuring sensitivity of $\Delta\epsilon = 10^{-5}$. The temperature of the liquid in the cell was maintained by an internal thermostat at 20°C (293 K).

3.RESULTS AND DISCUSSION:

The non-coincidence effect is the phenomenon where the peak frequencies of the isotropic (iso) and the anisotropic (aniso) components of Raman bands do not coincide. The frequency difference $\Delta\tilde{\nu}$ is defined by the equation

$$\Delta\tilde{\nu} = \tilde{\nu}_{aniso} - \tilde{\nu}_{iso} \qquad 4.3.1$$

The Raman spectra of pure PMA and BH show the I_{iso} and I_{aniso} components with the peak of I_{aniso} component shifted to a higher frequency position (Figs.4.1a and 4.1b). In the present work,the band profiles have been assumed to be symmetric and in this case the first moment and the peak position of a band coincide.

The origin of the non-coincidence effect in liquid polar molecules is mainly due to the orientationally dependent intermolecular forces. The intermolecular forces modulate the vibration of a symmetrical mode and split into in phase and out-of-phase components. The isotropic component of vibration is governed by the angular independent inter- and intra-molecular potentials, whereas the anisotropic component of vibration is affected by angular dependent inter- and intra-molecular forces. The bands corresponding to isotropic and anisotropic components differ not only in the shape, but also in the

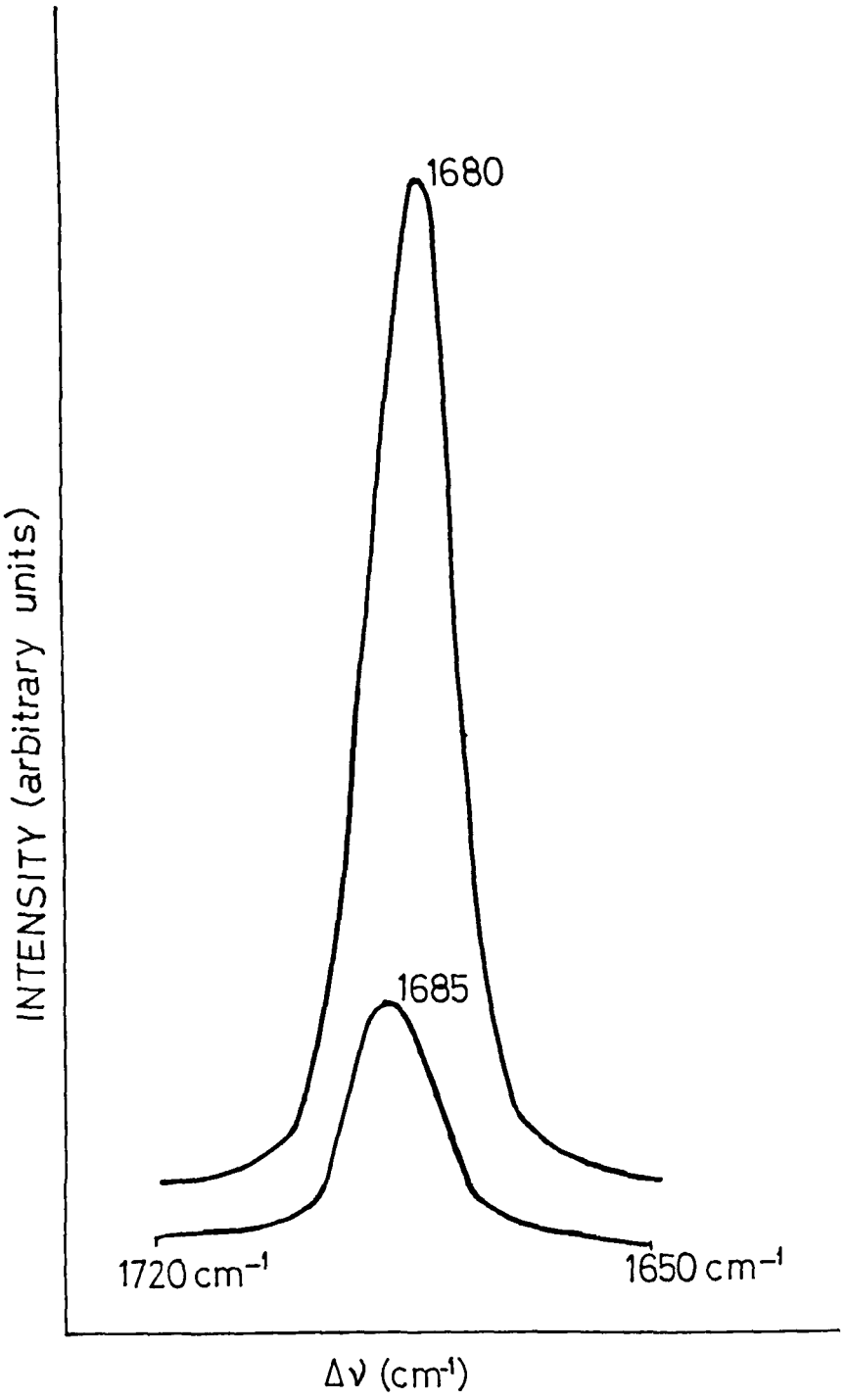

Fig.4.1(a) Raman Spectra of pure PMA

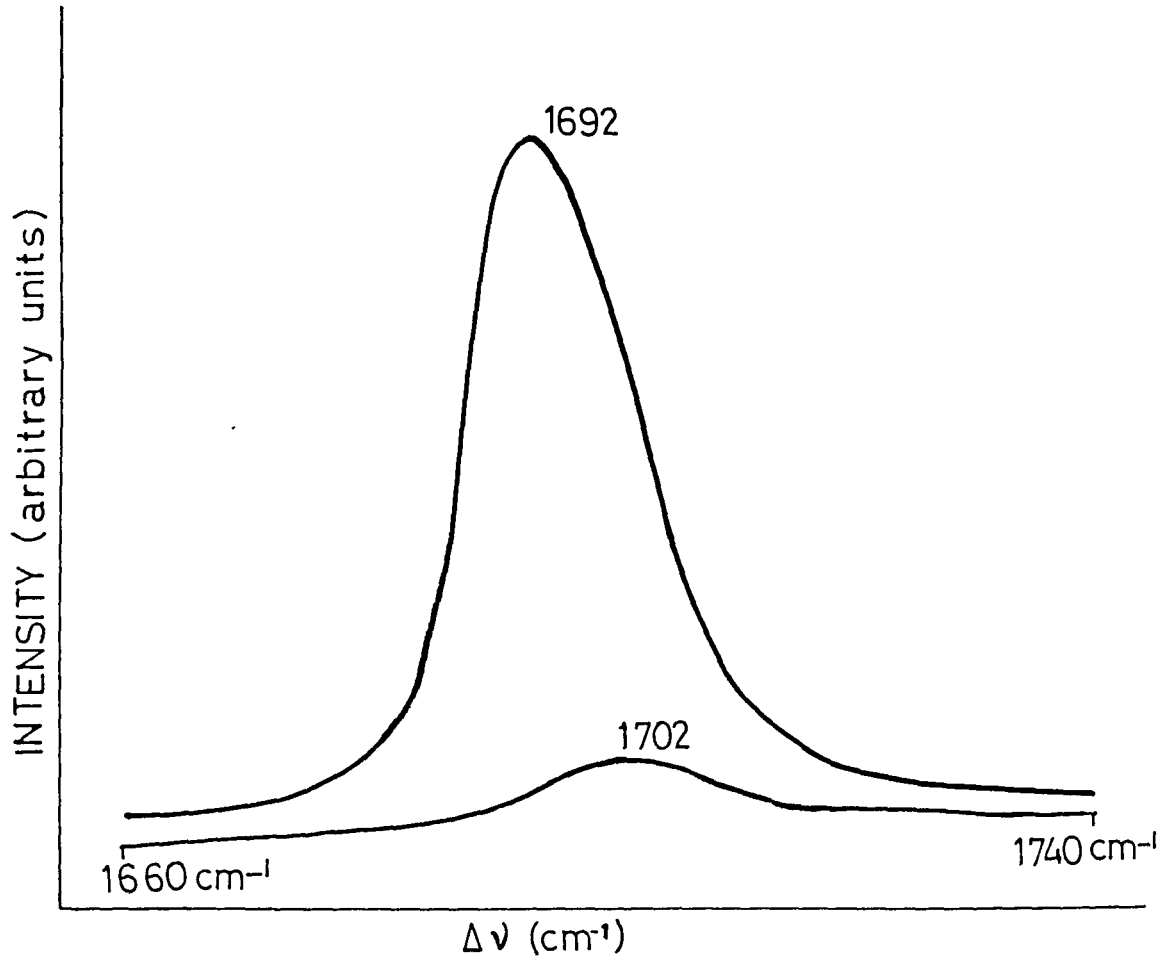

Fig.4.1(b) Raman spectra of pure BH

peak frequencies The non-coincidence effect is mostly associated with symmetric vibrational modes of polar molecules and is very pronounced for the modes which have strong IR band. In case of polar modes vibrational resonance coupling due to transition dipole-transition dipole (TD-TD) interaction may be the most important mechanism for perturbation of vibration. However, induction forces and dispersion forces etc. may also be important. The differences between the peak frequencies are expected to give information on the intermolecular forces and liquid structure.

The non-coincidence of the isotropic and anisotropic frequency maxima may be explained by taking into consideration the resonant coupling due to transition dipole - transition dipole (TD-TD) interactions of the vibrations of two adjacent molecules. The study of the non-coincidence effect needs considerations of the influence of the intermolecular forces, viz., dispersion forces, induction forces, and multipole-multipole interactions. The dispersion type of interactions usually explain the general additive attractions between arbitrary atoms and molecules. The dispersion energy has higher value even in the case of solvent molecules having a dipole moment, which is

mainly because of ϵ^{-2} dependence of the dipole-dipole and the dipole-induced dipole type of interactions for the solvents of high dielectric constant. The contributions to the observations due to induction forces are supposed to be present in both types of systems as a result of the dipolarity of the solute molecules under investigation, even for non-dipolar solvent molecules . The polarity of the solvent is also an important factor as it contributes to the potential field perturbing the vibration. This is particularly true at high dilution. The explanation that the anisotropy shift is an effect due to resonant coupling is supported by the experimental data related to the effect of solvent on the Raman band of PMA and BH molecules. This effect tends to vanish at high concentration of the solvents (Fig.4.2 and Fig. 4.3). The separation between the isotropic and anisotropic maxima of the Raman bands in different solvents varies with the concentration of the active substance.

If it is possible to separate the vibrational degrees of freedom from degrees of freedom of bath, because of the separation in frequencies, the vibrations will respond almost adiabatically to the changes in the environment. The coupling potential V can be expanded in a Taylor

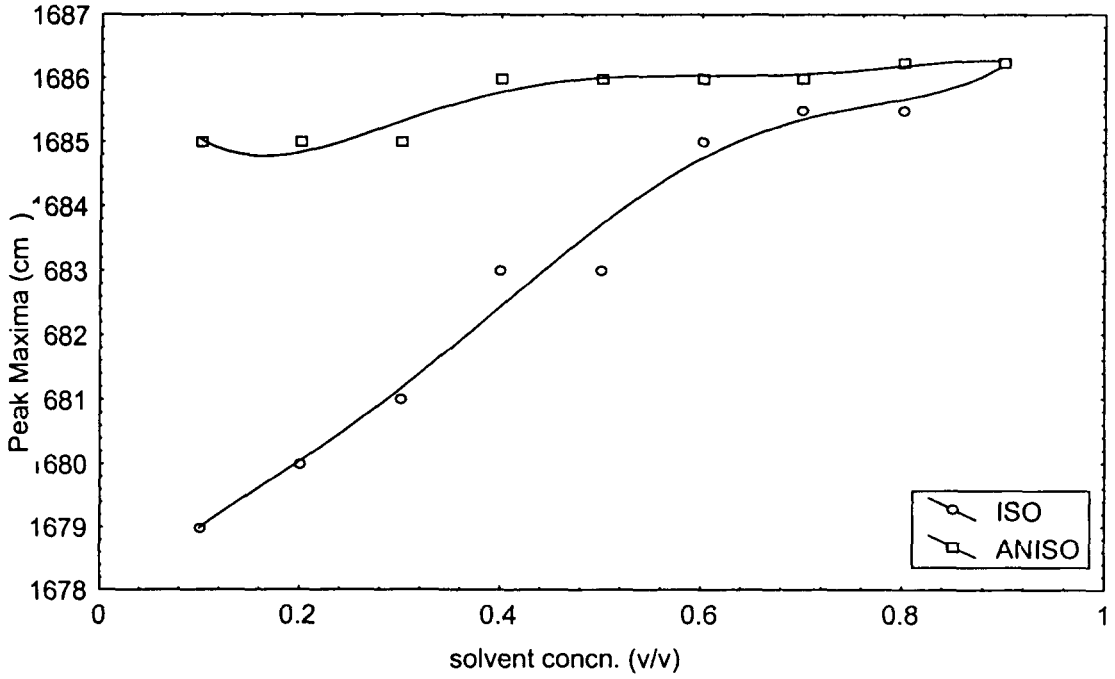

Fig. 4.2a. PMA in C_6H_6

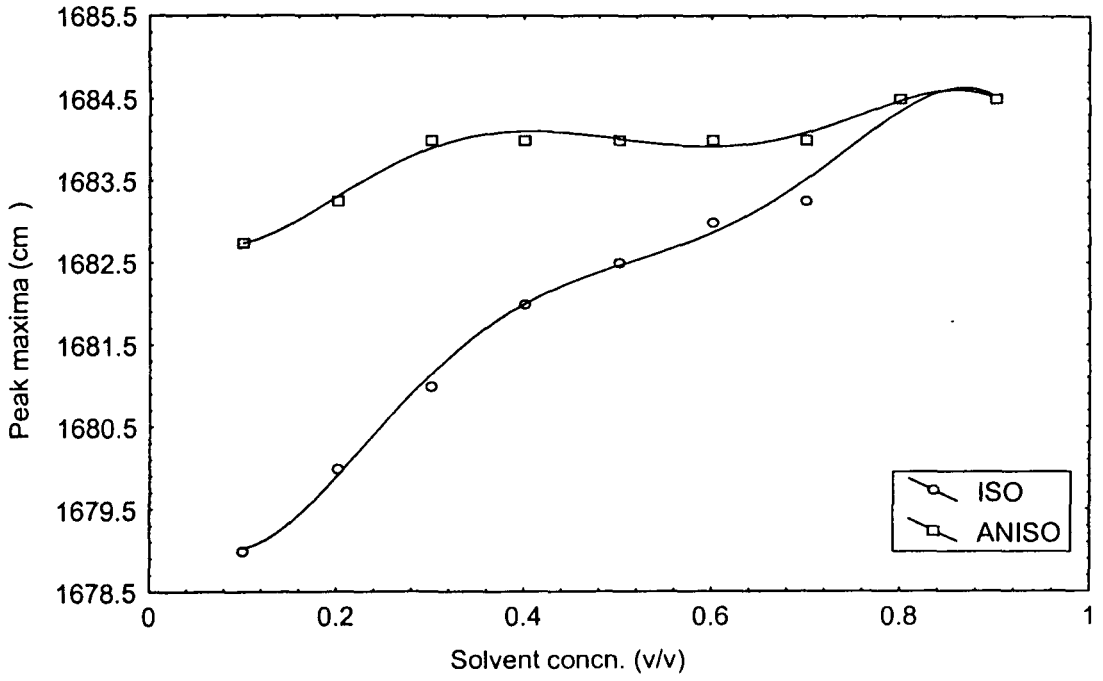

Fig. 4.2b. PMA in CCl_4

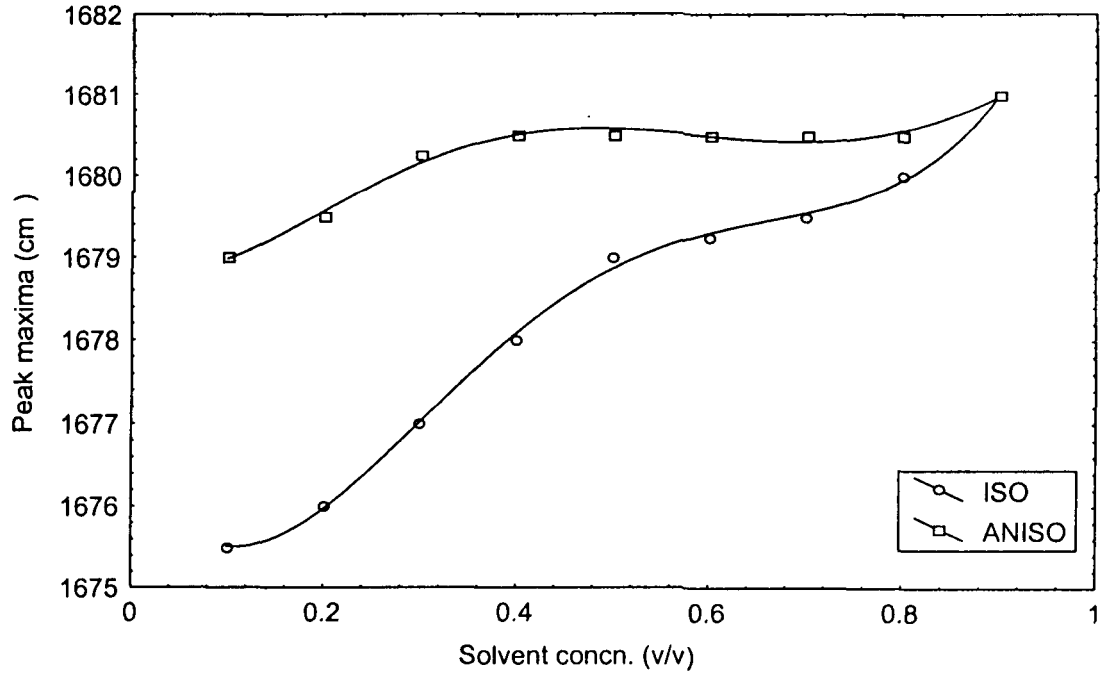

Fig. 4.2c. PMA in $CHCl_3$

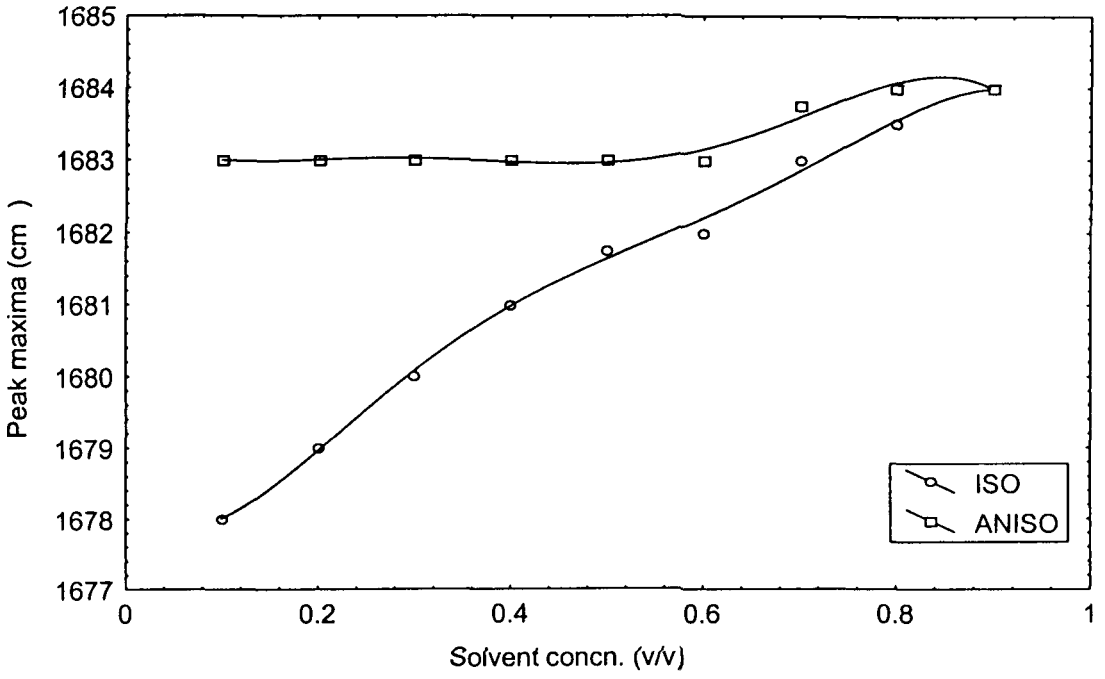

Fig. 4.2d. PMA in CH_3CN

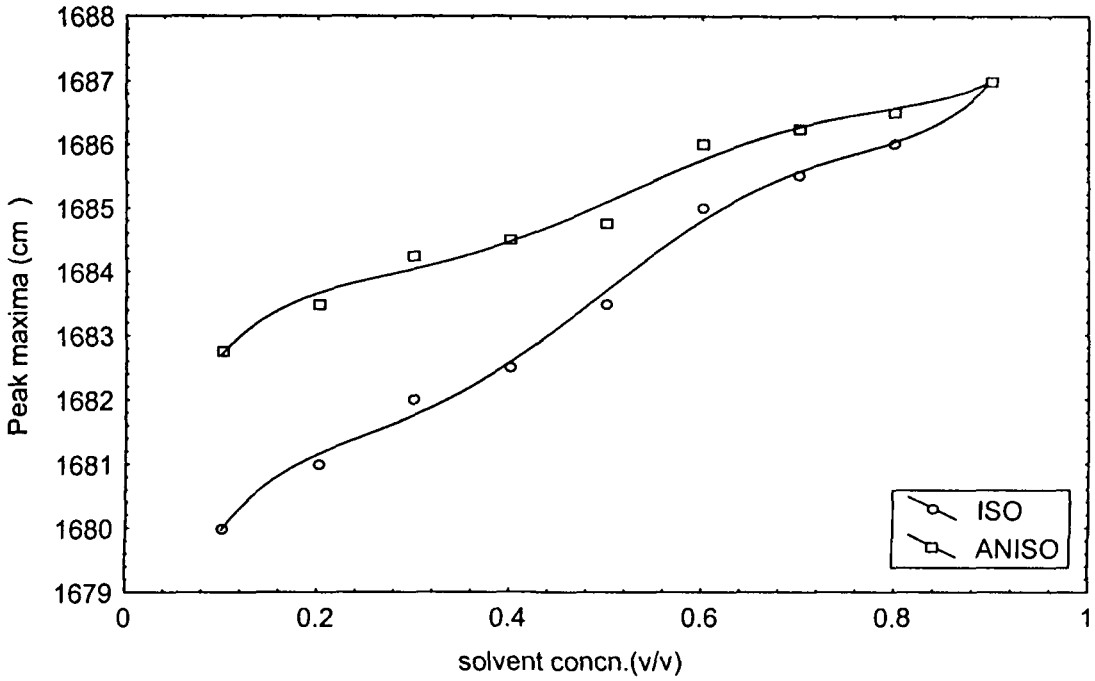

Fig. 4.2e. PMA in CH_2Cl_2

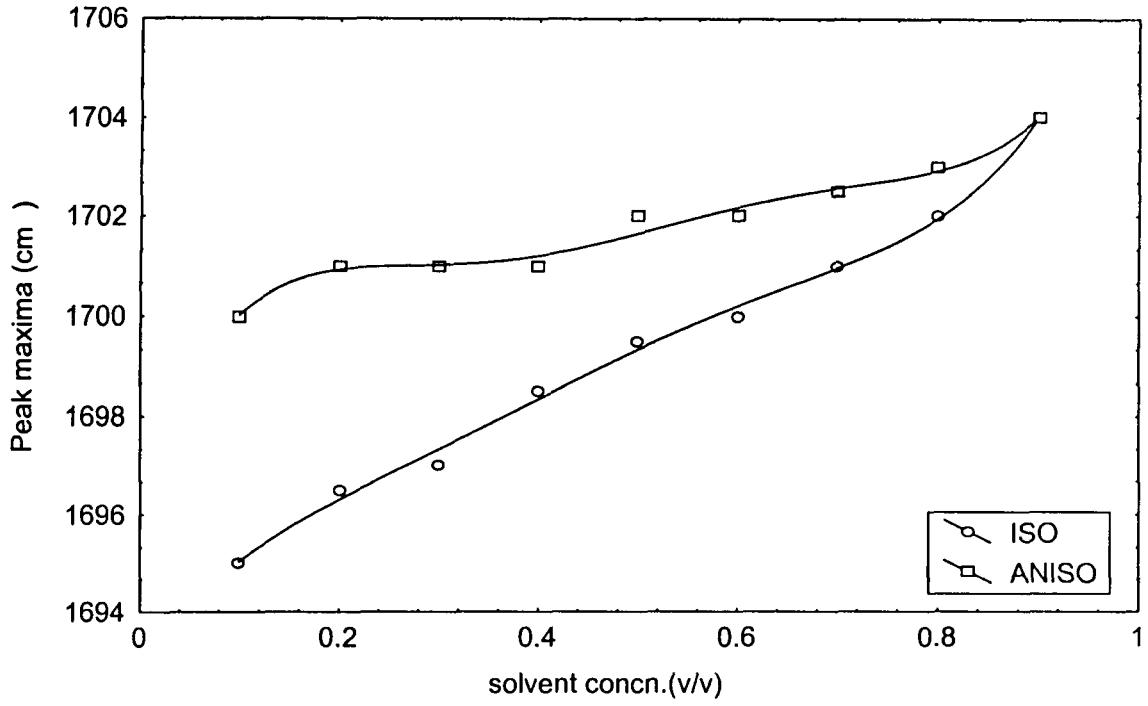

Fig. 4.3a. BH in C_6H_6

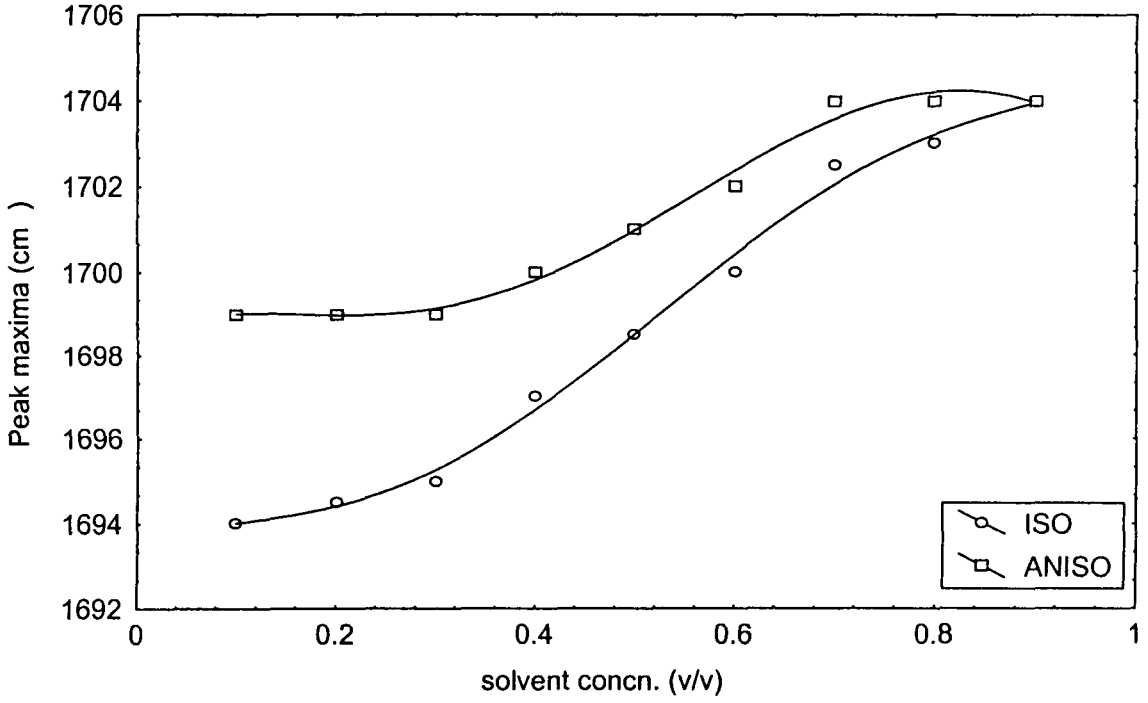

Fig. 4.3b. BH in CCl_4

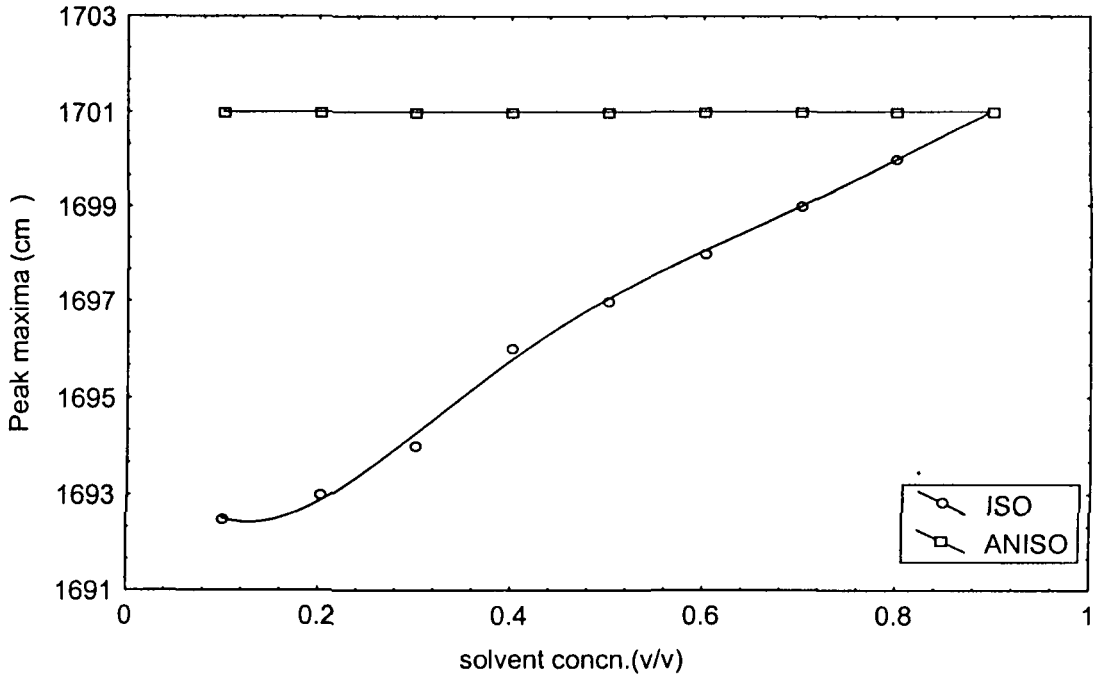

Fig. 4.3c. BH in $CHCl_3$

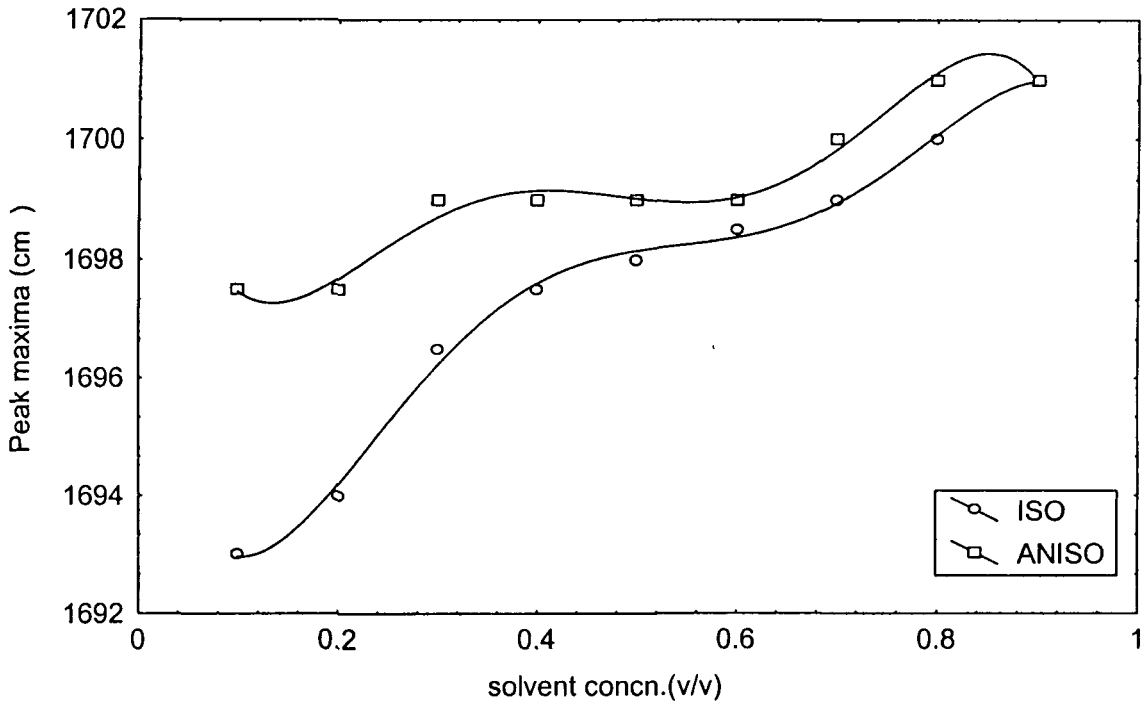

Fig.-4.3d. BH in CH_3CN

series in vibrational coordinates.

$$V = V_0 + \left(\frac{\delta V}{\delta Q_i}\right)_{Q_{i=0}} Q_i + \frac{1}{2}\left(\frac{\delta^2 V}{\delta Q_i^2}\right)_{Q_{i=0}} Q_i^2 + ... \qquad 4.3.2$$

The last term in the above expression is responsible for resonance energy transfer and leads to anisotropy shift or non-coincidence effect. Since $V << H_0$, where H_0 is the Hamiltonian for the vibrational degrees of freedom, the first order perturbation calculation for energy difference (leading to frequency difference) between the ground and first excited states leads to the expression (2.1.9). The main interaction term that couples the fundamentals of the νth mode of the molecules i and j can be written as[3,8–10,22],

$$\Delta E_{res} = \frac{\delta^2 V_{ij}}{\delta Q_i \delta Q_j} Q_{01_i} Q_{01_j} \qquad 4.3.3$$

where $Q_{01} = \langle 1|Q|0\rangle$ is the expectation value of the normal coordinate in the transition state. For transition dipole-transition dipole (TD-TD) interaction,

$$\Delta E_{(TD-TD)} = \left(\frac{\delta \mu}{\delta Q}\right)^2 \left\langle \frac{k_{ij}}{R_{ij}^3} \right\rangle (\langle 1|Q|0\rangle)^2 \qquad 4.3.4$$

For PMA and BH , the dipole-dipole interaction predominates in the liquid phase as far as C=O mode is concerned. Considering only

pair interactions and the first order term, the frequency shift is expressed by the proportionality relationship

$$\Delta\tilde{\nu} \propto \left(\frac{K_{ij}}{R_{ij}^3}\right)\left(\frac{\delta\mu}{\delta Q}\right)^2 \qquad 4.4.5$$

where R_{ij} is the distance between the molecules and K_{ij} is a factor describing the relative orientation of the two dipole moment vectors. This term is responsible for the splitting factor due to dipole-dipole coupling and the coupling potential V was given by

$$V = \left(\frac{\mu_i\mu_j}{R_{ij}^3}\right) K_{ij} \qquad 4.3.6$$

The coupling potential may originate from various interactions such as dipole-dipole, transition dipole-transition dipole (TD-TD), hydrogen bonding etc.

If a vibrational mode of an active material interacts with the same mode of an identical neighbouring molecule, this is called resonant intermolecular vibrational coupling. Then the pair of interacting active molecules vibrate in-phase or out-of-phase. In case of an out-of-phase motion the isotropic part of the transition probability tensor of the molecular pair vanishes. The in-phase mode has a transition probability for isotropic as well as anisotropic Raman scattering, whereas

the out-of-phase mode contributes only to the latter.

If we consider dipole-dipole coupling to be responsible for the interactions leading to orientational order between the molecules of PMA or BH, this causes a splitting of the vibrational mode into an in-phase and out-of-phase vibrations. The frequency of the completely polarized (in-phase) vibration corresponds to the band centre of the isotropic component whereas the frequency of the depolarized (out-of-phase) vibration is nearly equal to the centre of the anisotropic band. It was shown by McHale that the anisotropy shift $\Delta\tilde{\nu}$ can be expressed by the relation[12]

$$\Delta\tilde{\nu} = \frac{2\mu^2 \left(\frac{\delta\mu}{\delta Q}\right)_0^2 N_0}{25\pi^2 c^2 \tilde{\nu}_0 kT d^3 V_M} \Phi \frac{1}{\epsilon^2} \qquad 4.3.7$$

where N_0 is Avogadro's number, Φ is the volume fraction of the solute, $\tilde{\nu}_0$ is the vibrational frequency of the isolated molecule, d is the minimum intermolecular distance, V_M is the molar volume of the solute, kT is the thermal energy, μ is the dipole moment, Q is the mass weighted normal coordinate and $\left(\frac{\delta\mu}{\delta Q}\right)_0$ is the transition moment. The term $\frac{1}{\epsilon^2}$ may be considered as the screening factor S, i.e.,

$$S = \frac{1}{\epsilon^2}$$

The expression for $\Delta\tilde{\nu}$ then becomes

$$\Delta\tilde{\nu} = \frac{2\mu^2 \left(\frac{\delta\mu}{\delta Q}\right)_0^2 N_0}{25\pi^2 c^2 \tilde{\nu}_0 kT d^3 V_M} \Phi S \qquad 4.3.8$$

According to Giorgini *et al*[23], the screening factor S comprises two factors, S_p and S_t, related to the interaction of permanent and transition dipoles[15].The first term is given by

$$S_p = \left(\frac{n^2+2}{2\epsilon + n^2}\right)^2 \epsilon$$

and the second term is given by

$$S_t = \left(\frac{\left[n^2+2\right]^2}{9n^2}\right)$$

which comes after substituting $\epsilon = n^2$. Here ϵ is the dielectric constant of the medium and n is the refractive index of the solute. Since the refractive index does not vary much with the variation of the solvent, the term S_t may be considered to be constant. Therefore considering only the term S_p and following the dielectric model given by Onsager-Frölich, which treats the dielectric as continuum, the equation for $\Delta\tilde{\nu}$

takes the form

$$\Delta\tilde{\nu}\left(2\epsilon+n^2\right)^2\epsilon^{-1}=\frac{2\mu^2\left(\frac{\delta\mu}{\delta Q}\right)_0^2\left[n^2+2\right]^2N_0}{25\pi^2c^2\tilde{\nu}_0kTd^3V_M}\Phi \qquad 4.3.9$$

The quantity $\left(\frac{\delta\mu}{\delta Q}\right)_0^2$ is proportional to IR band intensity and the Raman band corrsponding to IR band for PMA and BH molecules under study are very strong which indicates that the splitting factor for these molecules should be quite large.

The vibrational frequencies of peak maxima for I_{VV} and I_{VH} components of C=O stretching mode of both PMA and BH were measured in case of pure liquid as well as when dissolved in different solvents, both polar and nonpolar. The experimental results in case of neat liquid show the non-coincidence of the isotropic and anisotropic frequency maxima of the order of 5 cm^{-1} in case of PMA (Fig4.1a) and that of 10 cm^{-1} in case of BH (Fig.4.1b). When dissolved in different solvents the separation between the isotropic and anisotropic peak maxima of the Raman bands varies with the concentration of the active substance and tends to vanish at high concentration of the solvent

As the concentration of the solvent is increased, the observed peak frequencies of both isotropic and anisotropic bands appear at higher

frequencies (commonly known as blue shift) which is attributed to attractive intermolecular forces.The frequency shift and the non-coincidence effect may be explained by taking into account the resonant coupling due to transition dipole-transition dipole interactions of the vibrations of two adjacent molecules.

The dielectric constant of PMA and BH were experimentally measured and found to be 16.25 and 17 respectively. The dielectric constant of the solution was calculated by using the relation

$$\epsilon_{solution} = \Phi.\epsilon_{solute} + (1 - \Phi).\epsilon_{solvent} \qquad 4.3.10$$

The quantity $F = \Delta\tilde{\nu}\left(2\epsilon + n^2\right)^2 \epsilon^{-1}$ was plotted as a function of the volume fraction Φ in different solvents (Fig.4.4a and 4.5a). The figures clearly show that the data points do not lie on a stright line for the entire range of dilution. It is, however, seen that the data points fit rather well in two straight lines with a discontinuity around $\Phi = 0.5$ in case of PMA dissolved in various solvents. In case of BH dissolved in various solvents the discontinuity arises around $\Phi = 0.6$. This discontinuity may be due to the structure breaking effect and local fluctuations[23,24] in liquid solution. The plot in the Fig.4.3a may be described by the non-linear relationship

$$F(\Phi) = \Lambda(\Phi_0 - \Phi)F_1 + F_2\Lambda(\Phi - \Phi_0) \qquad 4.3.12$$

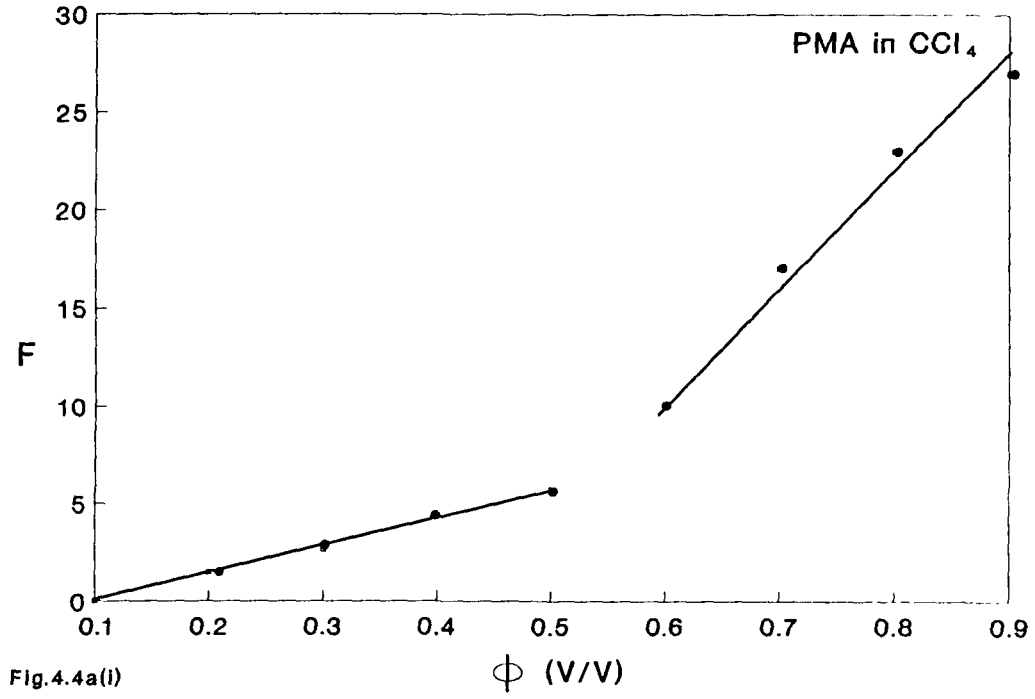

Fig.4.4a(I)

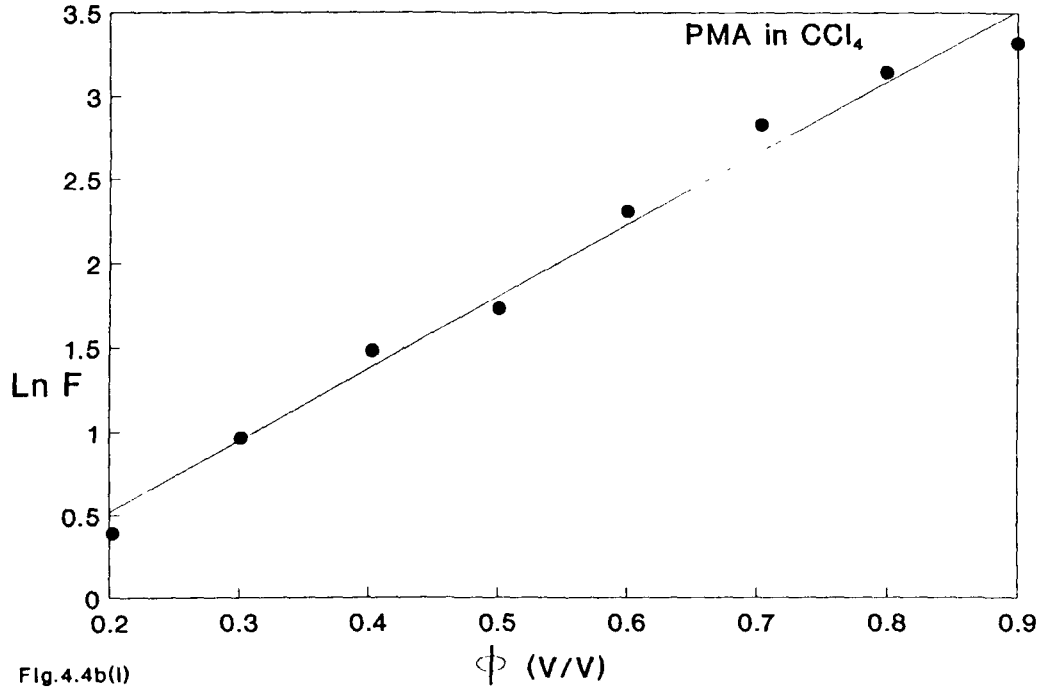

Fig.4.4b(I)

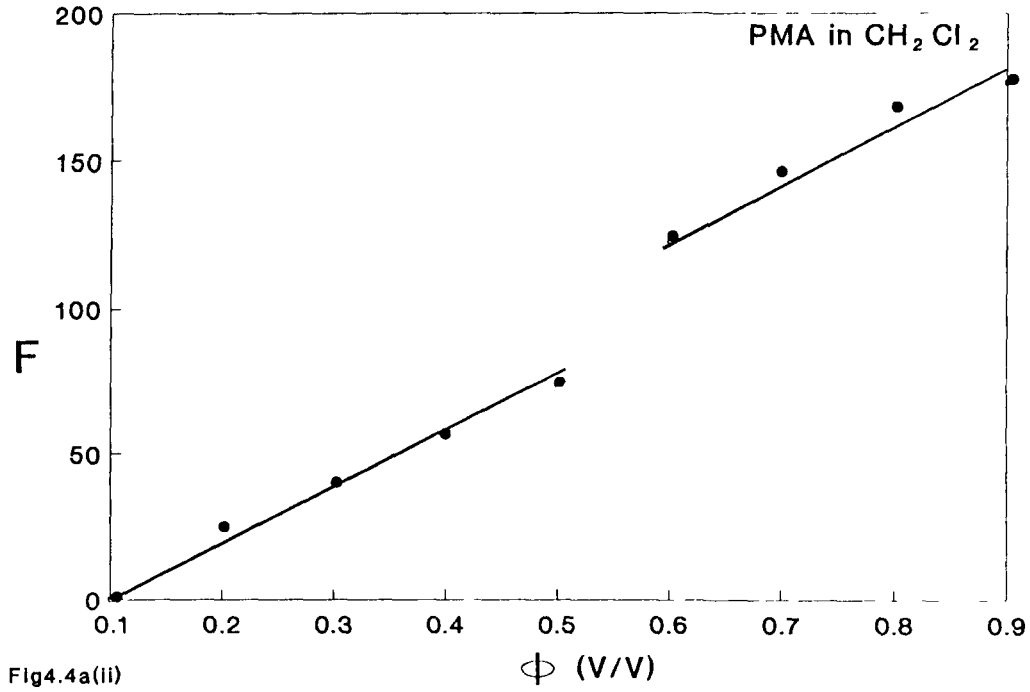

Fig4.4a(ii)

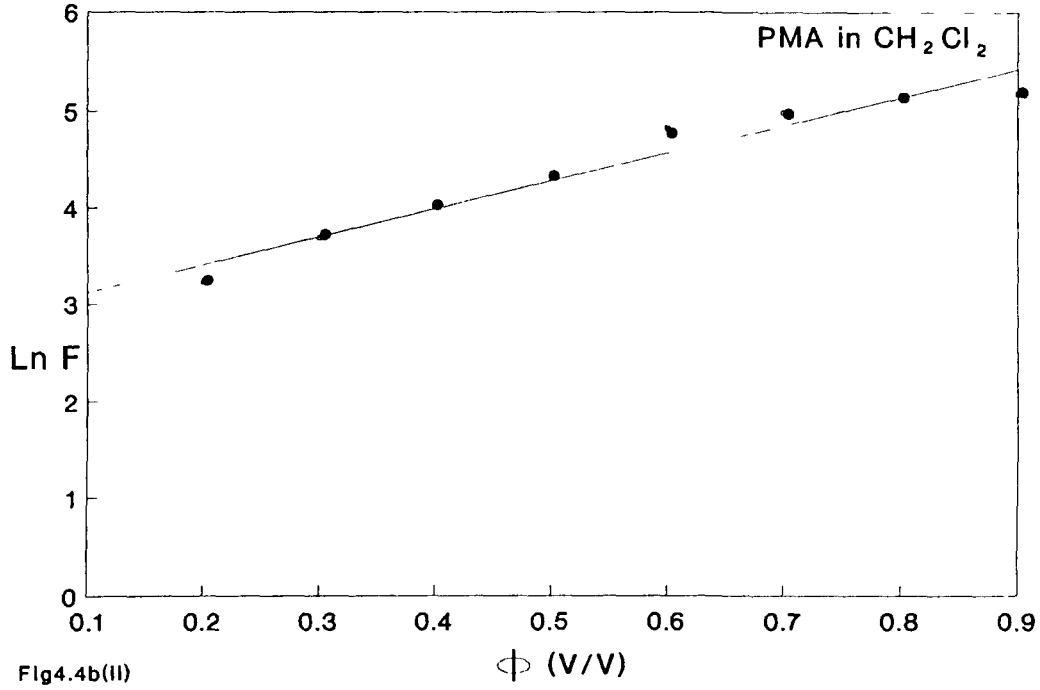

Fig4.4b(ii)

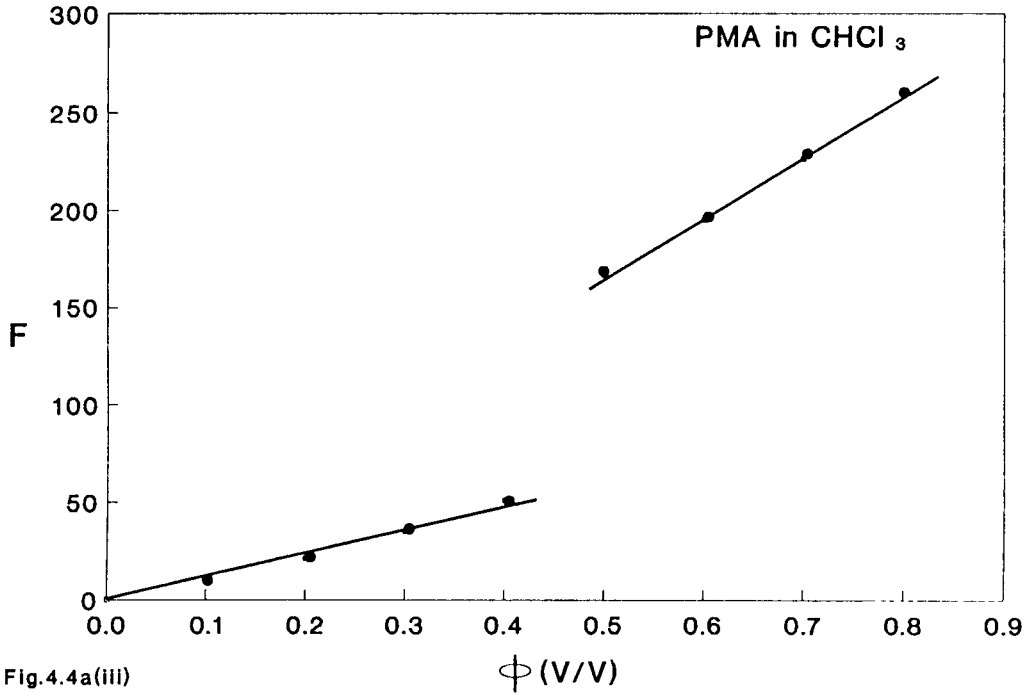

Fig.4.4a(iii)

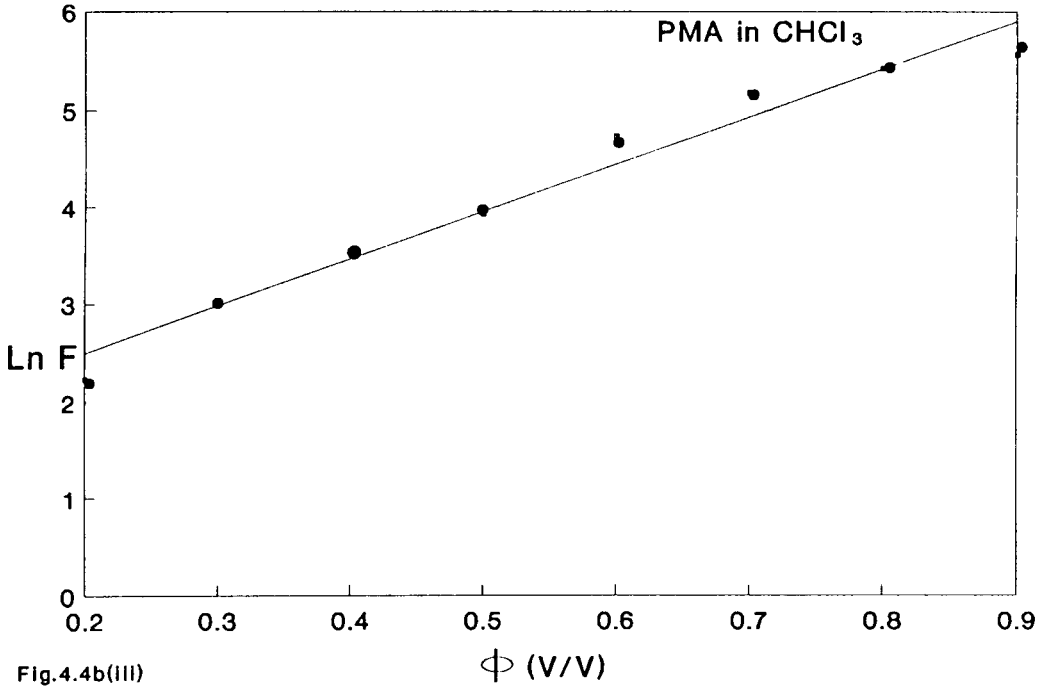

Fig.4.4b(iii)

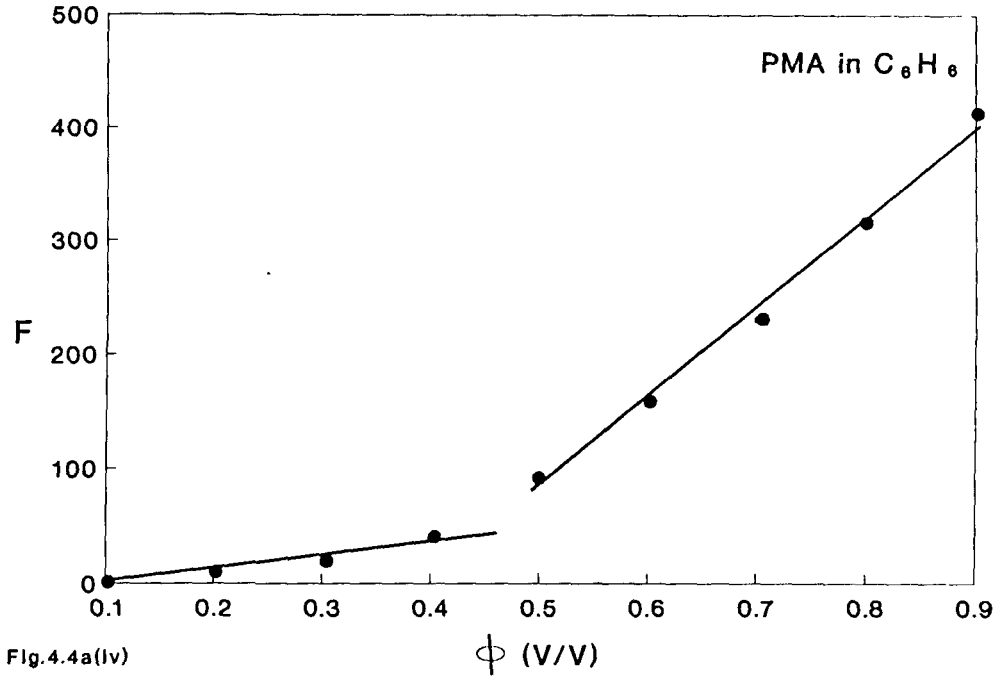

Fig.4.4a(iv)

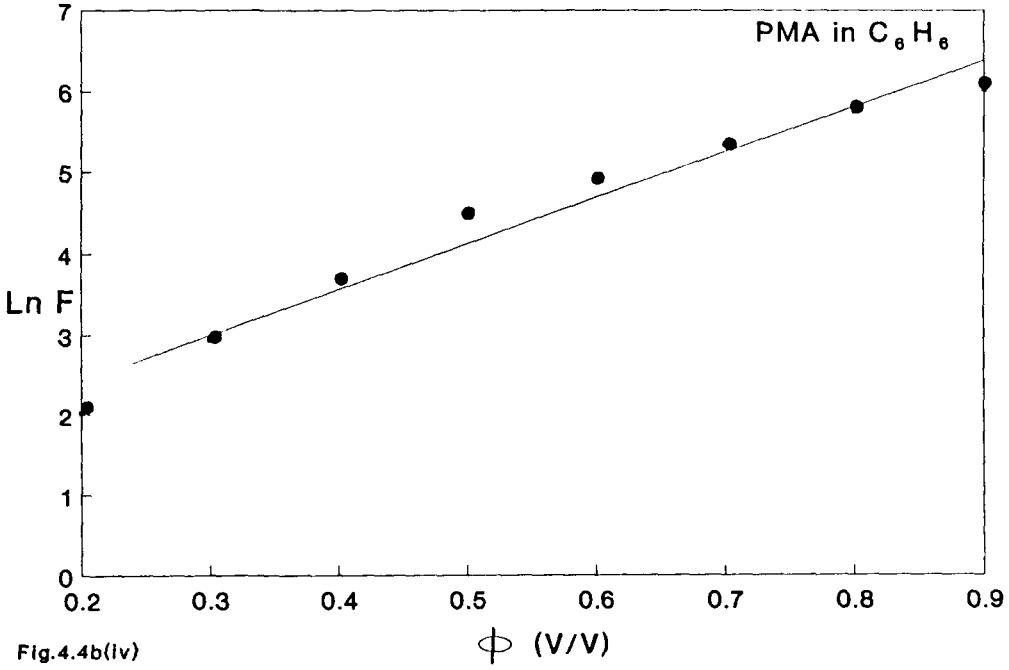

Fig.4.4b(iv)

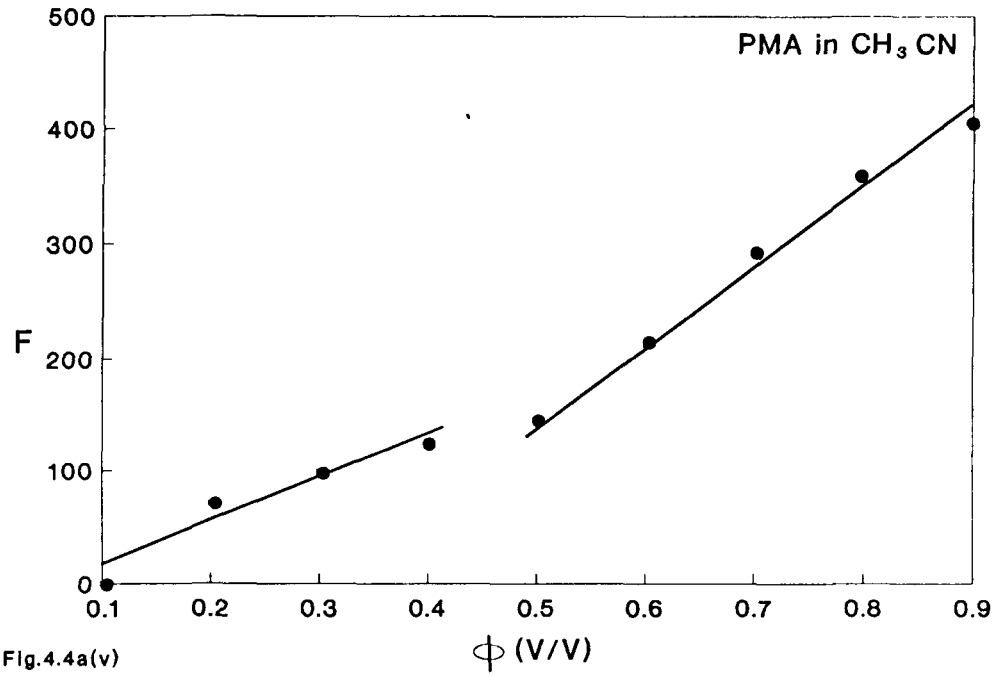

Fig.4.4a(v)

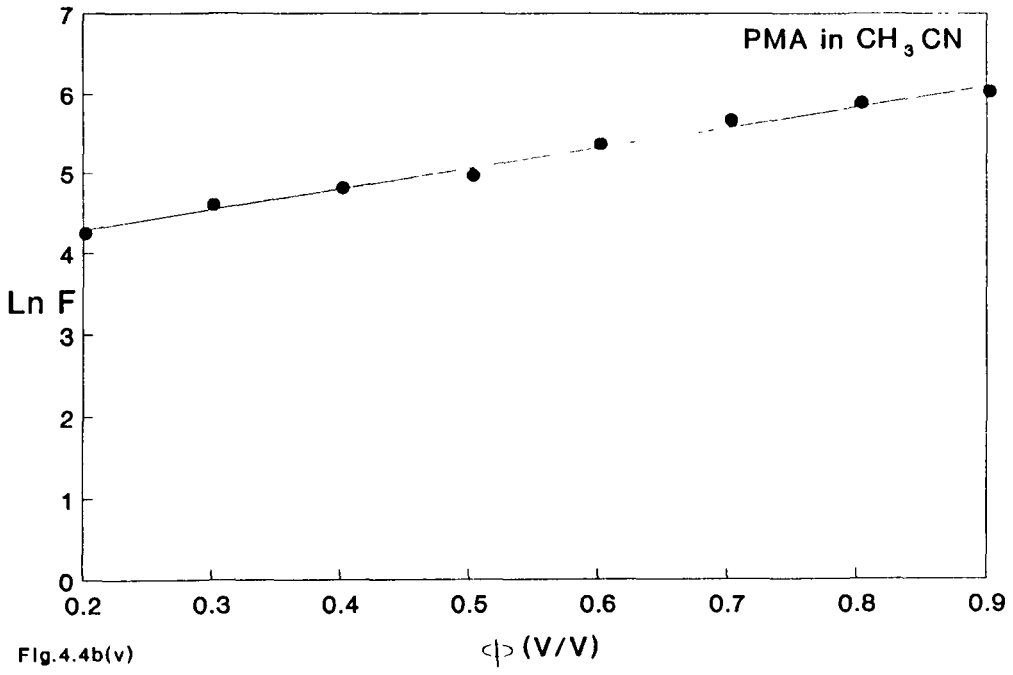

Fig.4.4b(v)

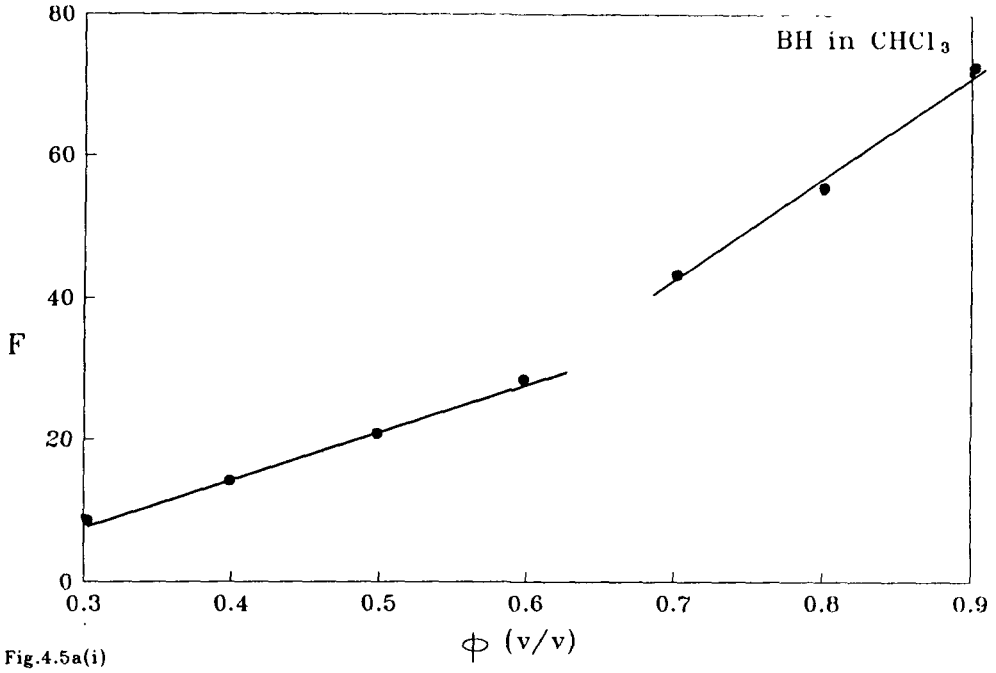

Fig.4.5a(i)

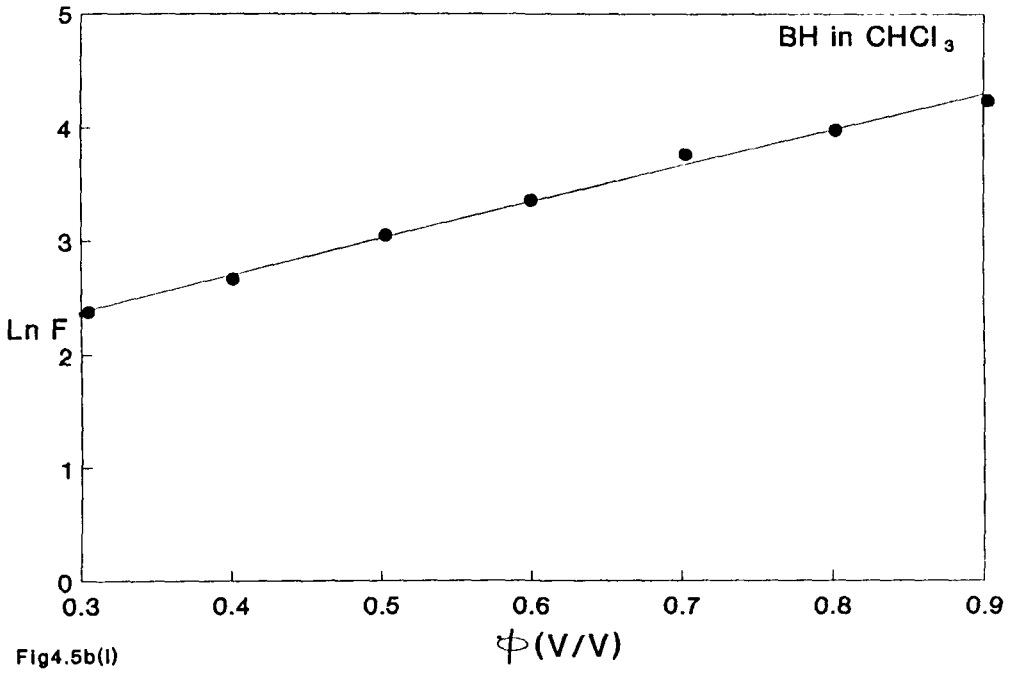

Fig4.5b(I)

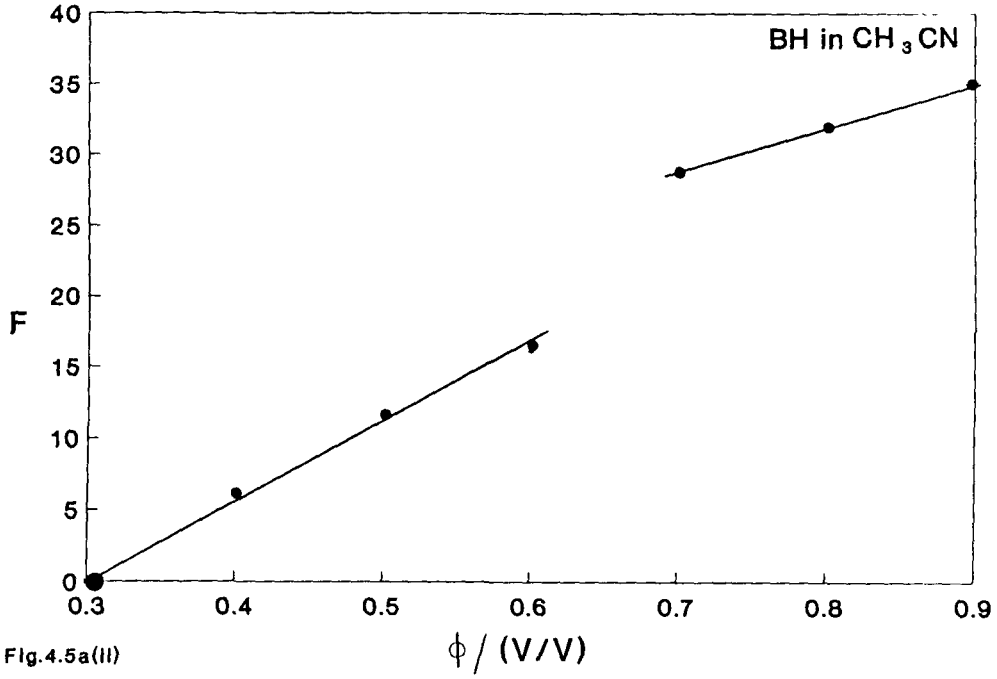

Flg.4.5a(II)

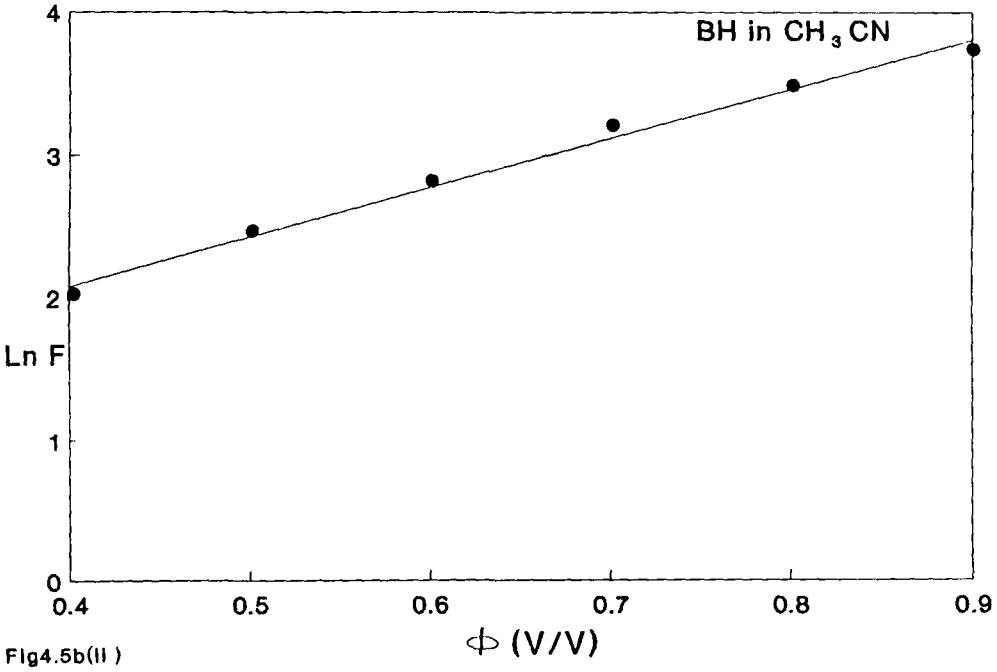

Flg4.5b(II)

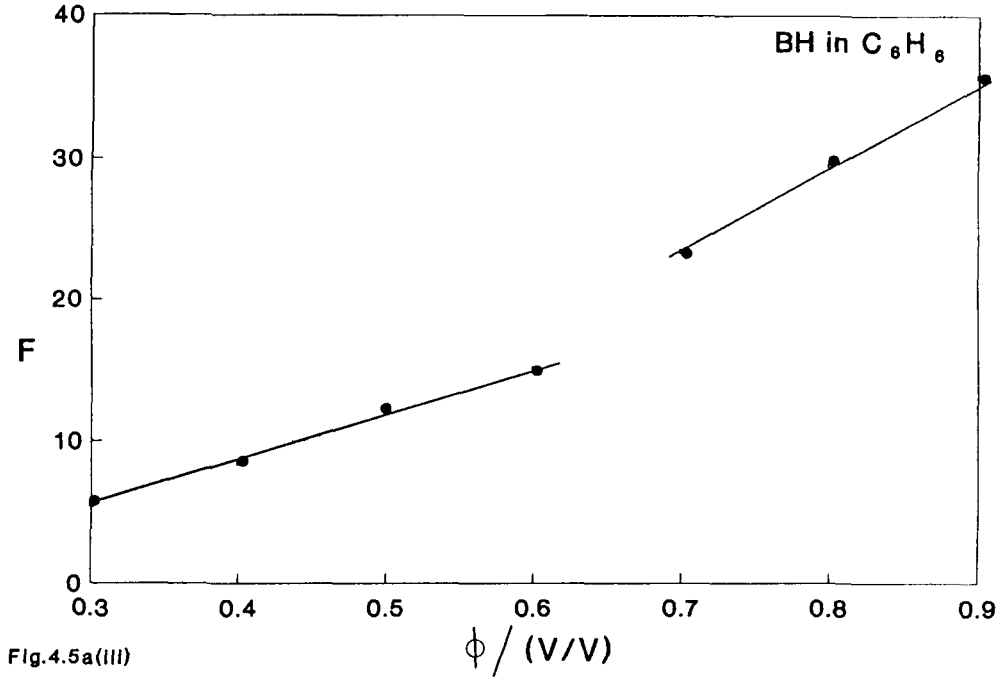

Fig.4.5a(III)

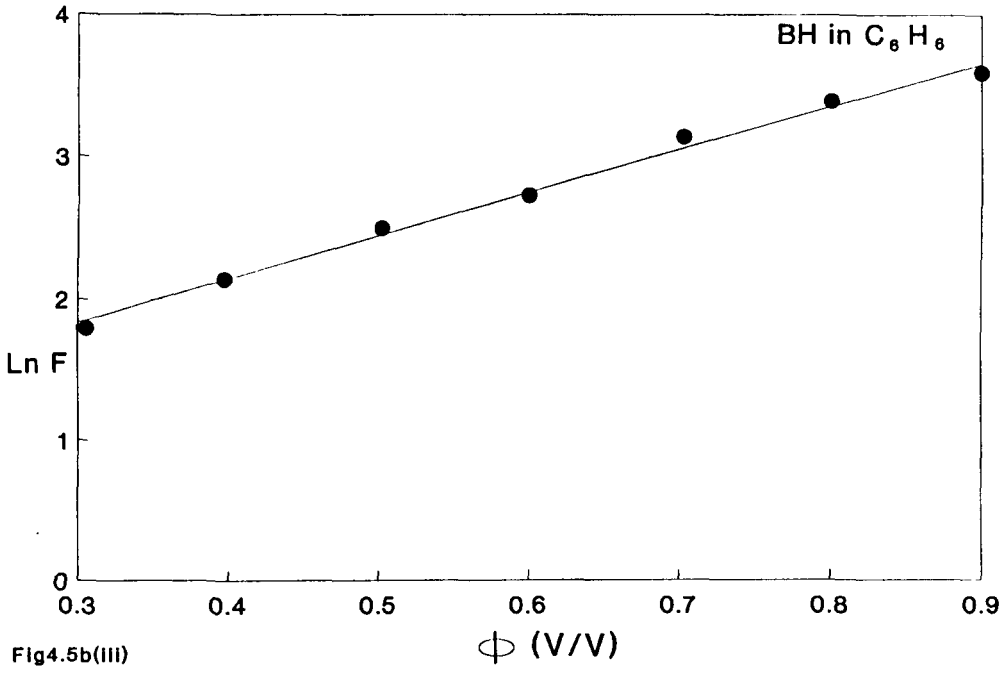

Fig4.5b(III)

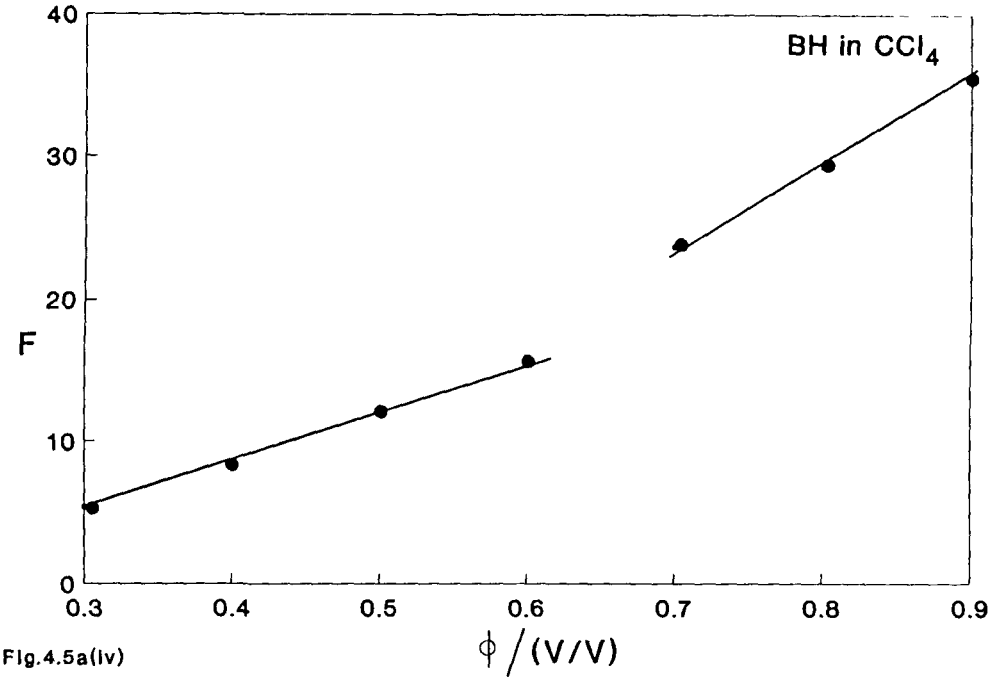

Fig.4.5a(iv)

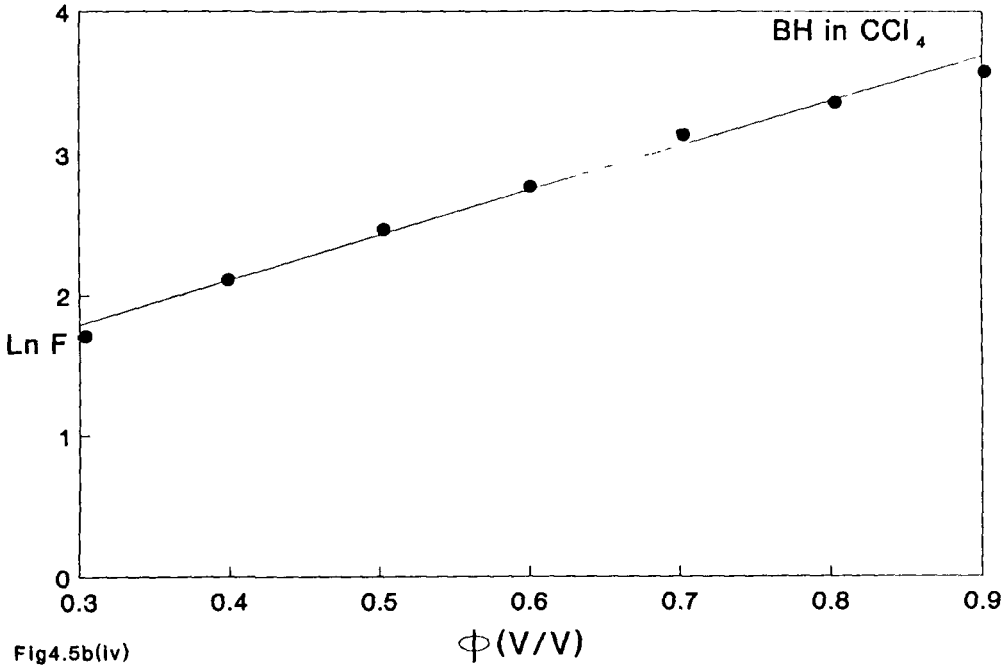

Fig4.5b(iv)

where $\Phi_0 = 0.6$. The splitting given by equation (4.3.9) was predicted by the TD coupling model and this expression was expected to be valid only for dilute solutions. At higher solute concentration the interactions are expected to occur more among solute molecules than solute-solvent interactions. The present study indicates that in order to explain the non-coincidence effect in complex molecular systems like PMA and BH, where the effects of dispersion interaction, multipolar interaction etc. are likely to vary from solvent to solvent, the screening effect may not be as effective as envisaged by the Onsager-Fröhlich model.The theories which use the continuum approach for the environment of the molecules may not be applicable as such. Therefore the methods of statistical mechanics may be used which provide a way of obtaining microscopic quantities when the properties of the molecules and the molecular interactions are known. In statistical mechanical theories of dielectric constant, simplified models are often used for the molecules and the intermolecular forces. For example, a molecule is represented by an ideal dipole at the centre of a dielectric sphere and the molecular interaction is taken to follow a hard sphere of Lennard-Jones potential.

However, the plot of the quantity lnF vs. Φ shows a linear graph as shown in Figs.4.4b and 4.5b. This kind of relationship whereby

a lnF vs. Φ graph has been found to be linear may be indicative of the repulsive potential function[26] of the type $e^{-\alpha R}$ playing an important role. Here R is the appropriate distance of closest approach and depends upon the fraction of the solute present and α is a constant. The different multipolar interactions which are repulsive in nature may be playing a significant role in such complex molecular systems containing benzene ring. For such cases where the permanent monopole, dipole and quadrupole effects need to be considered, the interaction potential may be given by the equation (2.5.8). Moreover, when quadrupole moment is important, an induced dipole effect may also take place due to the molecular polarizability leading to induction forces.

For molecules with a non-spherical shape the short range repulsion between two non-overlapping atoms is modified significantly by the shape of the molecules. The molecular shape influences the preferred orientations by controlling the distance of closest approach. For specific molecules there are often additional competing interactions such as dispersion which may lead to preferred orientation different from those favoured purely electrostatically.

When the dipole sizes are comparable with those of solvent molecules,

the fundamental problem lies in the determination of an effective electric permittivity of the medium . The free energy dependence of the pair formed by the dipolar forces on solvent polarity is given by the equation

$$\Delta G_{or} = -\frac{\mu_i \mu_j}{\epsilon r^3} \left(1 + 3cos^2\theta\right)^{1/2} cos\phi \qquad 4.3.13$$

where θ denotes the angle between the dipole μ_i and the line linking the centres of the two dipoles and ϕ is the angle between μ_i and the direction of the electric field generated by the dipole μ_j on a position μ_i. The expected free energy dependence on the inverse of the permittivity is rather doubtful in such cases and the agreement between theory and experiment may not be very useful. This idea based on the assumption that in strongly polar solvents (with large electric permittivity) the interaction between dipoles contributes little to the interaction energy may, however, be used for the qualitative discussion of both inter- and intra-molecular interactions responsible for non-coincidence effect.

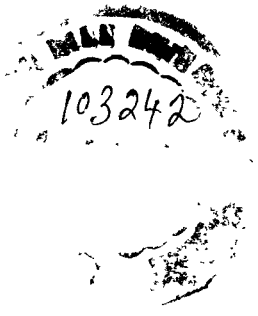

REFERENCES

1. H. D. Thomas and J. Jonas, *J. Chem. Phys.*,**90,** 4144 (1989).

2. H. D. Thomas and J. Jonas, *J. Chem. Phys.*,**90,** 4612 (1989).

3. W. Schindler, T. W. Zerda and J. Jonas, *J. Chem. Phys.*, **81,** 4306 (1984).

4. W. Schindler, P. T. Sharko and J. Jonas, *J. chem. Phys.*, **76,** 3493 (1982).

5. M. Shelley and J. Yarwood, *J. Chem. Phys.*, **137,** 277(1989).

6. V. M. Shelley, A. Talintyre, J. Yarwood and R. Buchner, *Faraday Discuss., Chem. Soc.*, **85** 211 (1988).

7. G. Fini and P. Mirone, *J. Chem. Phys.*, **79,** 639 (1983).

8. A. Purkayastha and K. Kumar, *Spectrochim. Acta,* **42A,** 1379 (1986).

9. A. Purkayastha and K. Kumar, *Spectrochim. Acta,* **43A,** 1269 (1987).

10 A Purkayastha and K. Kumar, *J. Raman Spectrosc.*, **22,** 721 (1991).

11. C. H. Wang and J. McHale, *J. Chem. Phys.*, **72,** 4039 (1980).

12. J. McHale, *J. Chem. Phys.*, **75,** 30 (1981).

13. G. Fini P. Mirone and B. Fortunato, *J. Chem. Soc., Faraday*

Trans., **1169**, 1243 (1973).

14. G. Fini and P. Mirone *J. Chem. Phys.*, **71**, 2241 (1979).

15. P. Mirone, *J. Chem. Phys.*, **77**, 2704 (1982).

16. G. Döge, R. Arndt and J. Yarwood, *Mol. Phys.*, **52**, 399 (1984).

17. G. Döge, D. Schneider and A. Morresi, *Mol. Phys.*, **80**, 525 (1993).

18. D. E. Logan, *Mol. Phys.*, **58(1)**, 79 (1986).

19. D.E. Logan, *J. Chem. Phys.*, **103**, 215 (1986).

20. D. E Logan, *J. Chem. Phys.*, **131**, 199 (1989).

21. S. Tarulli and E. J. Baran, *J. Raman Spectrosc.*, **26**, 139 (1995).

22. Z. Kecki and A. Sokolowska, *J. Raman Spectrosc.*, **27**, 429 (1996).

23. M. G. Giorgini, G. Fini and P. Mirone, *J. Chem. Phys.*, **79**, 639 (1983).

24. G. Tarjus and S. Bratos, *Mol. Phys.*, **42**, 307 (1981).

25. S. Bratos and G. Tarjus, *Phys. Rev. A*, **24**, 1591 (1981).

26. M. Karplus and R. N. Porter, *Atoms and Molecules, An Introduction for Students of Physical Chrmistry*, **pp.** 262-267, The Benjamin/Cummings Publishing Company, California (1970).

CHAPTER 5

Chapter 5

MICROENVIRONMENT DEPENDENCE OF VIBRATINAL RELAXATION IN p-METHYLACETOPHENONE AND BENZALDEHYDE

1.INTRODUCTION

The vibrational relaxation in molecular liquids has been the subject of many theoretical and experimental studies. Although considerable progress has been made towards a deeper understanding regarding the vibrational relaxation process in recent years[1], a detailed study is required to account for the discrete nature of the solute-solvent system at the microscopic level. This may involve the development of microscopic picture of the environment around the molecule. The

Raman band analysis especially the band width dependence on environment may provide useful information regarding the intermolecular forces. The vibrational relaxation process which is responsible for the broadening of the isotropic Raman component[2,3] may be due to the contribution from vibrational dephasing, population relaxation and resonant energy transfer via transition dipole - transition dipole (TD-TD) interactions[4–6]. Moreover, the microscopic environment affects the behaviour of a reference molecule. In a liquid mixture the bandshape of a reference mode is influenced by the concentration fluctuations of the environment.

The theoretical explanation for the vibrational relaxation may be given by correlating the vibrational relaxation rate (τ_v^{-1}) with some molecular parameter which takes into account the effect of reaction field (solvent electric field) on the solute[7], and using the basic concept of dielectric relaxation processes. To have a better picture of the solute-solvent systems one may consider the so called **solvent cage effect** where the molecules of a solute are confined in a potential well created by solvent molecules. The molecule is considered to be vibrating against its immediate neighbours, with an occassional escape to its adjacent position. The explanation for the vibrational relaxation process in complex molecular systems, cannot be understood only on

the basis of a macroscopic perception of the solute-solvent system. A marked difference is likely between the interacting situations in the pure solute and when it is dissolved in solvents, especially at high dilution. For detailed information about the relaxation processes involved in complex molecular systems, p-methylacetophenone (PMA) and benzaldehyde (BH) molecules have been chosen . The present work deals with the solvent dependent studies on the Raman band corresponding to C=O stretching vibration of these two molecules. The C=O stretching Raman bands of both PMA and BH are well isolated from other bands corresponding to other modes of vibration. The dipole moment of these molecules is also concentrated on the C=O bond.

2.EXPERIMENTAL:

Raman spectra of PMA and BH in different solvents were recorded by using the excitation wavelength of 4416 Åprovided by a liconix model 4240 He-Cd laser for BH and that of 4880 Åprovided by Spectra Physics model 165 Ar^+ laser for PMA. The liquid sample was taken in a quartz cell [(2-3)ml] and the laser beam was made to strike at the bottom of the cell very near to its perimeter. The sample of PMA and

BH and the solvents were obtained commercially and were used without further purification. The Raman spectra were recorded in a 90^o scattering geometry with a SPEX Ramalog 1403 double monochromator equipped with a cooled RCA 31034 photomultiplier and photon counting arrangement. The spectrometer control and data processing were achieved with the help of DM-3000 software. Other spectral conditions were adjusted to get the best possible spectra. The isotropic component was obtained by using the formula

$$I_{iso}(\tilde{\nu}) = I_{VV}(\tilde{\nu}) - \frac{4}{3} I_{VH}(\tilde{\nu}) \qquad 5.2.1$$

and

$$I_{aniso}(\tilde{\nu}) = I_{VH}(\tilde{\nu}) \qquad 5.2.2$$

where $I_{VV}(\tilde{\nu})$ and $I_{VH}(\tilde{\nu})$ represent the polarized and depolarized Raman spectra respectively. $\tilde{\nu}$ is the frequency in wave number. The reported Raman spectral measurements are accurate to ± 0.5 cm^{-1}.

3. RESULTS AND DISCUSSION:

The vibrational Hamiltonian of a dephasing system can generally be written as

$$H = H_0 + H_B + H_{coup} \qquad 5.3.1$$

where H_0 is the Hamiltonian for the isolated active oscillator, H_B

includes the translational and rotational degrees of freedom of the bath and H_{coup} describes the coupling of the vibrations to the bath. The general theory of vibrational dephasing involves calculation of the expression for coupling, H_{coup}. Experimentally measured bandshape of the isotropic and anisotropic components of Raman bands help us to know more about the spherically symmetric and anisotropic part of the intermolecular forces respectively[8–12]. Vibrational phase relaxation leads to broadening of the isotropic Raman band. The spectral bandshape can be expressed by Kubo lineshape function as

$$\phi(t) = exp\left\{-\langle\Delta\omega_i(t)\rangle^2\left[\tau_c\left(e^{t/\tau_c}-1\right)+t\tau_c\right]\right\} \qquad 5.3.2$$

The vibrational relaxation may be explained on the basis of three mechanisms, viz.,lifetime broadening, environmental broadening and resonance transfer. The fluctuations in the solute-solvent interaction forces lead to the fluctuations in the solute vibrational frequency which contribute to the width of the vibrational band. According to Fischer and Laubereau[13], the vibrational dephasing arises exclusively from the repulsive component of the interaction between the molecules, which was later generalised by Oxtoby[1]. Although the solvent's contribution to the vibrational frequency and band width in liquids is mainly due to repulsive interactions, the interactions due

to attractive forces and rotovibrational coupling components are also playing important role[14-17]. The inhomogenious and homogenious contributions to the band width, which is required for understanding the molecular dynamics, may be separated by time dependent techniques.

The information regarding the spherically symmetric part of the intermolecular forces can be obtained from experimentally measured bandshape of the isotropic component of Raman band. It is possible to adopt a stochastic approach[18] to the dephasing process, treating the molecule as an active oscillator perturbed by random forces. Its original spectrum will be broadened around the centre by a random modulation giving a distribution of frequency. With the hypothesis that the process is a Gaussian one, the correlation function $\psi(t)$ is exponential given by the equation

$$\psi(t) = e^{-t/\tau_c} \qquad 5.3.3$$

and dephasings due to different physical processes are statistically independent. Different decay rates of $\psi(t)$ leads to slow or fast processes of modulation. In the slow modulation limit ($\tau_c \rightarrow \infty$), the active molecule undergoes a perturbation for a long time and its phase is rapidly lost. In this case $I_{iso}(\tilde{\nu})$ is a Gaussian function with $t < \tau_c$.

In the fast modulation limit, i.e., for $t > \tau_c$ the perturbation is for a short time on the active molecule, so its phase is retained for longer times. In this case the corresponding $I_{iso}(\tilde{\nu})$ is a Lorentzian curve. Thus the bandshape is Lorentzian for homogeneous broadening. Very often dephasing rates are severely modified by inhomogeneous broadening and by hot or isotopic impurity bands which are slightly separated from the prominent band under study. For reliable values of dephasing rates, the chosen isotropic profile must be a symmetric band, not perturbed by other modes; eventual neighbouring bands must be subtracted, if necessary.

In the case of long range dipolar interactions τ_c is directly proportional to dynamic viscosity and therefore, τ_v is expected to depend on the viscosity of the medium. The electrical and electronic properties of an environment consisting of solvent molecules will also play a role in determining the vibrational relaxation based on considerations similar to dielectric relaxation in disordered systems[19]. The steady state conductivity (σ) for disordered systems is given by

$$\sigma = Nqm \qquad 5.3.4$$

where N is the density of a moving charge q and m is the mobility. If we consider the correspondence between disordered systems and

liquids, q may be taken as a partial charge[20] generated on the solute molecules by the solvent molecules. The average relaxation time τ , for a system may be given as

$$\tau = \tau_0 exp\left(\frac{\Delta w}{k_B T}\right) \qquad 5.3.5$$

In a liquid the molecules are in a potential well and this confinement is usually referred to as the **solvent cage effect** (Fig. 5.1). The molecule is considered to be vibrating against the walls of the cage, i.e., against its immediate neighbours with an occassional escape to the position adjacent to it. According to this model, the random diffusional motion of molecules in the liquid is taken to occur as a sequence of jumps from one molecular position to the next, so that collisions with identical molecules are involved. With dilute solutions, the solute molecule may be assumed to be in a cage of solvent molecules. Two different molecules (solute and solvent) that collide are likely to undergo successive collisions because they are surrounded by other molecules that tend to form a cage around them. This succession of collision is called an encounter. Therefore strong intermolecular interactions (non-bonded) are probable. These interactions may be diffusion controlled that is the interaction will depend upon the rate at which the solvent and solute can diffuse together. Accordingly

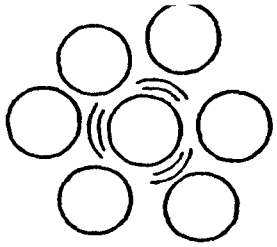

(a)

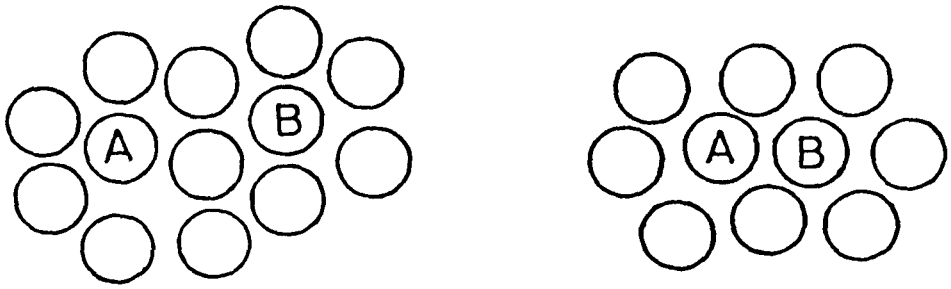

(b)

Fig. 5.1 (a) The solvent cage

(b) Diffusional encounter between A and B molecules

changes in the concentration and nature of the atoms present in the molecules have significant effects on the vibrational relaxation rate in the liquid phase.

One may take the approximation, however, that the molecules of the solvent and the solute are of same size. The frequency with which two solute molecules will accidentally become neighbours by the process of diffusion may then be estimated. The elementary jump distance, λ, is about $2r$, where r is the radius of the molecule. The diffusion coefficient is given by

$$D = \frac{\lambda^2}{6\tau} \qquad 5.3.6$$

where τ is the average time between collisions. In the case of polar molecules the hopping from one localized position to an adjacent one may result in a transfer of charge. This process is also associated with an activation of energy since the energy of a given localized position is different from that of another position. The conductivity due to such a process may depend on the hopping probability between two adjacent molecular positions i and j. The electrical conductivity tensor may be expressed abstractly by the Kubo equation as

$$\sigma_{\mu\nu} = \frac{1}{k_B T} \int_0^\infty \langle j_\mu(t) j_\nu(0) \rangle dt \qquad 5.3.7$$

The conductivity therefore depends on the time correlation between a component of the current operator $j_\nu(0)$ at time zero and the component $j_\mu(t)$ at some later time t, integrated for expectation value of the product over the equilibrium ensemble. The conductivity (σ) may be expressed by using equation(5.3.4) as

$$\sigma = \frac{Nq\lambda}{\tau E} \qquad 5.3.8$$

It is also related to the dynamic viscosity (η) as[21]

$$\sigma = \frac{Nq^2}{\sigma\pi\eta r} \qquad 5.3.9$$

Here E is the electric field, which the reaction field of the solvent molecules and may be taken as due to the dispersion forces at high frequencies given by

$$E = \frac{2\mu}{a^3}\left(\frac{n^2-1}{2n^2+1}\right) \qquad 5.3.10$$

where μ is the dipole moment of the solute and a is the radius of the spherical cavity in which the solute molecule is sitting. Eliminating σ from equation(5.3.7) and (5.3.8) and substituting the value of E we obtain

$$\tau = \frac{6\pi\eta r^2 a^3}{\eta\mu}\left(\frac{n^2-1}{2n^2+1}\right)^{-1} \qquad 5.3.11$$

Assuming that the radius of the cavity is small enough, a may be approximated as the radius of the molecule, r. The quantity ηr may then be taken as the dipole moment of the solute molecule. The above equation then reduces to

$$\tau = \frac{6\pi\eta r^6}{\mu^2}\left(\frac{n^2-1}{2n^2+1}\right)^{-1} \qquad 5.3.12$$

This collision time τ may be considered as the correlation time τ_c. Applying the Kubo correlation function τ may be related to the vibrational relaxation time τ_v as

$$\tau_v^{-1} = \frac{6\pi\eta r^6}{\mu^2}\langle(\Delta\omega_i^2)\rangle\left(\frac{n^2-1}{2n^2+1}\right)^{-1} \qquad 5.3.13$$

The second moment $\langle(\Delta\omega_i^2)\rangle$ may be related to the density(ρ) of the liquid as

$$\langle(\Delta\omega_i^2)\rangle = A\rho \qquad 5.3.14$$

Then equation(5.3.13) assumes the form[22]

$$\tau_v^{-1} = \frac{6\pi\eta r^6}{\mu^2}A\rho\left(\frac{n^2-1}{2n^2+1}\right)^{-1} \qquad 5.3.15$$

$$\tau_v^{-1} = C_m f(\rho,\eta,n) \qquad 5.3.16$$

where

$$C_m = \frac{6\pi r^6}{\mu^2} A \qquad 5.3.17$$

and

$$f(\rho, \eta, n) = \rho\eta \left(\frac{n^2 - 1}{2n^2 + 1} \right)^{-1} \qquad 5.3.18$$

The vibrational relaxation rate may then be calculated assuming a Lorentzian shape for the isotropic Raman component under study at higher solvent concentration according to the following relationship.

$$\tau_v^{-1} = \pi c \Gamma_{\text{iso}} \qquad 5.3.19$$

where Γ_{iso} is the fwhm of the isotropic component of the Raman band.

In the present work the band width of the isotropic components Γ_{iso} (fwhm) of the Raman band corresponding to the C=O stretching mode of PMA were measured in various polar as well as nonpolar solvents (CH_3CN, CH_2Cl_2, CCl_4, C_6H_6, $CHCl_3$) at 80% concentration. The Γ_{iso} for BH were also measured in solvents (CH_3CN, CCl_4, C_6H_6, $CHCl_3$) at 90% concentration. At these concentrations (80% for PMA and 90% for BH) the isotropic bandshapes for both the systems were found to be Lorentzian (Figs. 5.2 and 5.3). Therefore, the vibrational

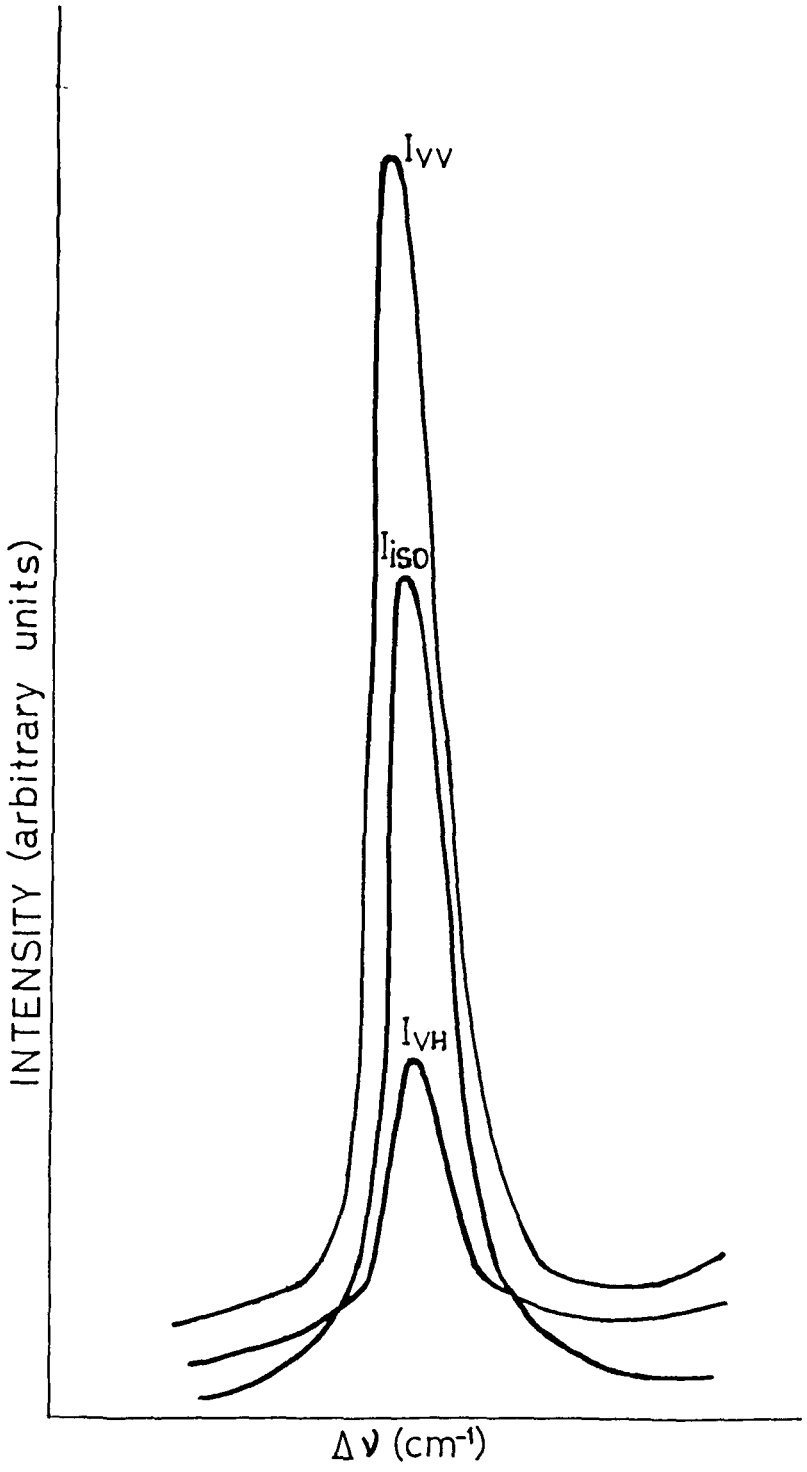

PMA in CCl_4

Fig. 5.2 (a)

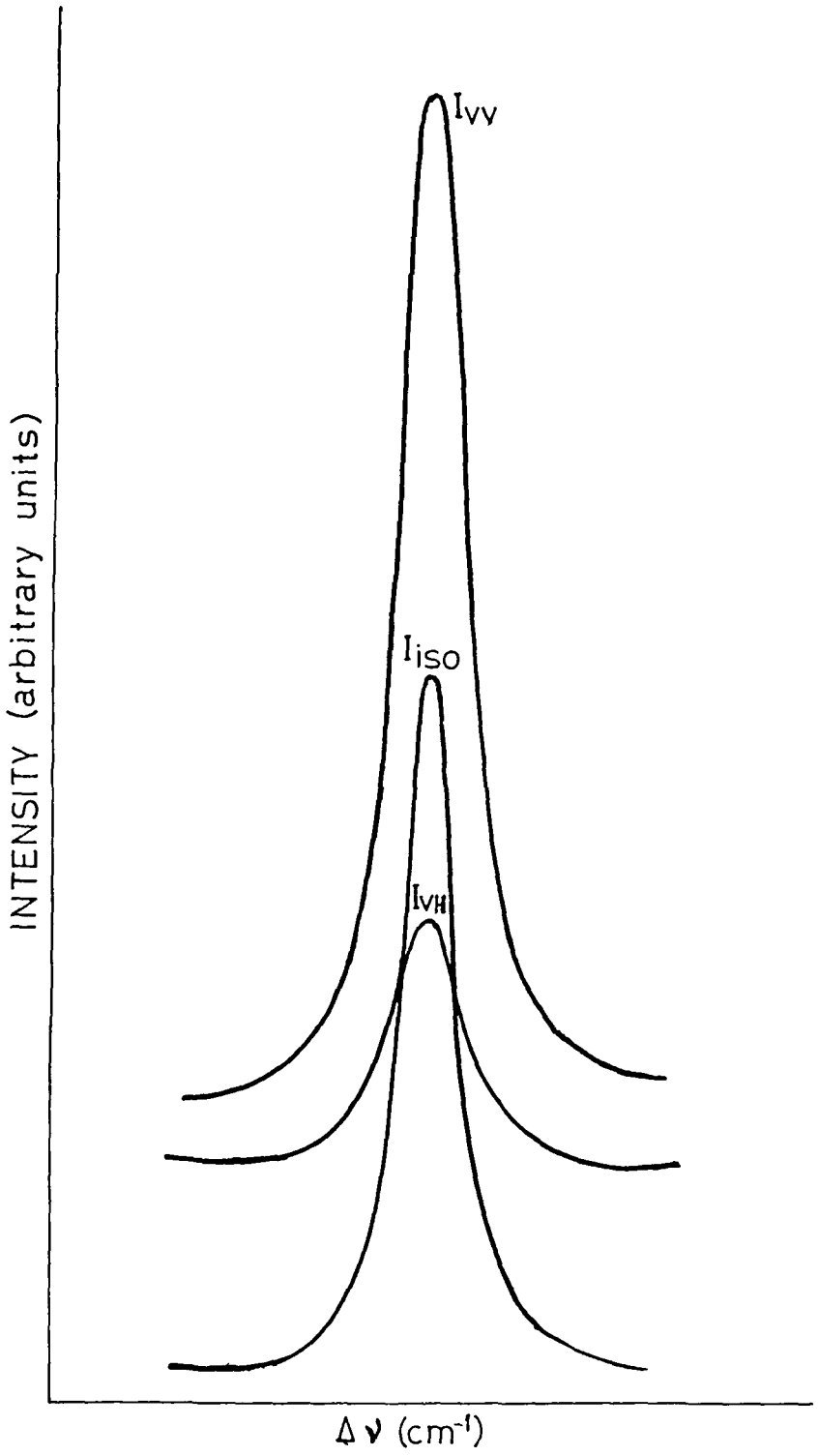

PMA in CH_3CN

Fig.5.2(b)

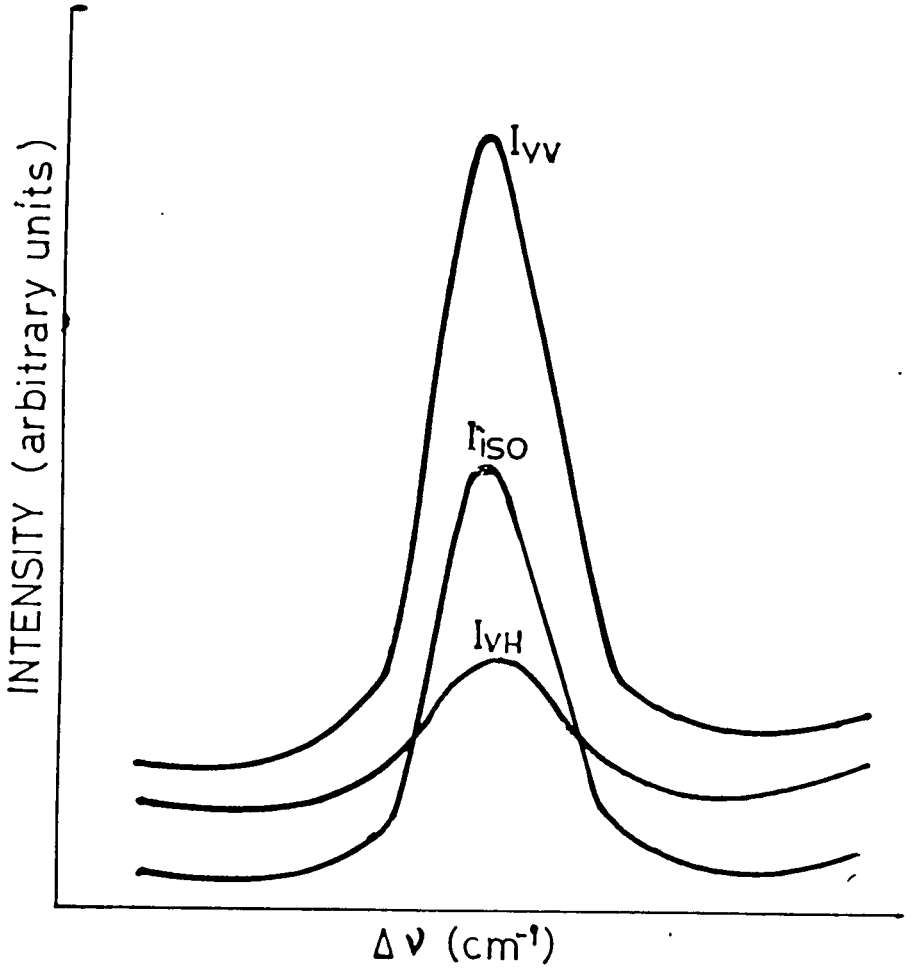

PMA in $CHCl_3$

Fig.5.2(c)

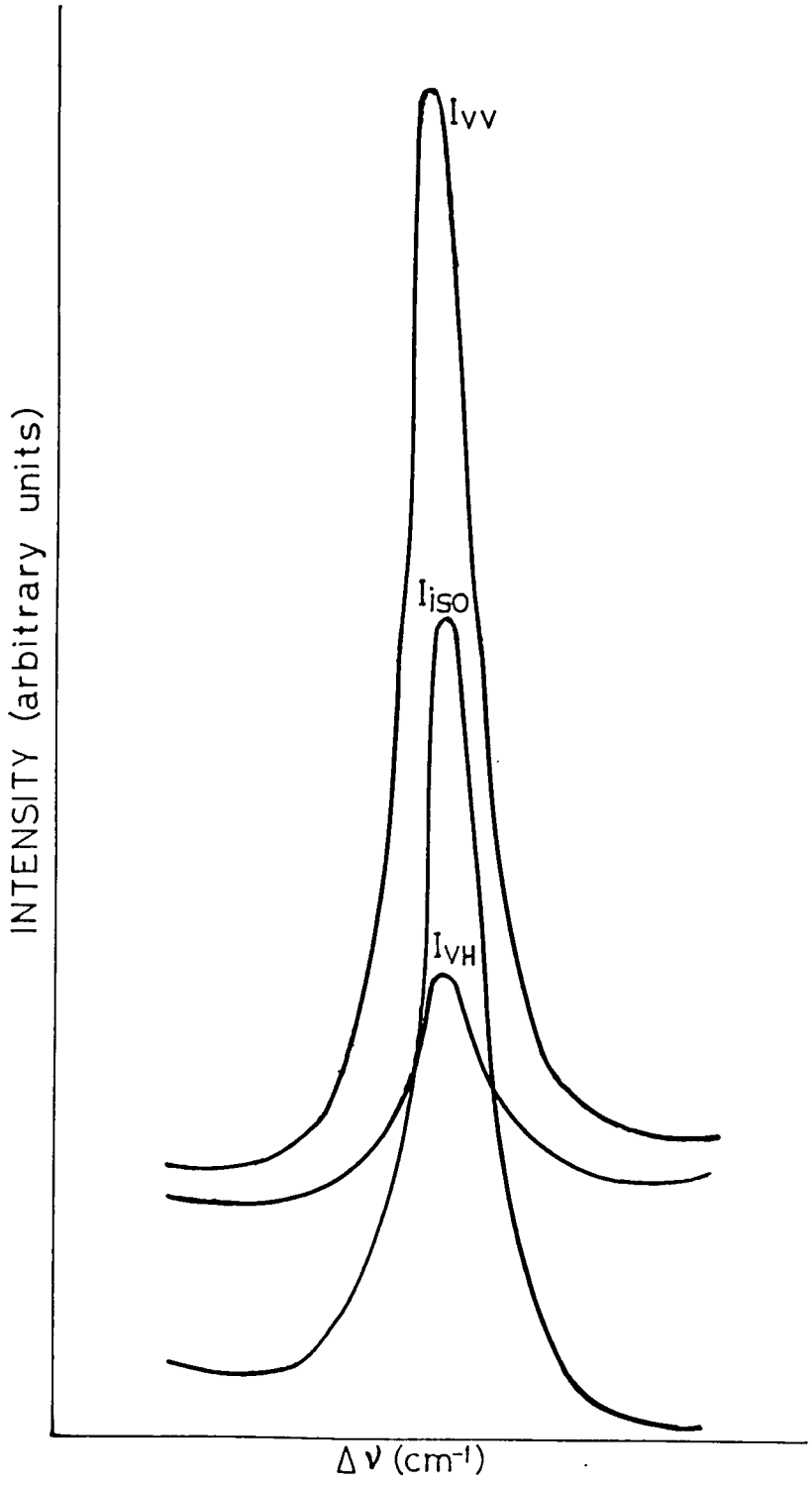

PMA in C_6H_6

Fig.5.2(d)

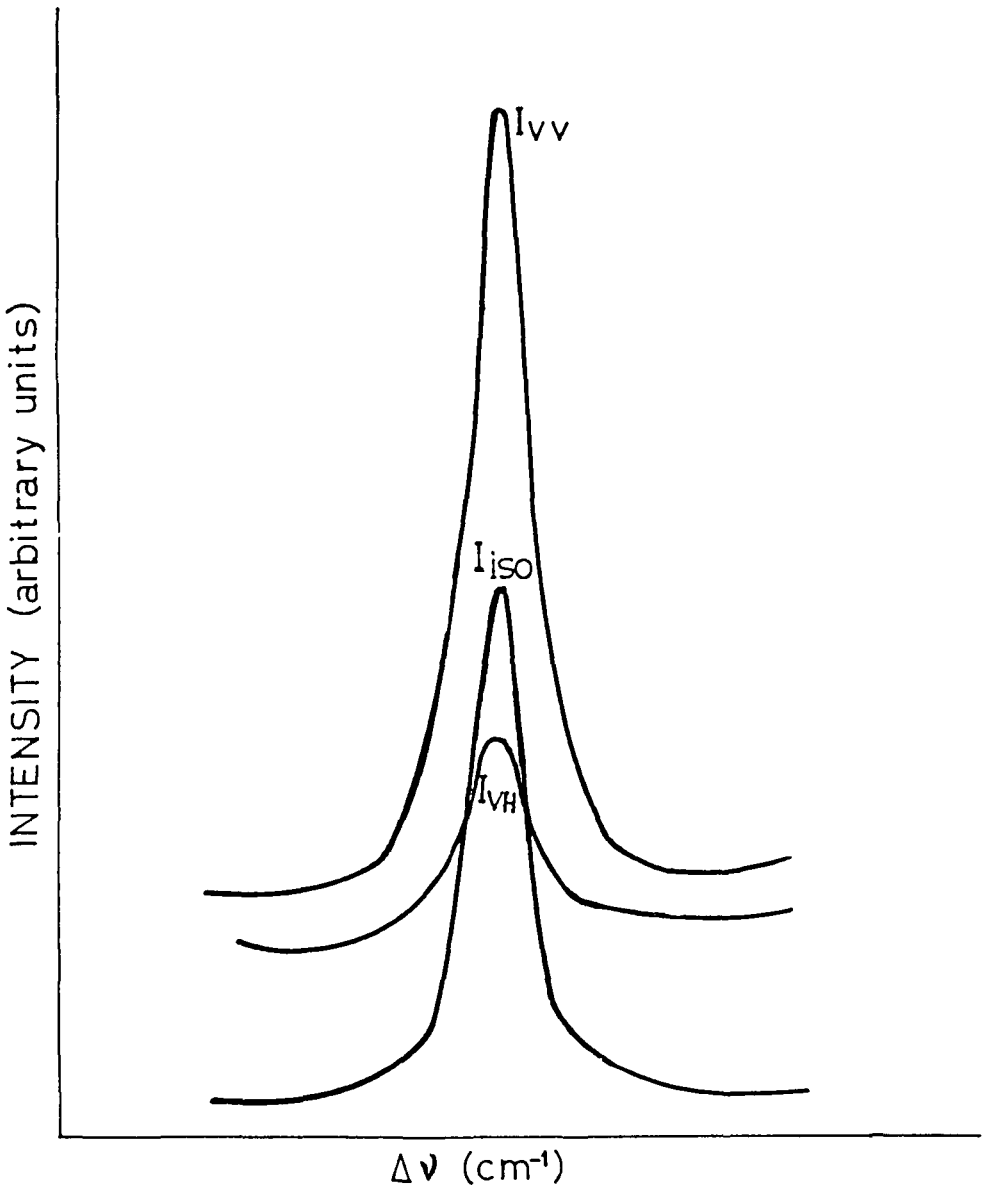

PMA in CH_2Cl_2

Fig.5.2(e)

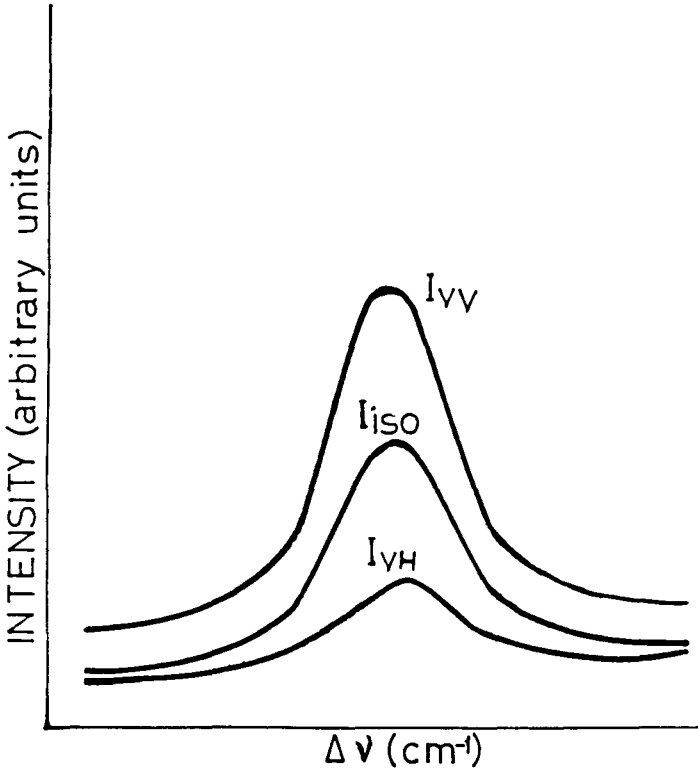

BH in CCl_4

Fig.5.3(a)

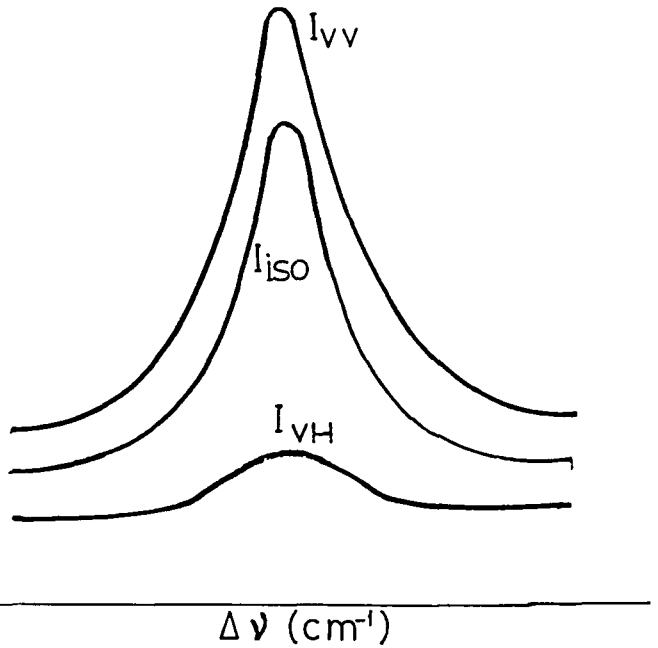

BH in CH_3CN

Fig.5.3(b)

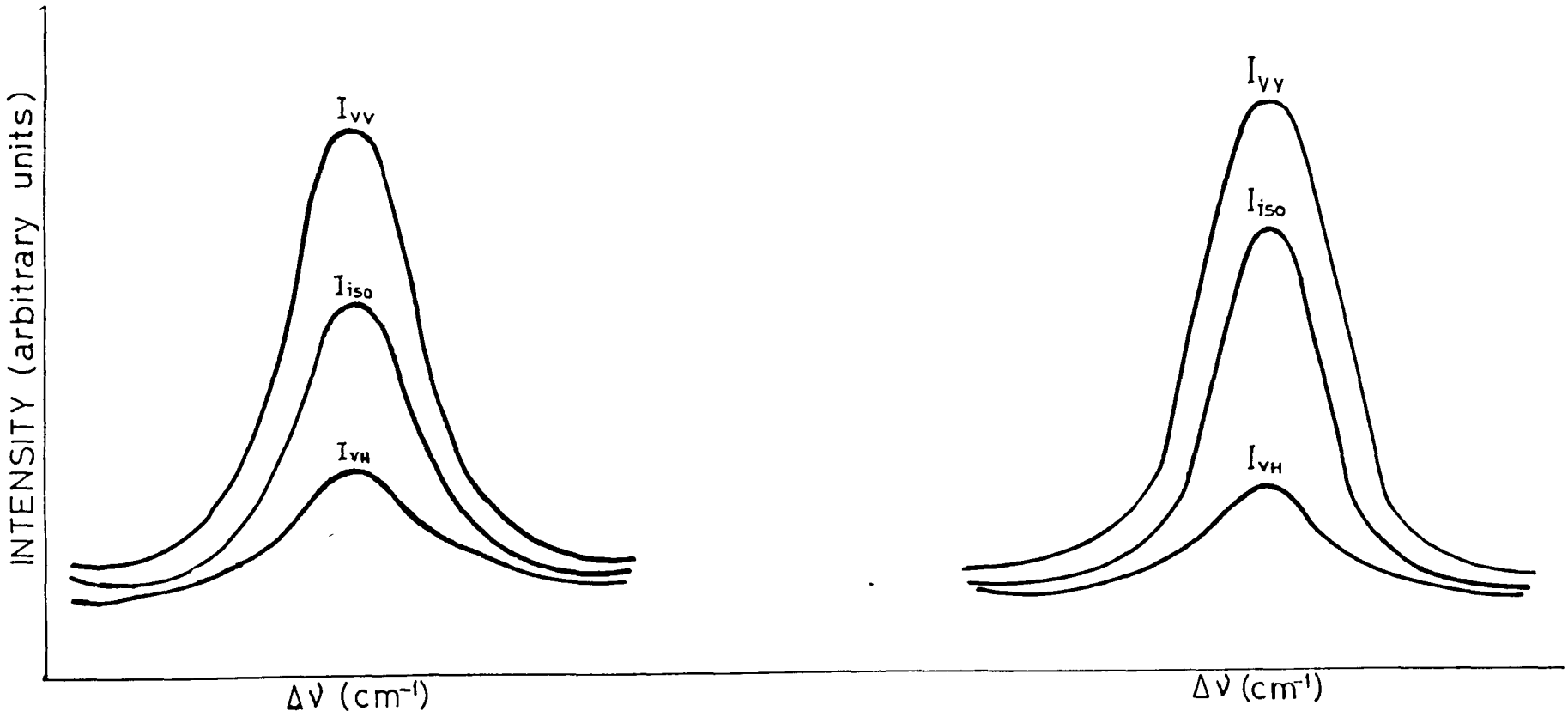

BH in $CHCl_3$

Fig.5.3(c)

BH in C_6H_6

Fig.5.3(d)

relaxation rates (τ_v^{-1}) were calculated from the isotropic band width using the relation (5.3.19).

The various models proposed for examining the dephasing process took into account the dynamic viscosity (η) which is a macroscopic property. However, the liquid state especially a finer details of the liquid structure requires a microscopic model incorporating the microviscosity(η_m) which may be calculated using the relation[23–25]

$$\eta_m = \eta \left[0.16 + 0.4 \left(\frac{a}{b}\right)\right] \qquad 5.3.20$$

$$\eta_m = \eta\gamma$$

where

$$\gamma = \left[0.16 + 0.4 \left(\frac{a}{b}\right)\right]$$

is the microfriction factor. The molecular parameters used for the calculation and the corresponding values of f_m and τ_v^{-1} are given in Tables 5.1 and 5.2. Here a and b are the radii of the solute and the solvent molecules respectively. The parameter f (equation 5.3.18) then takes the form[23–25]

$$f_m = \rho\eta_m \left(\frac{n^2 - 1}{2n^2 + 1}\right)^{-1} \qquad 5.3.21$$

Table 5.1

MOLECULAR PARAMETERS

Solvent	Density (ρ)	Dielectric constant (ε)	Refractive index (n)	Viscosity (η) (cp)
$CHCl_3$	1.479	4.77	1.45	0.452
CCl_4	1.548	2.23	1.46	0.843
CH_2Cl_2	1.319	9.14	1.42	0.393
CH_3CN	0.776	37.5	1.34	0.345
C_6H_6	0.873	2.28	1.50	0.564

Table 5.2(a)

Relaxation rate (τ_V^{-1}) and the function f_m for PMA in various solvents

Molecular system	Γ_{iso} (cm^{-1})	a (Å)	b (Å)	f_m	$\tau_V^{-1}(ps)^{-1}$
PMA-$CHCl_3$	16	2.60	1.20	3.90	1.51
PMA-CCl_4	12	1.77	3.50	2.20	1.13
PMA-CH_2Cl_2	10	1.77	1.80	1.44	0.94
PMA-CH_3CN	9	1.77	1.50	1.00	0.84
PMA-C_6H_6	15	1.70	1.00	3.30	1.40

Table 5.2(b).

Relaxation rate (τ_V^{-1}) and the function f_m for BH in various solvents

Molecular system	Γ_{iso} (cm^{-1})	a (Å)	b (Å)	f_m	$\tau_V^{-1}(ps)^{-1}$
BH-$CHCl_3$	13	2.6	1.2	2.85	1.18
BH-CCl_4	12	1.77	3.5	2.28	1.13
BH-CH_3CN	9	1.77	1.5	0.97	0.84
BH-C_6H_6	10	1.77	1.77	1.24	0.94

The experimental results have been presented as the plot of the vibrational relaxation rate τ_v^{-1} as a function of the parameter f_m for both PMA and BH molecules (Figs. 5.4 and 5.5). If we assume the PMA and BH molecules to be planar the dipole-dipole interaction may create stacking of solute molecules. The benzene molecule may move with respect to the stack so formed while still interacting with the molecular fragments of the PMA and BH molecules present. Due to molecular motion and diffusion the orientation of benzene molecule will not be fixed with respect to any particular fragment. The distance of closest approach may be limited by the CH_3 group present in the para position of the benzenoid ring of PMA. The anisotropy shifts in DMF, DMA, CH, BH and PMA molecules show a decreasing trend (Table 5.3) which is indicative of the fact that the local order in the liquids and the alignment of the dipoles in the neat liquid is very much dependent upon the size of the substituents. The above conclusion that the benzene ring may not be able to come as near to the benzenoid fragment in case of PMA as it would come in case of BH molecule was drawn in analogy with the above mentioned observation.The benzene ring may occupy any random position and may not be able to influence much through its π electron system. Therefore the entire molecular volume would not be effective in the

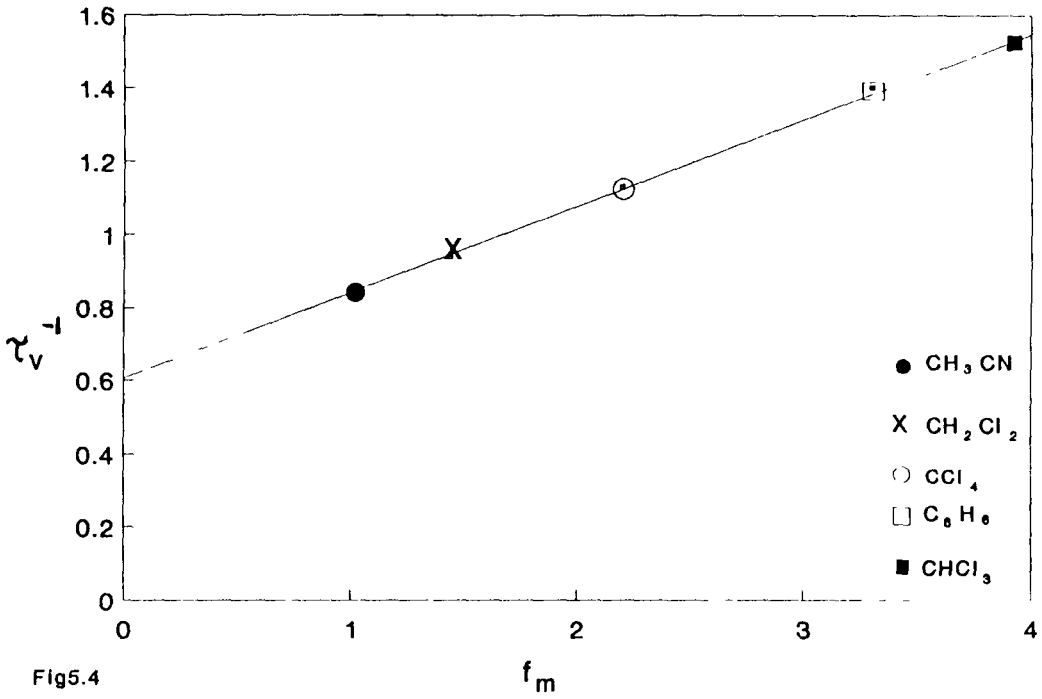
1.6
1.4
1.2
1
0.8
0.6
0.4
0.2
0
0
1
2
3
4
τ_v^{-1}
f_m
● CH_3CN
X CH_2Cl_2
○ CCl_4
□ C_6H_6
■ $CHCl_3$

Fig5.4

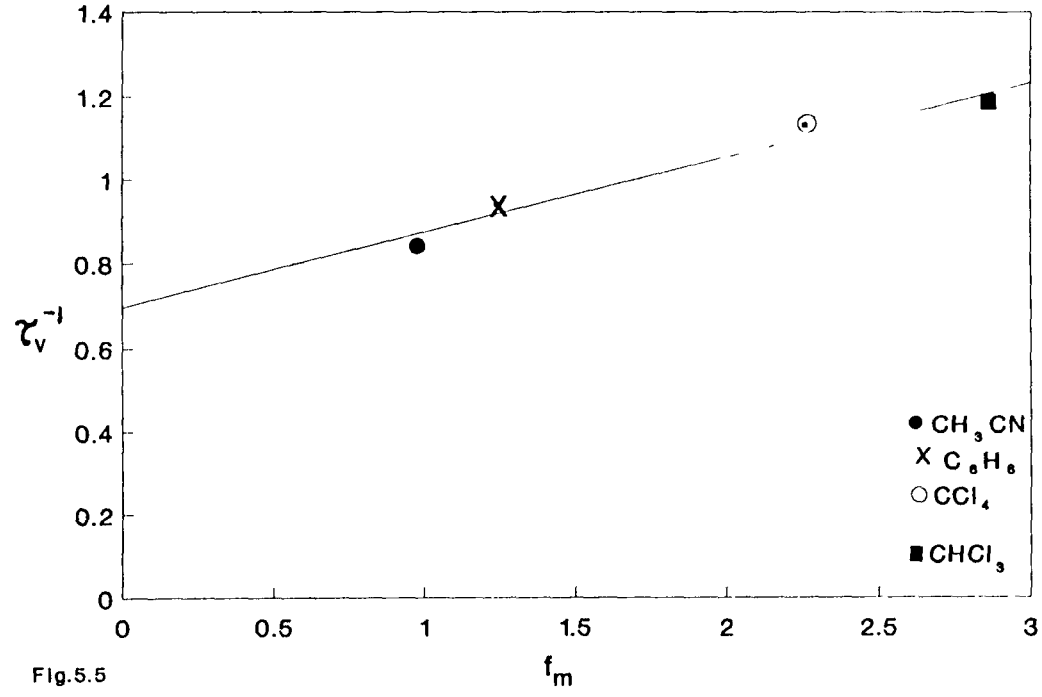
1.4
1.2
1
0.8
0.6
0.4
0.2
0
0
0.5
1
1.5
2
2.5
3
τ_v^{-1}
f_m
● CH_3CN
X C_6H_6
○ CCl_4
■ $CHCl_3$

Fig.5.5

Table 5.3a

Concentration of solute(v/v)	$\Delta\nu(cm^{-1})$ for different Molecular System				
	DMF-C_6H_6	DMA-C_6H_6	CH-C_6H_6	BH-C_6H_6	PMA-C_6H_6
50%	10	7	1.5	1.5	1
70%	10	9.5	3.5	3.5	3
80%	12	11	4.5	4.5	4
90%	12	12	5	5	4

Table 5.3b

Concentration of Solute (v/v)	$\Delta\nu(cm^{-1})$ for different Molecular System				
	DMF-CCl_4	DMA-CCl_4	CH-CCl_4	BH-CCl_4	PMA-CCl_4
50%	8	6	2	1.5	1
70%	10.5	10	4	3.5	2.5
80%	11	11	4.5	4.5	3.5
90%	12	12	6	5	4

Table 5.3c

Concentration of Solute(v/v)	Δν(cm-1) for different Molecular System				
	DMF-$CHCl_3$	DMA-$CHCl_3$	CH-$CHCl_3$	BH-$CHCl_3$	PMA-$CHCl_3$
50%	13	9.5	5	5	1
70%	15	12	7	7	2
80%	16	13	8	8	3
90%	17	14	9	8.5	4

Table 5.3d

Concentration of Solute (v/v)	Δν(cm^{-1}) for different Molecular System				
	DMF-CH_3CN	DMA-CH_3CN	CH-CH_3CN	BH-CH_3CN	PMA-CH_3CN
50%	10	6	2	1.5	1
70%	12	11	3.5	3	2
80%	13	12	4.5	4	4
90%	14	13	5	5	4

interaction process. It is also well known that the dipole-dipole interaction is maximum when the dipoles are in head to tail configuration (Fig.5.6). Any angle between the dipoles leads to a decrease in the interaction energy.

Therefore the solvent molecular radius for PMA-C_6H_6 system can be taken as the H atom van der Waals' radius (1.0Å). However, the benzene solvent may interact with the benzenoid portion of the BH molecule in its entirety and the interaction may be governed by the π electron system of the solute and solvent molecules. The solvent radius has therefore been chosen as the the benzene van der Waals' radius (1.77Å) for the BH-C_6H_6 molecular system(26).

For solute-CH_3CN system, the interaction is mainly between the dipole moment of the C=O bond of the solute and the dipole moment of the solvent. In this case the dipole-dipole interaction between the fragments of the molecules in solution are comparable to the interactions in the neat liquid. The dipole of CH_3CN molecule will try to interact with the dipole of the solute and align along the electric field of solute dipole. In this process it is likely that the dipole of an individual CH_3CN molecule may align along one of the components of the quadrupole moment of the benzenoid fragment of the solute molecule. The solvent molecules can then easily move with respect

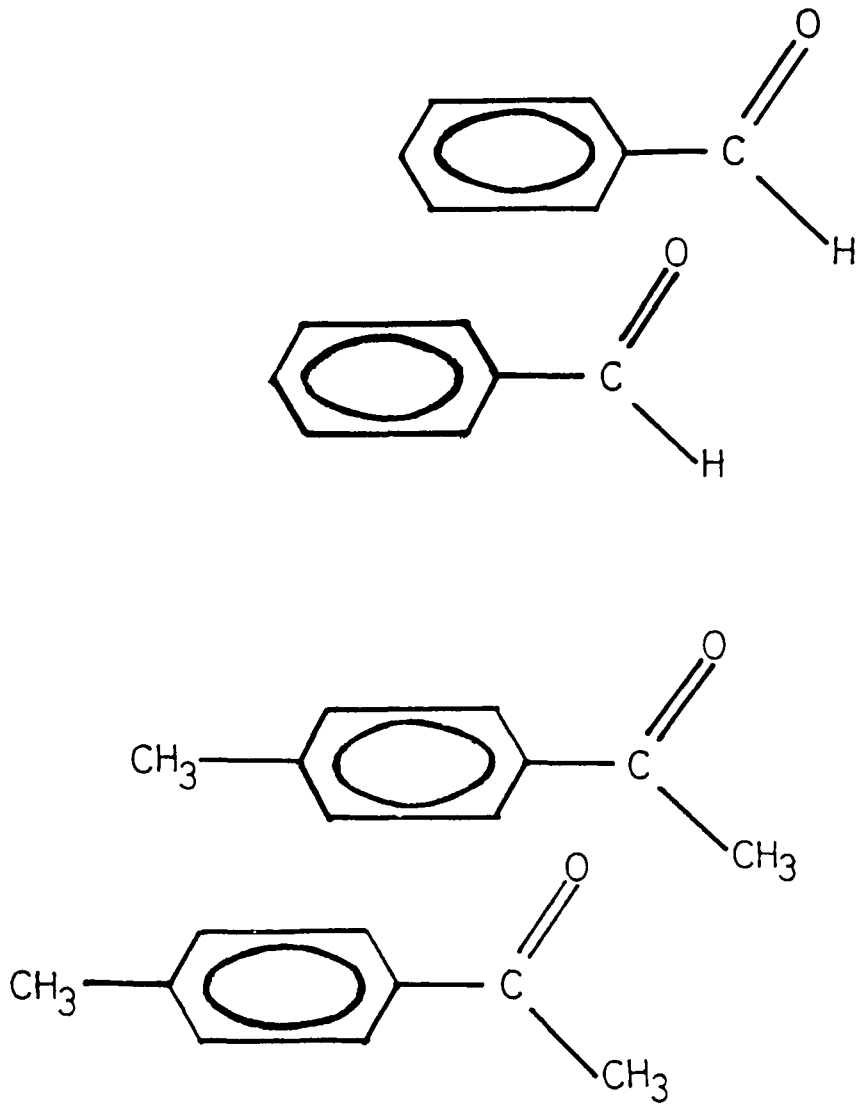

Fig.5.6 Head to tail orientation of the dipole moment of C=O bonds of PMA and BH molecules

to the stacks formed by the solute molecules while still interacting through the dipoles . The distance of closest approach will be determined by the orientation of C-C≡ N fragment of the solvent molecule. The acetonitrile molecule may be considered to have a cylindrical like structure so far as C-C≡N portion is concerned and it may be reasonable to assume that the CH_3CN molecule is interacting with the dipole of the C=O bond by forming an antiparallel configuration. This will facilitate it to interact simultaneously with the dipole of C=O bond and quadrupole of benzenoid fragment. This particular interacting situation may also be favoured by the motion of the solvent molecules with respect to the solute molecules in fluid state. Hence the solvent molecular radius has been chosen as the van der Waals' radius[26] of N atom (1.5Å) this being the largest atom in C-C≡N fragment of the acetonitrile molecule.

In case of solute-CCl_4 molecular system, when CCl_4 molecule approaches the solute molecule, it acquires a net electrical charge due to the high polarizability of the CCl_4 molecule. In addition, the CCl_4 has comparatively less dielectric constant than the PMA and BH molecules, hence it acquires a negative charge. As a result of the build-up of this charge an electrostatic potential is developed in the locality of the molecule whose value decreases with increasing distance

between the two molecules (solute and solvent).

Moreover, when the quadrupole moment is present in a molecule a quadrupole-induced dipole interaction is also likely to play an important role. The quadrupole moment of the benzenoid fragment of the solute molecule induces dipole moment in the solvent molecules approaching it. This is in addition to the induced dipole moment produced by the permanent dipole moment of the C=O bond.

The solute molecules PMA or BH may be assumed to have a planar structure. The spherical CCl_4 molecule can then easily roll over the planes of the solute molecules. The CCl_4 molecule is highly polarizable and has spherical shape, therefore the radius of the sphere which is the sum of C-Cl bond distance (1.7 Å) and the van der Waals' radius of Cl atom (1.8 Å) has been taken as the radius of the solvent molecule[26].

In case of PMA-CH_2Cl_2 molecular system, the dielectric constant of the CH_2Cl_2 solvent also has comparatively less value than that of PMA. Moreover, in CH_2Cl_2 molecule the Cl atom is more polarizable than the H atom. Therefore, in this molecular system the interaction is more likely through the Cl_2 group of the solvent. Due to the partial negative charge acquired, the CH_2Cl_2 molecule tends to orient towards the benzenoid fragment of PMA rather than the C=O bond.

A quadrupole-induced dipole interaction may as well be playing a significant role in this system besides the usual dipole-induced dipole and dispersion forces.

If we assume that the PMA molecule is planar the CH_2Cl_2 molecule will have a tendency to float with its Cl_2 group oriented towards the benzenoid fragment of PMA. The solvent and the solute molecules may be flowing with respect to each other and still interacting; hence the hydrodynamic properties may be expected to play an important role. Therefore the solvent radius in this molecular system has been chosen as the van der Waals' radius (1.8 Å) of the Cl atom[26].

The solute radius in all these cases has been chosen as the van der Waals' radius[26] of benzene (1.77Å) which corresponds to the benzenoid fragment for all practical purposes.

In case of $CHCl_3$ and PMA or BH molecular system, the acidic nature of the proton in $CHCl_3$ molecule may lead to an interaction where the hydrogen bonding effect may have to be taken into account. The solute molecules (PMA and BH) will have a tendency to form hydrogen bond through the carbonyl group. The $CHCl_3$ molecule while coming into proximity with the PMA or BH molecule has a possibility to orient itself in a head to tail configuration with the dipole of the C=O group through the C-H bond. However, due to

the molecular motion in liquid a more general case whereby there is an angle between the two dipoles is more near to the real situation (Fig.5.7)

In such hydrogen bonded systems, the complex formation is not expected as the proton in the $CHCl_3$ molecule is bonded to C and is having only an acidic nature. It may only be weakly associated with the C=O bond and the oscillations between the oxygen and carbon atoms may not be feasible as in the case of strongly hydrogen bonded systems. Nevertheless, the interaction may be sufficient to weaken the pair interaction at sufficiently higher concentration of the solvent where several chloroform molecules may surround the solute in a **cage** effect fashion.

Due to the orientation of C-H bond of $CHCl_3$ towards C=O bond of PMA or BH, the solute radius in this case is taken as the sum of van der Waals' radius of O atom (1.4 Å) and the C=O bond distance (1.2 Å) as the entire C=O bond may be considered as the interacting system in the hydrogen bonded solute-solvent system. The solvent radius is taken as the van der Waals' radius[26] of H atom (1.2 Å) as this is the atom which may be mainly the interacting one in the chloroform molecule due to its particular orientation in the hydrgen bonded structure.

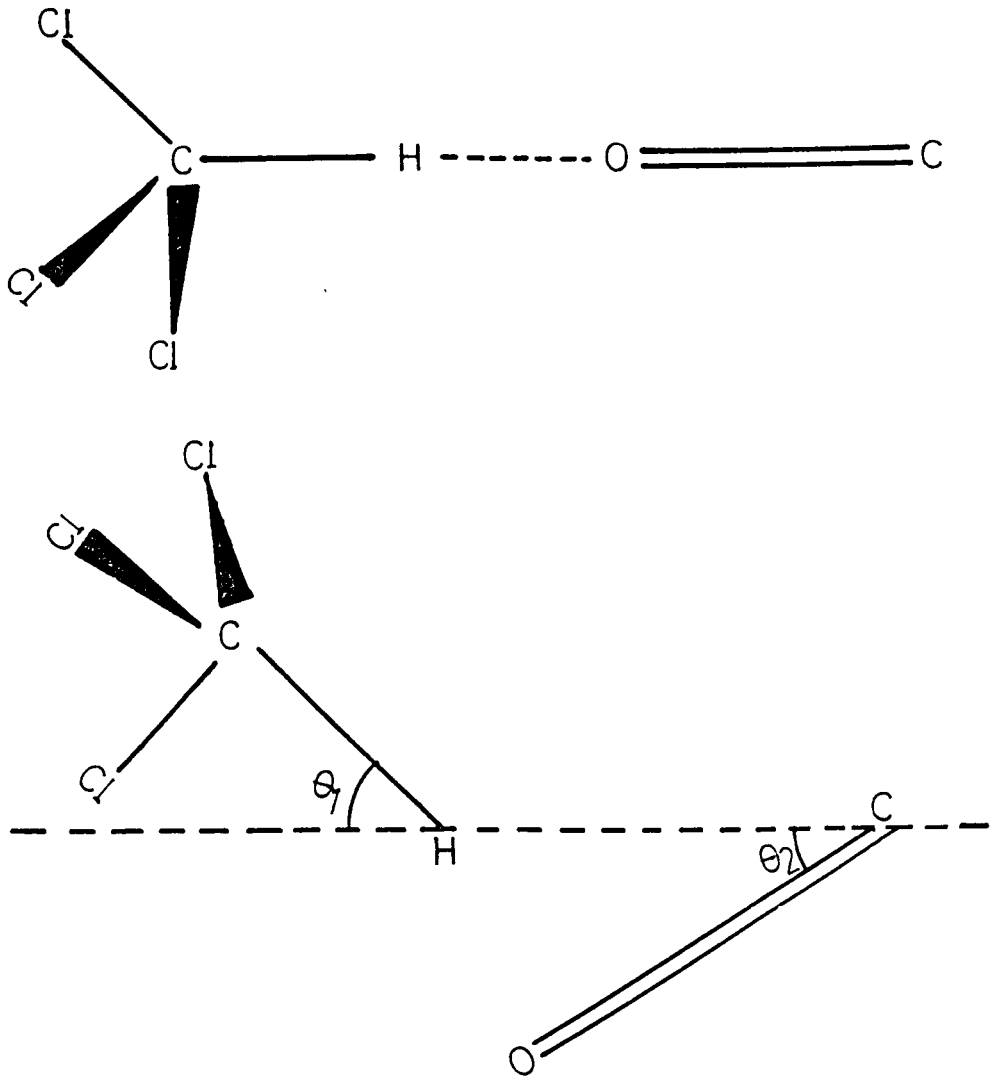

Fig.5.7 Hydrogen bonding of C-H bond of solvent molecule and C=O bond of solute molecule

The variation of τ_v^{-1} with respect to f_m is clearly linear which indicates that the discreteness of the medium due to the solvents has a significant influence in such complex molecular systems. It is, therefore, probable that the solvent microviscosity is playing a major role. The concept of microenvironment takes into account the band broadening as it is not only the microviscosity but the entire environment around the solute molecule which plays role in determining the band width observed in the present study.

REFERENCES:

1. A morresi, L. Mariani, M. R. Distefano and M. G. Giorgini, *J. Raman Spectrosc.,* **26,** 179 (1995).

2. D. W. Oxtoby, *J. Phys. Chem.,* **87,** 87, 3028 (1983).

3. F. Seifert, K. E. Oehme, G. Rundikoff, W. Hölzer, W. Carius and O. Schrötter, *Chem. Phys. Letts.,* **105,** 635 (1984).

4. D. E. Logan, *Chem. Phys.,* **103,** 215 (1995).

5. S Tarulli and E. J. Baran, *J. Raman Spectrsc.,* **26,** 139 (1995).

6. Z. Kecki and A. Sokolowska, *J. Raman Spectrsc.,* **27,** 429 (1996).

7. J. Jonas, *Acc. Chem. Res.,* **17,** 74 (1983).

8. A. Purkayastha, R. Das and K. Kumar, *Spectrchim. Acta,* **47A,** 525 (1991).

9. E. W. Knapp and S. F. Fischer, *J. Chem. Phys.,* **76,** 4730 (1980).

10. E. W. Knapp and S. F. Fischer, *J. Chem. Phys.,* **74,** 89 (1981).

11. E. W. Knapp, *J. Chem. Phys.,* **81,** 643 (1984).

12. T. Bein and G. Döge, *J. Raman Spectrosc.,* **12,** 82 (1982).

13. V. F. Kalasinsky and T. S. Little, *J. Raman Spectrosc.,* **14,** 253 (1983).

14. S. F. Fischer and A. Laubereau, *Chem. Phys. Lett.,***35,** 6 (1975).

15. K. Schweizer and D. Chandler, *J. Chem. Phys.,* **76,** 2296 (1982).

16. A. Ben-Shaul, Y. Haas, K. L. Kompa and R. D. levine, *in Lasers and Chemical change, Springer Series in Chemical Physics,* edited

by V. I. Goldanski, R. Gomar, S. P. Schafer and J. P. Toennies, **pp.** 201-205, Springer, Berlin (1981).

17. D. Ben-Amotz and D. R. Harshback, *J. Phys. Chem.,* **97,**2295 (1993).

18. D. Ben-Amotz, M. -R. Lee, S. Y. Cho and D. J. List, *J. Chem. Phys.*, **96,** 8781 (1992).

19. R. Kubo, *in Fluctuation, Relaxation and Resonance in Magnetic Systems,* edited by D. ter. Haar, **pp.** 23, Oliver and Boyd, Edinburgh (1962).

20. S. Bone, J. Eden, P. R. C. Gasloyne and R. Pethig, *J. Chem. Soc., Faraday Trans. 1,* **77,** 1729 (1981).

21. J. S. Dhull and D. R. Sharma, *J. Phys,* **D15,** 2307 (1982).

22. B. Tareev, *Physics of Dielectric Materials,* **pp.** 50, Mir, Moscow (1975).

23. A. Purkayastha and K. Kumar, *J. Raman Spectrosc.,* **19,** 249 (1988).

24. A. Purkayastha, R. Das and K. Kumar, *Spectrochim. Acta,* **46A,** 1545 (1990).

25. A. Purkayastha, R. Das and K. Kumar, *J. Raman Spectrosc.,* **21,** 227 (1990).

26. A. Bondi, *J. Phys. Chem.,* **68,** 441 (1964).

CHAPTER 6

Chapter 6

RAMAN ANISOTROPIC BAND WIDTH DEPENDENCE ON VAN DER WAALS' VOLUME OF INTERACTING SYSTEMS

1.INTRODUCTION

The effect of dilution on the shape of Raman bands of liquids has always been a subject of considerable interest. Both the usual chemical and isotopic solvents have been employed in many experimental works. Theoretical investigations initiated by Bondarev and Mardaeva[1] and later continued by Fujiyamaa, Kakimoto and Suzuki[2] consider the effect of dilution in binary mixtures. These authors proposed a simple model in which the spectral effect of dilution in binary mixtures was

interpreted in terms of concentration fluctuation of particles on a fictitious space lattice. Knauss[3] and Wartheimer[4] examined this problem in the framework of the Zwanzig Mori theory of Brownian motion. But their theory is limited to the case where the modulation of the solvent-induced frequency shift is fast. Bratos and Tarjus[5,6] have proposed a theory to interpret Raman bandshapes of pure van der Waals' liquids. Widely different spectral effects are predicted for chemical and isotopic solutions[7]. Finally, Knapp and Fischer[8] elaborated a kinetic model applicable to all modulation speeds which permitted an analysis of Raman band shapes of binary mixtures of van der Waals' liquids.

The Raman bandshape of a reference mode in a molecule is dependent upon the microscopic environment. In liquid mixtures, the band shape is influenced by the concentration fluctuations of the environment. Therefore, the solvent dependent studies for the anisotropic Raman band corresponding to C=O stretching vibration of different molecules p-methylacetophenone (PMA), benzaldehyde (BH), cyclohexanone (CH), N, N-dimethylacetamide (DMA) and N, N-dimethylformamide (DMF) were made. The C=O stretching mode in these molecules is well isolated from other modes of vibration and exhibits

strong Raman band. Therefore, it is suitable for studies involving vibrational relaxation. These molecules are also known to exhibit non-coincidence effect through C=O stretching mode[9–13]. The present study is concerned with the anisotropic component of the Raman band where the anisotropic component of the intermolecular forces plays role.

2. EXPERIMENTAL

The samples used for spectroscopic measurements were of either spectroscopic or extra pure analytical-reagent grade and were used without further purification. Raman spectral measurements were made for the totally symmetric C=O stretching band of PMA, BH. CH. DMA and DMF molecules in the solvents CH_3CN and C_6H_6. Raman spectra for different molecules were recorded in 90^o scattering geometry with a SPEX Ramalog 1403 double monochromator equipped with a cooled RCA 31034 Photomultiplier and photon counting arrangement. The spectrometer control and data processing were achieved with the help of datamate by using either DM-01 or DM-3000 software. Excitation wavelength of 4880Åprovided by a Spectra Physics Model 165 Ar^+ laser was used for recording Raman spectra of PMA, CH, DMA,DMF and that of 4416 Åprovided

by Liconix Model 4240 He-Cd laser was used for recording Raman spectra of BH dissolved in different solvents. All the spectra showed good reproducibility and were recorded at least three times. A slit width of 1.5 cm^{-1} was used for recording the spectra. Other spectral conditions were adjusted to get the best possible spectra.

The anisotropic band shape can be obtained from the $I_{V//}$ component as

$$I_{aniso} = I_{VH}$$

and gives information about the anisotropic forces and molecular reorientation. The effect of the finite slit width on the observed band width was corrected by the equation[14]

$$\Gamma_t = \Gamma_a \left[1 - \left(\frac{S}{\Gamma_a}\right)^2\right]$$

where Γ_t and Γa are the true and apparent Raman band width (full width at half maximum intensity, fwhm) respectively, and S is the spectral slit width in cm^{-1}. The accuracy of the band width measurements is believed to be ± 0.5 cm^{-1}.

3. RESULTS AND DISCUSSION

In the present work, the band width of the anisotropic component corresponding to the C=O stretching mode of PMA, BH, CH, DMA

and DMF were measured (Γ_{aniso}) for different solvent concentrations varying from 10% to 90% in the solvents CH_3CN and C_6H_6. The observed data for these solvents were found to be highly concentration dependent. It is, therefore, interesting to interpret the solvent dependent anisotropic Raman band width. The full width at half maximum (fwhm) of the anisotropic Raman band obtained were plotted as a function of the solvent concentration. The plot is quite complicated in the sense that the nature of the curve depends upon the range of the concentration of the solvent. It is observed that the graph is straight line for higher concentration of the solvent whereas it shows a curvature for lower concentration of the solvent (Figs. 6.1 and 6.2). Moreover, it is also observed that in case of PMA and BH dissolved in the solvents the curve is deep while that for CH, DMA and DMF the curve is shallow. It is apparent from such a graph that molecular interactions are quite complicated in the range of higher solute concentration. This may be due to the competitive nature of the interactions between the similar molecules of the solute and the solute-solvent molecules. The interpretation of the plot of such a complicated nature, therefore, may require an understanding of the molecular interactions.

For a system containing N_A solute molecules and N_B solvent molecules,

$$N_A + N_B = N$$

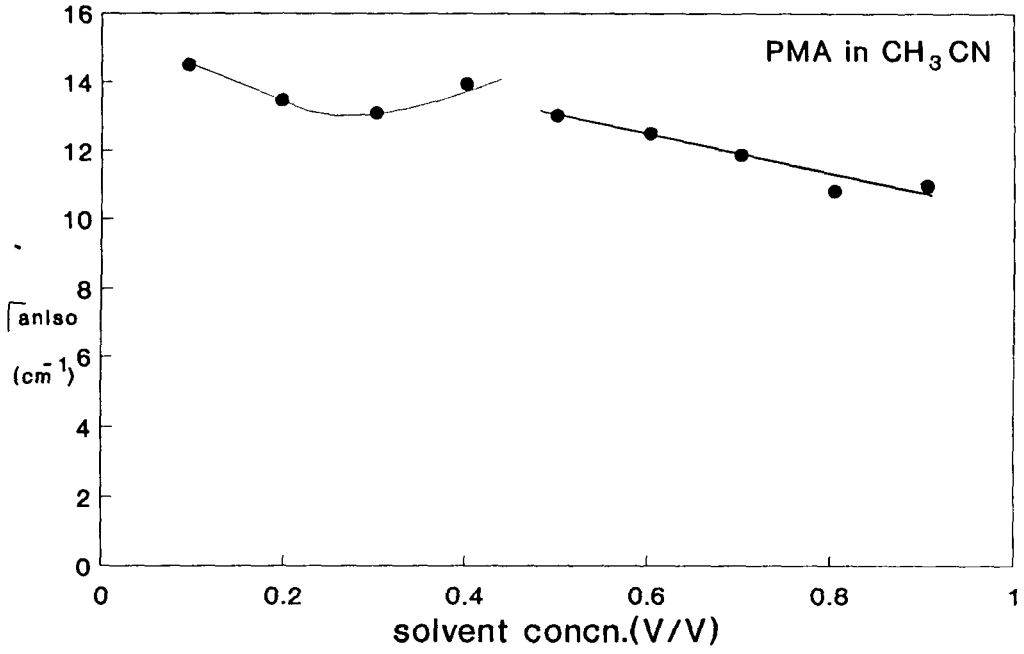

Fig. 6.1a

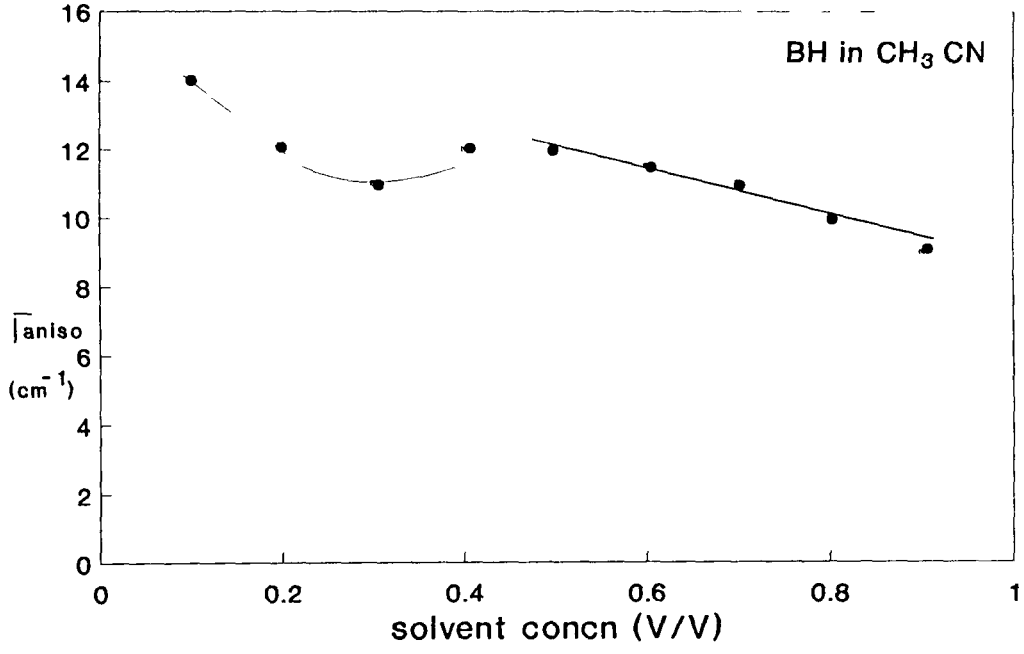

Fig.6.1b

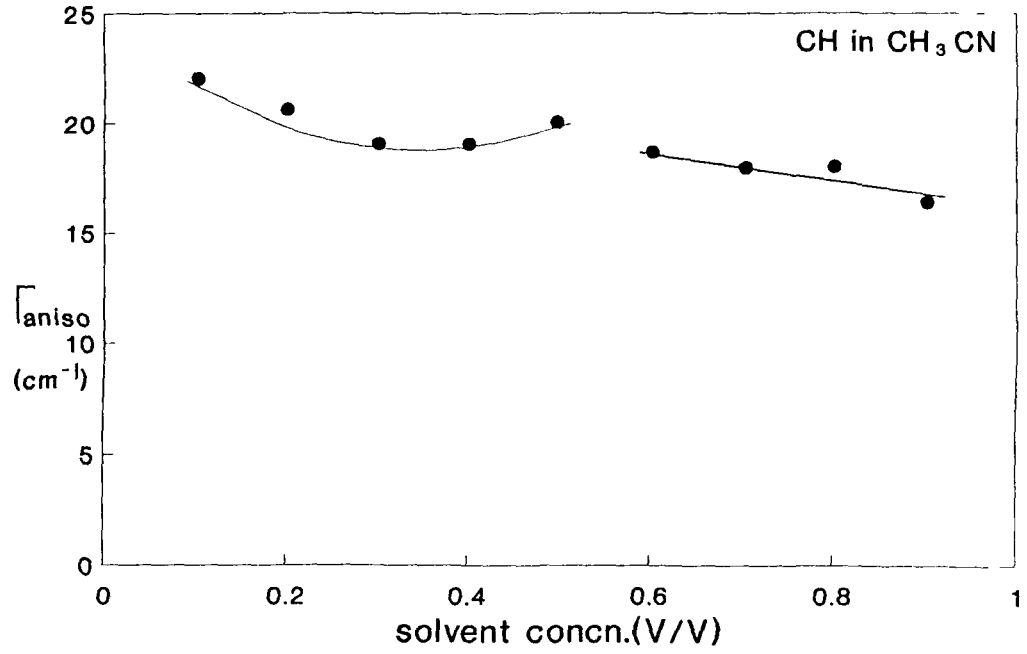

Fig.6.1c

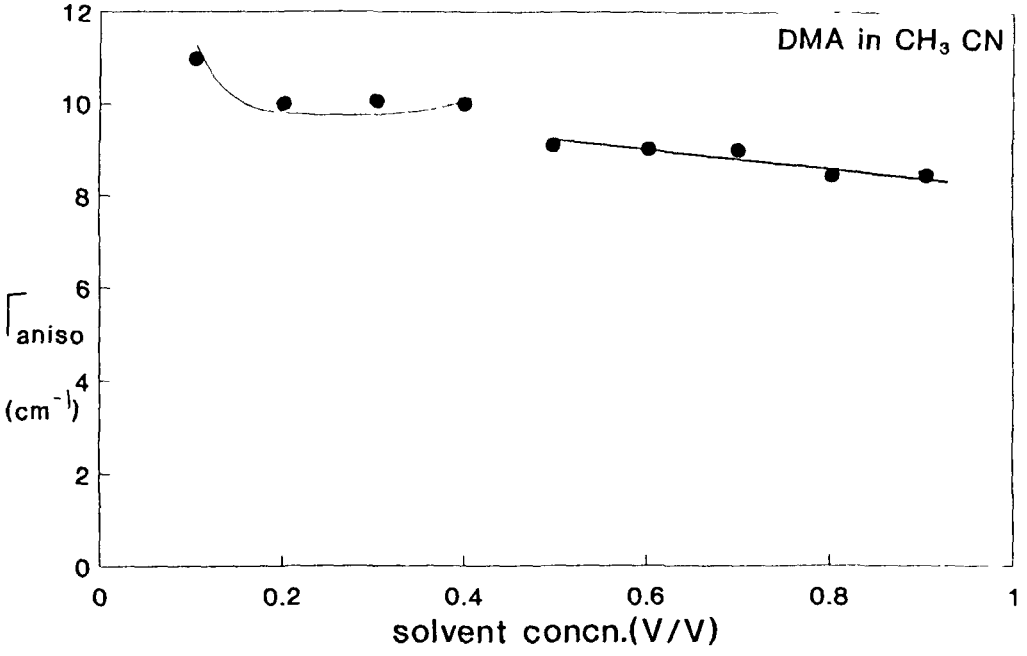

Fig.6.1d

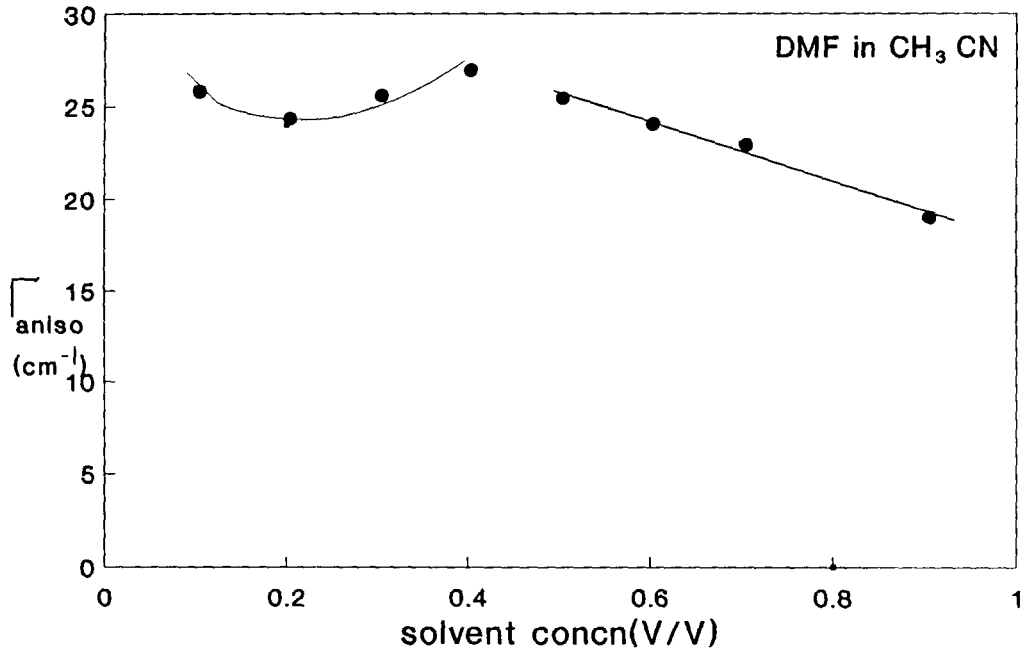

Fig.6.1e

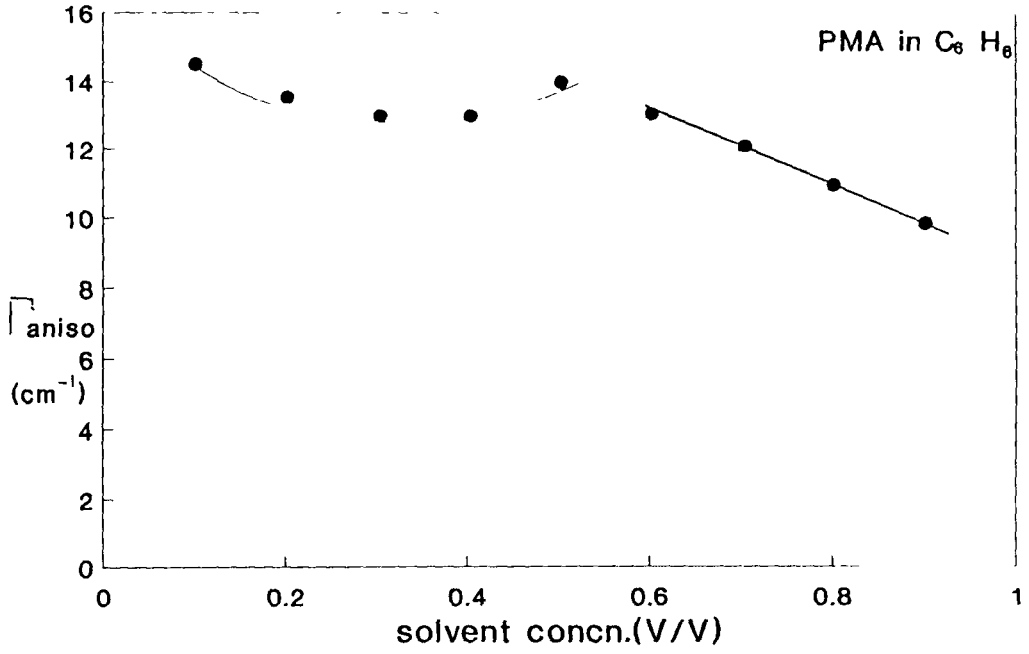

Fig6.2a

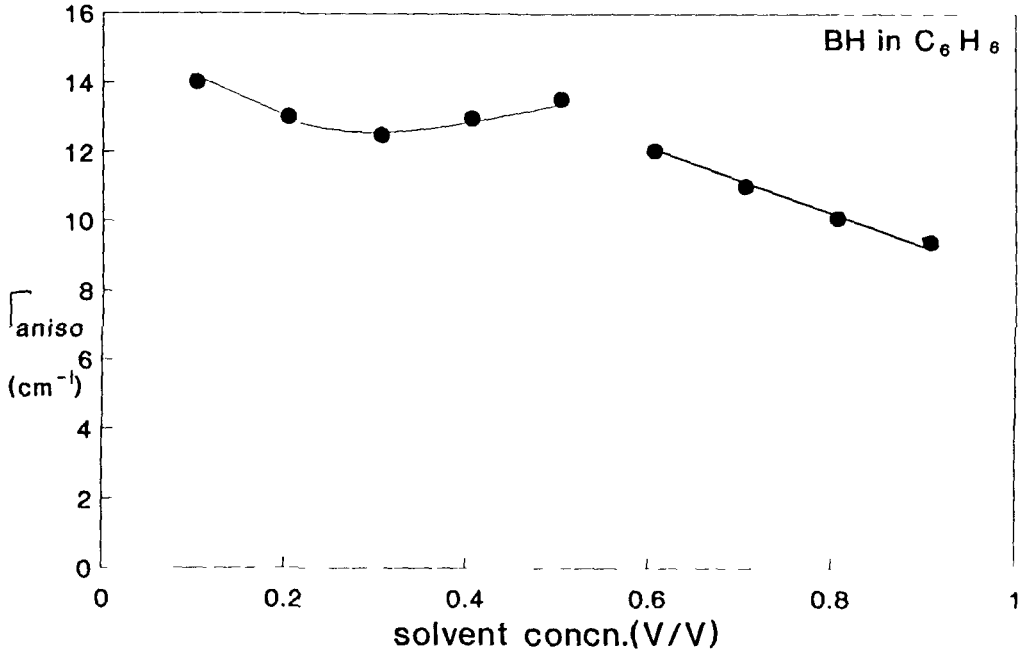

Fig.6.2b

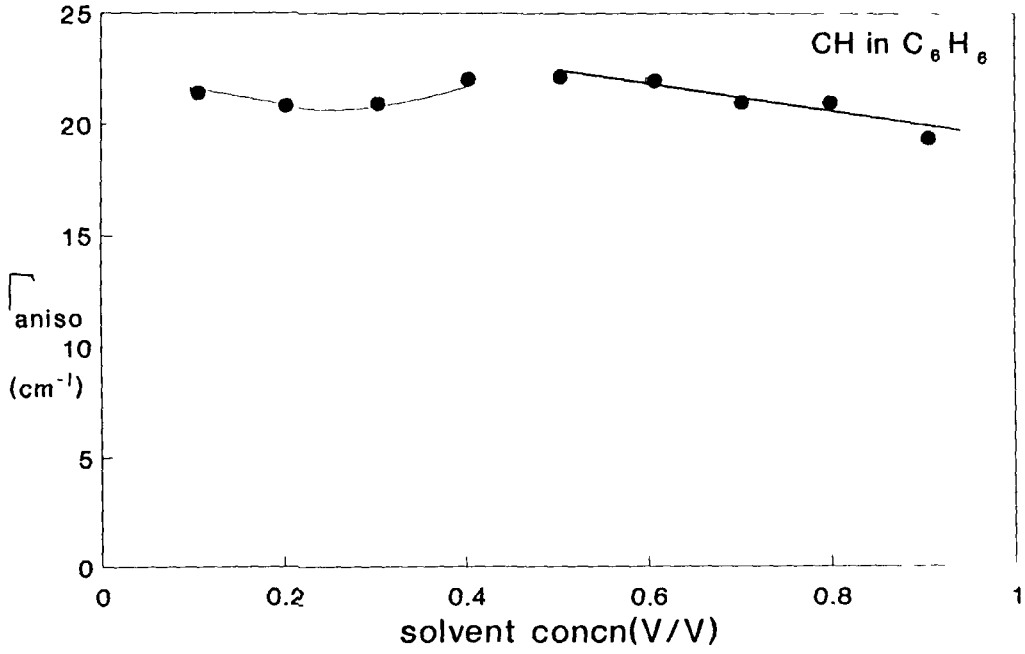

Fig. 6.2c

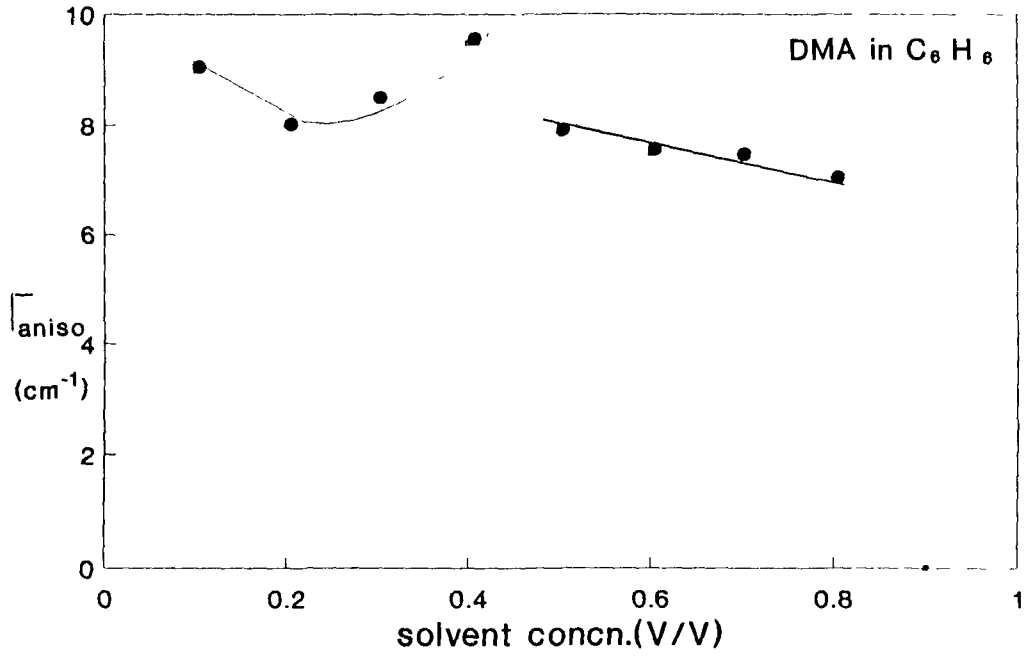

Fig. 6.2d

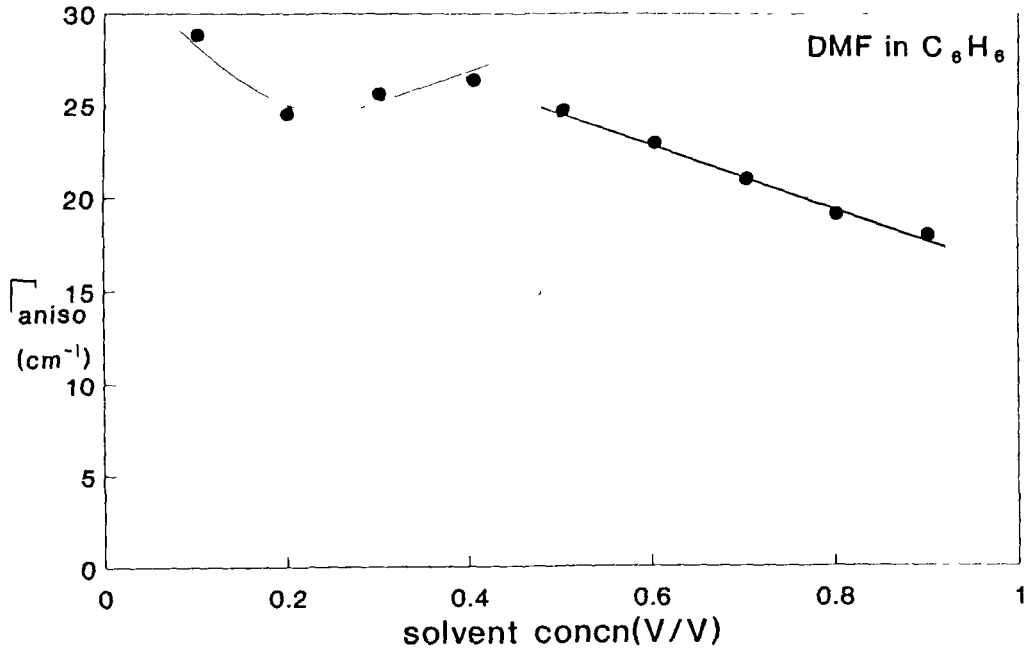

Fig.6.2e

For a system containing N_A solute molecules and N_B solvent molecules,

$$N_A + N_B = N$$

The solvent may be an isotopic variant of the spectrally active molecule or belong to entirely different chemical species, If the molecules of the species A executes anharmonic vibrations described by internal coordinates $r = (r_1, r_2, r_3, ...r_N)$, the semiclassical Hamiltonian can be written[8] as

$$H(r,t) = \left[\frac{1}{2}\sum_{i=1}^{N_A} p_i^2 + \frac{1}{2}\sum_{i=1}^{N_A} K r_i^2 + \frac{1}{6}\sum_{i=1}^{N_A} f r_i^3 + ...\right] + [V(r,t)] \quad 6.3.1$$

Here K and f are the harmonic and anharmonic force constants respectively; p_i are the momentum coordinates.

$$V(r,t) = \sum_{i,j=1}^{N_A} V_{ij}^{(AA)}(r,t) + \sum_{i=1}^{N_A}\sum_{j'=1}^{N_B} V_{ij'}^{(AB)}(r,t) \quad 6.3.2$$

where the pair potential $V_{ij}^{(AA)}$ and $V_{ij'}^{(AB)}$ describe the solute-solute and solute-solvent interactions, respectively. These potentials differ from each other for chemicals, but coincide for isotopic solvents.

In this model[8] the molecules of the species A and B are considered to execute stochastic rotations and translations, described by

the coordinates

$$\theta = \left(\theta_1^{(A)}, \theta_2^{(A)}, ..., \theta_{N_A}^{(A)}, \theta_1^{(B)}, \theta_2^{(B)}, ...\theta_{N_B}^{(B)}\right)$$

$$R = \left(R_1^{(A)}, R_2^{(A)}, ...R_{N_A}^{(A)}, R_1^{(B)}, R_2^{(B)}, ...R_{N_B}^{(B)}\right)$$

whereas the correlation between vibrations and rotations, although present is weak. Moreover, there is no collision induced scattering. The direct vibrational interactions between the solute and the solvent molecules are also neglected whereas the rotational and translational interactions are fully accounted for. Investigations by Levesque, Weis and Oxtoby[15] as well as by Tarjus and Bratos[7] show that the use of assumption regarding rotovibrational coupling is legitimate and no definite statement can be made about collision induced scattering.

Examination of spectral properties of isotopic solutions[16] reveals that the vapour-liquid frequency shift $\Delta\omega$ of an isotropic Raman band is a linear function of the concentration (Φ_A) of the solute molecules. On the other hand, the position of an anisotropic Raman band is independent of concentration. Also the variation with concentration of the halfwidth of an isotropic Raman band, strongly depends on the speed of vibrational modulation. The slow modulation expression

$\Delta\omega_{1/2}^{SM}$ and the fast modulation counterpart $\Delta\omega_{1/2}^{FM}$ are given by

$$\Delta\omega_{1/2}^{SM} = (2ln2))^{1/2} \{ [\langle(\Delta\Omega_{11})^2\rangle] + \Phi_A [2N\langle\Delta\Omega_{11}\Delta\Omega_{12}\rangle + N^2\langle(\Delta\Omega_{12})^2\rangle] \}$$

$$+\Phi_A^2 [N^2\langle\Delta\Omega_{12}\Delta\Omega_{13}\rangle] + ...\}^{1/2} \qquad 6.3.3$$

$$\Delta\omega_{1/2}^{FM} = \{[\langle(\Delta\Omega_{11})62\rangle] + \Phi_A [2N\langle\Delta\Omega_{11}\Delta\Omega_{12}\rangle + N^2\langle(\delta\Omega_{12}^2\rangle]$$

$$+\Phi_A^2 [N^2\langle\delta\Omega_{12}\Delta\Omega_{13}\rangle\tau_{12,13}]\} \qquad 6.3.4$$

where τ is a representative correlation time and Ω is a NXN frequency matrix.

One then concludes that the halfwidth $\Delta\omega_{1/2}$ is a quadratic function of Φ_A if the vibrational modulation is fast; it depends on the square root of this function if it is slow; and it exhibits an intermediate behaviour for intermediate modulation speeds. Moreover, from the wellknown Bondarev-Mardaeva expression[1] one concludes that the halfwidth $\omega_{1/2}$ is a linear function of Φ_A in the fast modulation limit, it depends on the square root of Φ_A in the slow modulation limit and it exhibits an intermediate behaviour for intermediate modulation speed. The half width of an anisotropic Raman band is, in practice, weakly concentration dependent.

Spectral properties of solutions involving chemical solvents are much

more difficult to analyze than those of isotopic solutions. For chemical solutions, the peak frequencies of both isotropic and anisotropic Raman bands are concentration dependent. The expressions

$$\Delta\omega_{iso} = \left[N\langle\omega_{12}^{AB}\rangle\right] + c_A\left[\left(N\langle\omega_{12}^{(AA)}\rangle - N\langle\omega_{12'}^{(AB)}\rangle\right) + N\langle\bar{\omega}_{12}^{(AA)}\rangle\right] \quad 6.3.5$$

$$\Delta\omega_{aniso} = \left[N\langle\omega_{12}^{AB}\rangle\right] + c_A\left[\left(N\langle\omega_{12}^{(AA)}\rangle - N\langle\omega_{12'}^{(AB)}\rangle\right)\right] \quad 6.3.6$$

in fact are nonlinear in Φ_A. The half width of isotropic and anisotropic Raman bands is also concentration dependent. However, this dependence is complex, even in the slow and fast modulation limits. In chemical solutions, the solvent induced effects on the band shape are of a similar magnitude in isotropic and anisotropic Raman spectra. This behaviour is different from that found in isotopic solutions. This difference is due to the fluctuations of the chemical composition in a given site of the liquid and to the structure-breaking effects which are present in the former case and absent in the latter. The environmental fluctuations of transition frequency and rotational fluctuations depend on Φ_A in chemical, but not in isotopic solutions.

To have a more clear picture about the intermolecular interactions involved which are responsible for such a complicated behaviour we have taken into account the concept of van der Waals' volume of the sphere of influence in solution. The calculation of van der Waals

volume (V_w) assumes a knowledge of bond distance[17], bond angles and contact distance i.e. intermolecular van der Waals radii (r_w) and shapes of atoms in various molecular configurations. It has been observed that for heavy atoms the van der Waals radius under the most drastic environmental changes, i.e., irrespective of its chemical combination and of its nearest non bonded neighbours as well as of the phase state in which it is found remain invarient. The van der Waals radius may thus be estimated from the point of view of the electron density distribution around an atom.

The electron density ψ^2 at distance r from the core of a hydrogenic one electron atom is given by

$$\psi^2 = C^2 exp\left(-\frac{2\sqrt{2m_e I_0}}{h}r\right) \qquad 6.3.7$$

where m_e is the rest mass of the electron, I_0 is the first ionization potential of the atom, and C is a normalization constant chosen such that $\int \psi^2 d\omega = 1$ of space (ω). As two atoms approach each other from $r = \infty$ their electron clouds interpenetrate more and more. The Pauli exclusion principle then causes a repulsion of the two atoms in direct proportion to the electron density in the region of interpenetration. The van der Waals radius then might be defined in terms of that distance r, at which this repulsion just balances the attraction

force between the two atoms, But it is difficult to formulate a critical electron density and calculate r_w from it because of the low degree of accuracy.

However,equation (2.6.1) contains a parameter $h\sqrt{m_e I_0}$, the de Broglie wavelength λ_B of the outermost valence electron of an atom, which might be related to the van der Waals radius (r_w). In fact, it has been observed that $r_w = (const.)\lambda_B$. The constant is 0.61 for the rare gas atoms, 0.53 for halogens and about 0.48 for the remainder of the non metallic elements. Deviation from this correlation are in the direction of predicting too large a diameter for the lightest elements.

In general for a detailed analysis, the method used to estimate V_w from bond distance l and from r_w is shown in the fig. 6.3.

Here,

r_1,r_2 = van der Waals radius

l = covalent bond distance

m = auxiliary parameter

h_1. h_2 = height of sphere segments

$m = \left(\frac{r_2^2 - r_1^2 + l}{2l}\right)$

$h_1 = r_1 + l - m; h_2 = r_2 - m$

$V_1 = \pi h_1^2 \left(r_1 - \frac{h_1}{3}\right)$

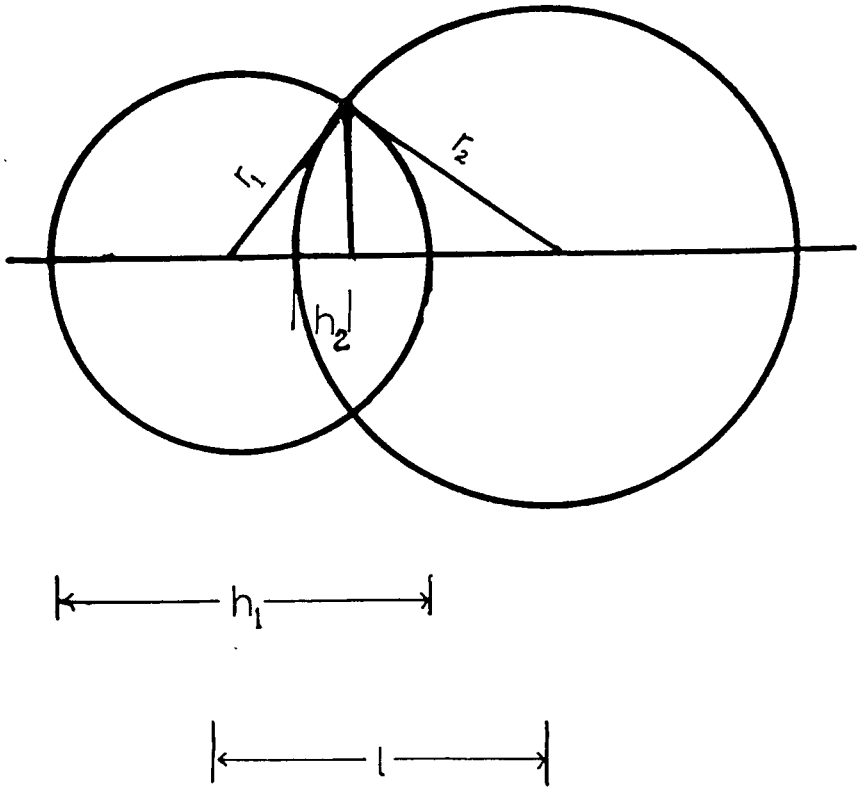

Fig.6.3 Calculation of van der Waals' volume

$\Delta V_2 = \pi h_2^2 \left(r_2 - \frac{h_2}{3}\right)$

$V_2 = \frac{4\pi}{3} r_2^3$

In this simple model for calculation of van der Waals volume V_w of molecules shown in the Fig. 6.3, care must be taken not to cut larger sphere segments off the central atom than it has volume to provide. Neighbouring atoms around a three or four valent central atom would interpenetrate if the sphericities of their shells were preserved to the root. Actually they do not even squeeze each other very hard, as the bound atoms are probably pear shaped due to the tighter binding of valence electrons halfway between the two radii. Moreover, strong association causes sufficient deformation of the perticipating atoms that it has to be taken into consideration in the selection of contact distance and in calculation of V_w.

$$V_w \approx N_A \left(\frac{\pi}{6}\right) \sigma^3$$

The van der Waals' volume of the interacting system with solute dissolved in the solvents CH_3CN and C_6H_6 has been calculated by using the relation

$$V_w = \Phi V_w(solute) + (1 - \Phi) V_w(solvent) \qquad 6.3.8$$

keeping in view the varying nature of the solute-solvent distance in a

solution.

For solute-acetonitrile system, the solvent's van der Waals' volume has been calculated by considering that the acetonitrile molecule has a cylindrical like structure as far as C-C≡N portion is concerned. The van der Waals' volume[17] for acetonitrile has been taken to be equal to the van der Waals' volume of $(C - C \equiv N)$.

In solute-benzene system, the van der Waals' volume of benzene[17] has been taken to be equal to 48.4. On the other hand the effective solute van der Waals' volume has been taken as the van der Waals' volume 11.70 of one C=O bond[17], because the primary interaction is dominated by the dipole moment of the C=O bond of the molecules.

Keeping in view the role of the van der Waals' volume, a quantity $\Gamma_w = ln\left(\frac{\Gamma_{anise}}{V_w}\right)$ was defined as one of the parameter in these systems. This quantity has been plotted as a function of the solvent concentration. the graph (Figs. 6.4[a-j]) shows a straight line for the entire region. This nature is somewhat similar to that reported earlier in Chapter IV where the repulsive potential is playing a significant role[13].

While explaining the non-coincidence effect[9–13], we have considered the pair interaction between the solute molecules which leads to the

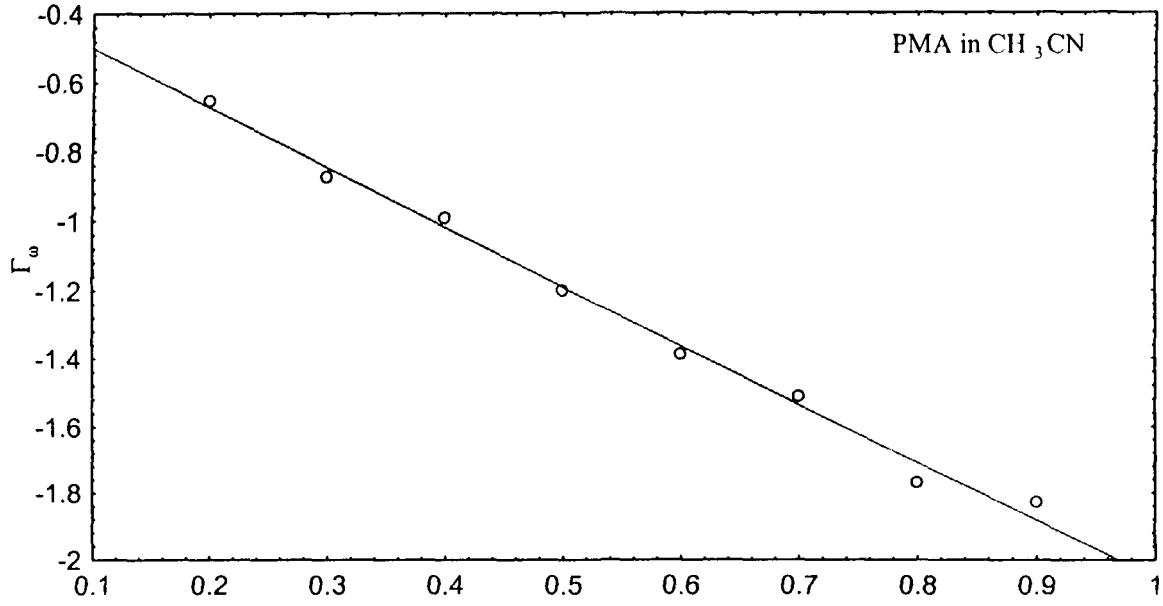

Fig. 6.4a

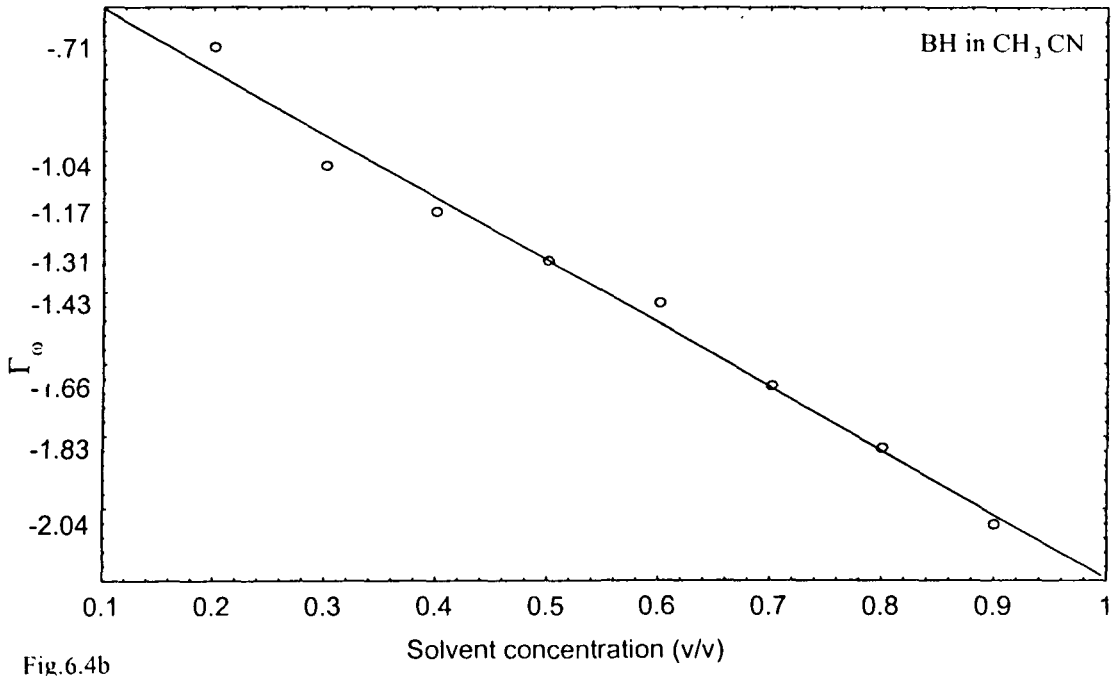

Fig.6.4b

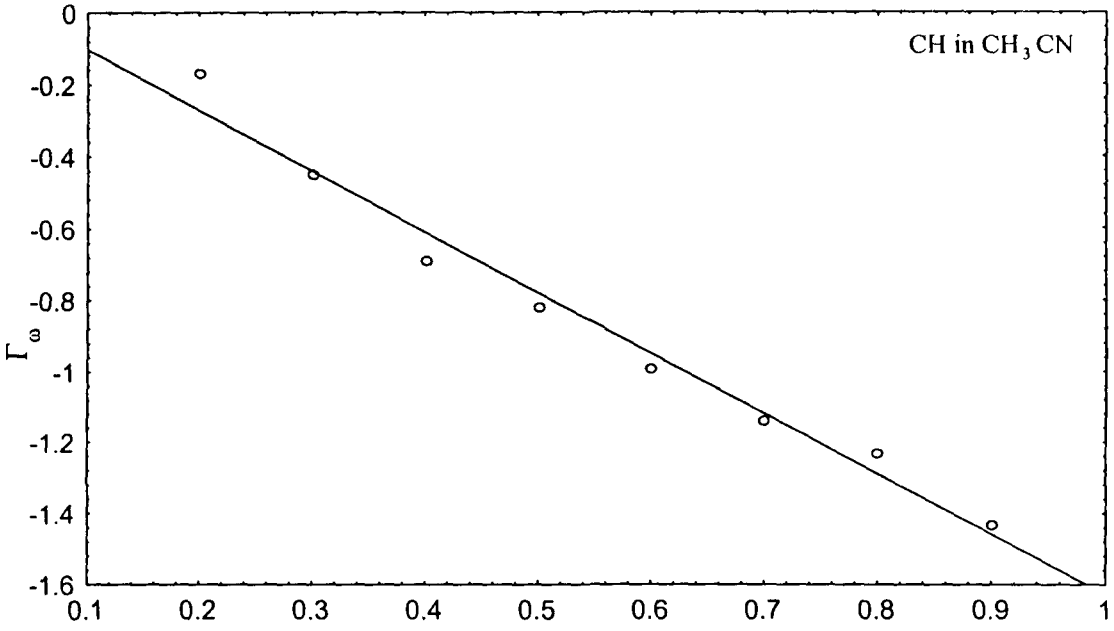
CH in CH_3CN
0
-0.2
-0.4
-0.6
-0.8
-1
-1.2
-1.4
-1.6
Γ_ω
0.1
0.2
0.3
0.4
0.5
0.6
0.7
0.8
0.9
1
Solvent concentration (v/v)

Fig 6.4c

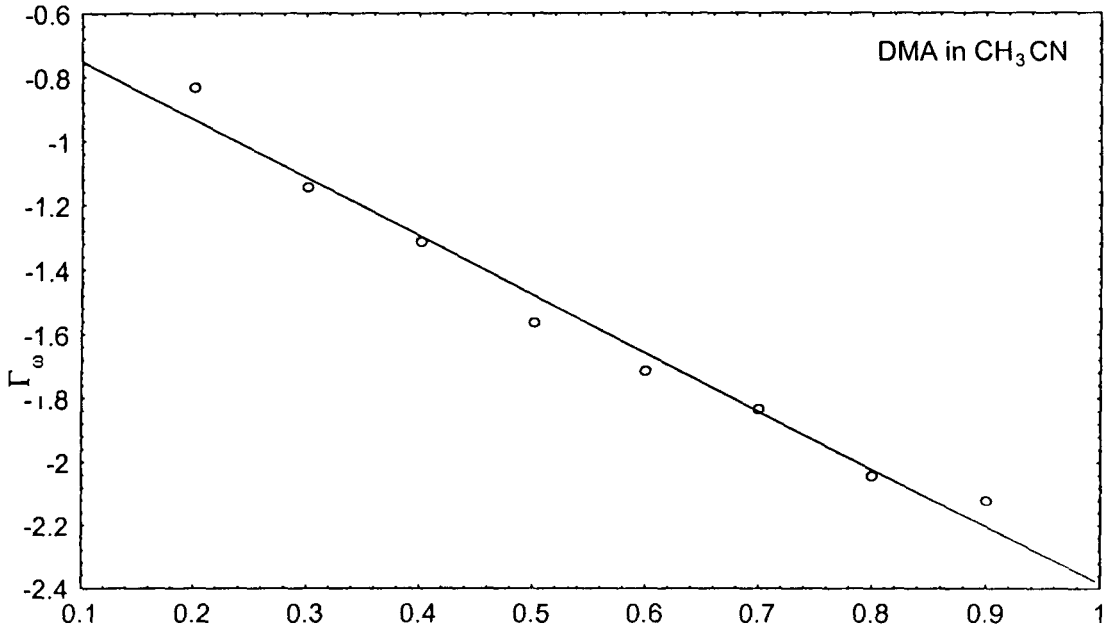

Fig. 6.4d

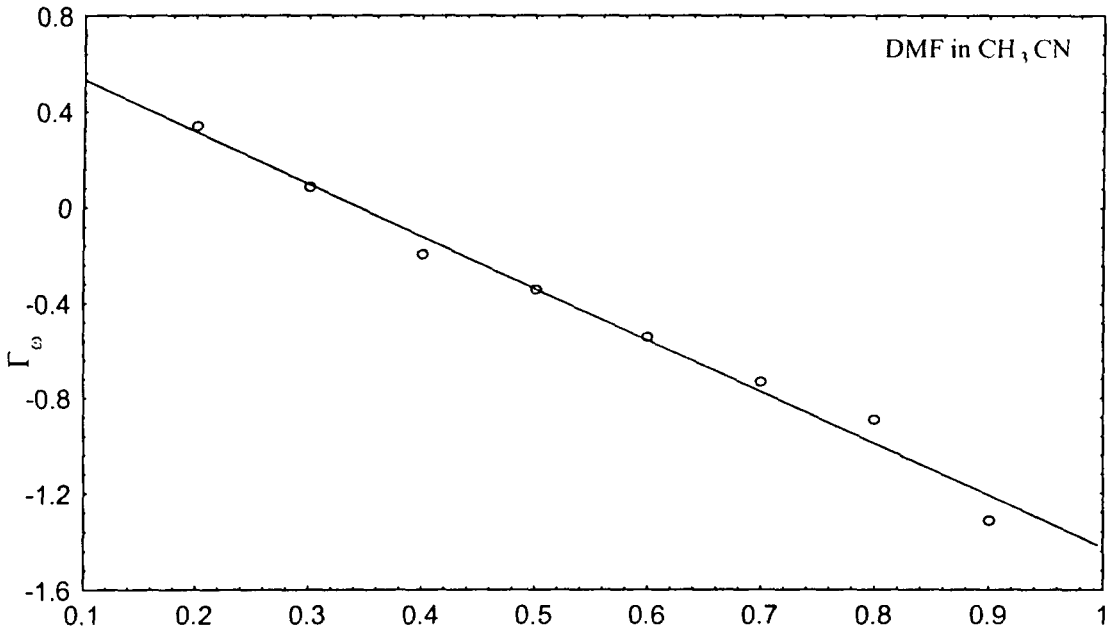

Fig.6.4e

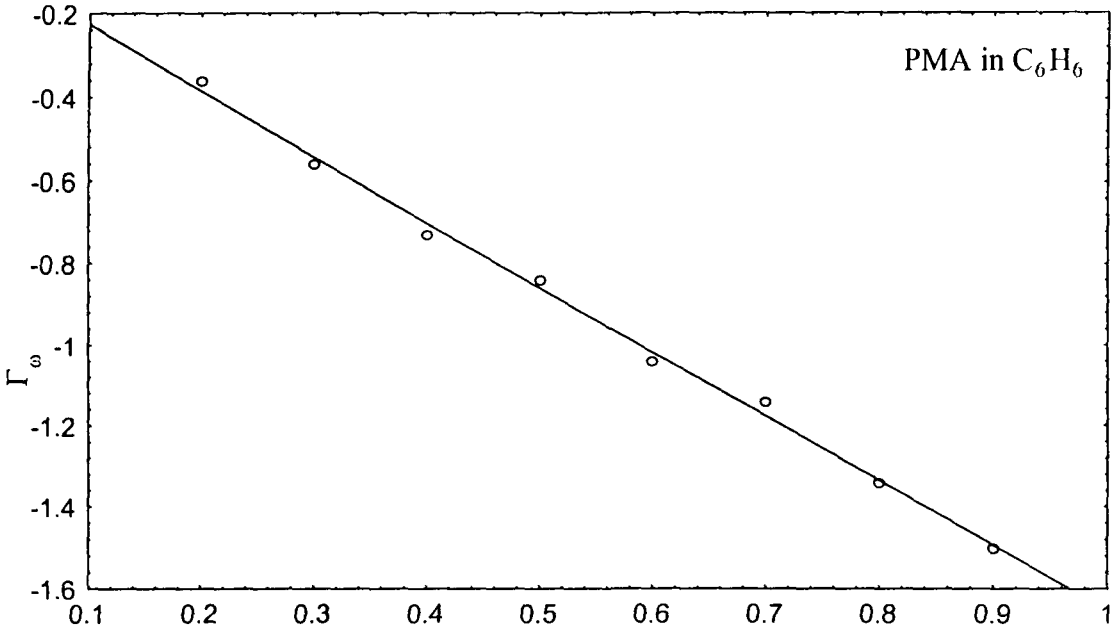

Fig.6.4f

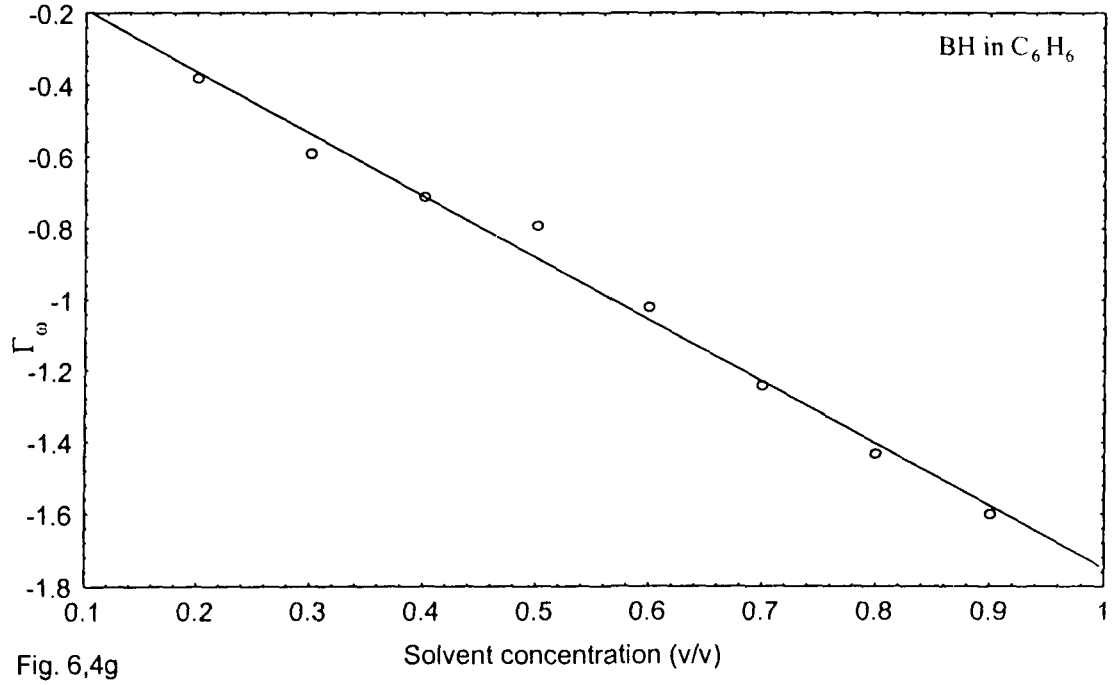

Fig. 6,4g

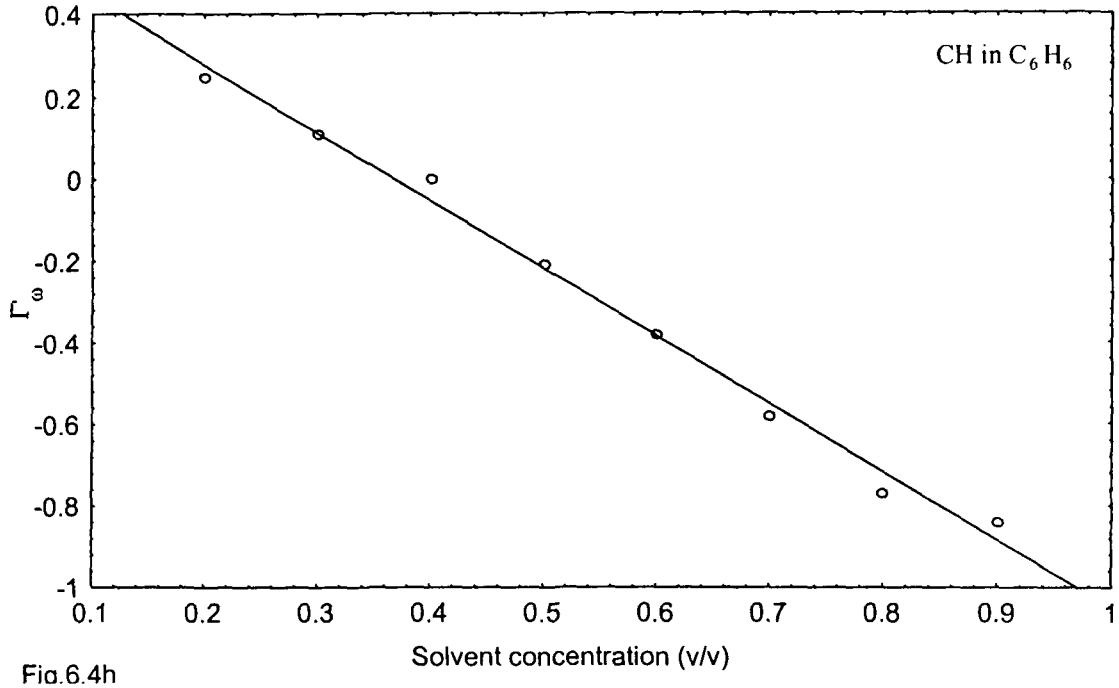

Fig.6.4h

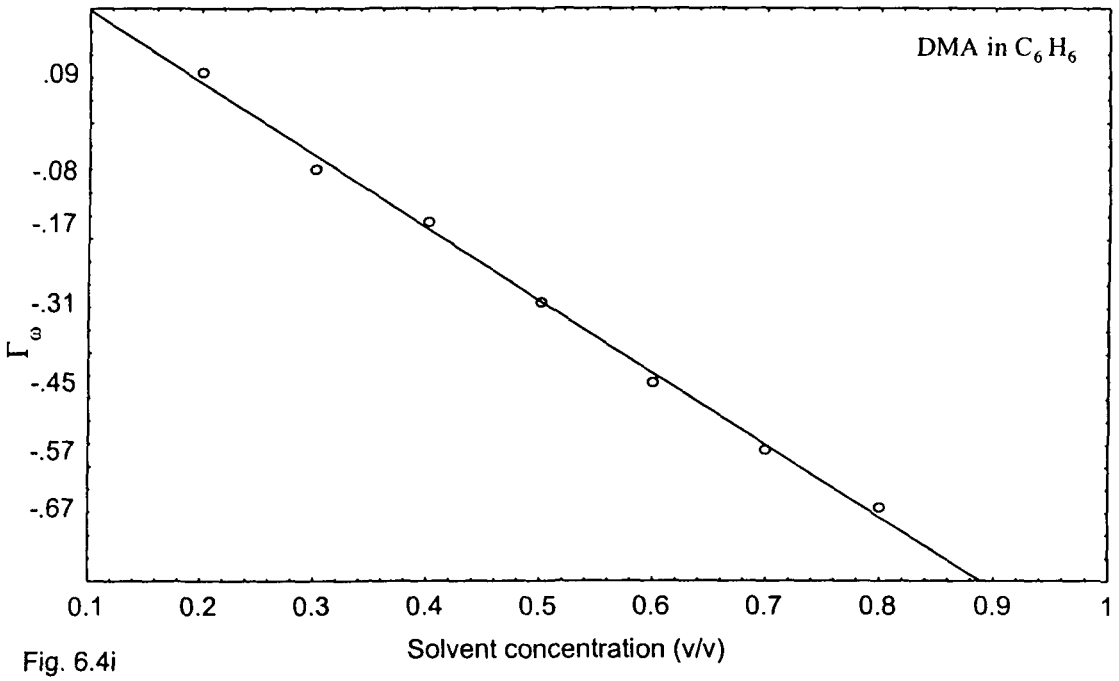

Fig. 6.4i

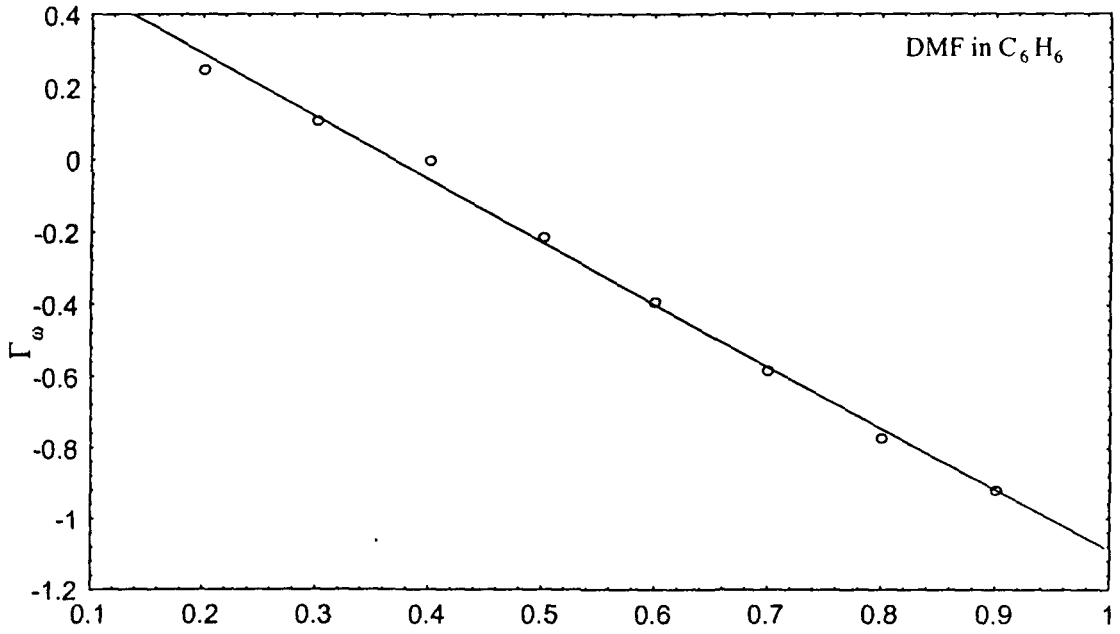
DMF in C_6H_6
0.4
0.2
0
-0.2
-0.4
-0.6
-0.8
-1
-1.2
Γ_ω
0.1
0.2
0.3
0.4
0.5
0.6
0.7
0.8
0.9
1
Solvent concentration (v/v)

Fig. 6.4j

local ordering in liquids. This leads to in-phase and out-of-phase type of vibrations. However, due to increasing concentration of the solvent the weakening of the pair correlation may occur. This is possible if the interactions between the fragments of the molecules are of comparable nature to the interactions in the neat liquid.

In solute-CH_3CN system, the dipole-dipole interaction is likely to be strong which may lead to the weakening of the pair interaction between the solute molecules. It is possible to write the torque exerted on a dipolar molecule by a field $\bar{F}$ due to the dipole moment of the C=O bond of the solute (hearafter called as director)

$$-\mu F Sin\theta = \xi \frac{d\theta}{dt} + I \frac{d^2\theta}{dt^2} \qquad 6.3.9$$

where ξ is the frictional force constant and I is the molecular moment of inertia.

A simplified picture of solvent effect may be obtained by considering the effect of a dipolar field upon its surroundings. The components of the field $\bar{F}$ due to a dipole moment μ are given by,

$$F_x = \frac{3\mu}{r^3} Cos\theta Sin\theta Cos\phi$$

$$F_y = \frac{3\mu}{r^3} Cos\theta Sin\theta Sin\phi$$

$$F_z = \frac{\mu}{r^3}\left(3Cos^2\theta - 1\right)$$

where θ is the angle between r and the Z axis, and ϕ is the angle between the projection of r in the XY plane and the X axis (Fig. 6.5). μ is supposed to be at the centre of a spherical solute molecule.

The dipole of CH_3CN will try to align along the $\bar{F}$ of the dipole of the solute molecule and thus an average component will be there along the director. In this process for the solute molecules containing benzene ring (PMA or BH molecules), it is likely that the dipole of an individual CH_3CN molecule may align along the quadrupole of the benzenoid fragment. This being a situation of minimum energy[18] hence may be a favourable situation for the flow of the molecules in the fluid state. However, this situation may lead to repulsive interaction as far as the π electron system of C=O and C-C≡N fragments of the solute and solvent molecules are concerned. Moreover, the orientation of the PMA or BH molecule may be such that the benzene rings come near to each other and form a plate like structure to maintain a smooth flow while still interacting (pair interaction in liquids) through dipoile-dipole interactions. When PMA or BH is dissolved in CH_3CN, the dipole-dipole interaction between the solute-solvent system will affect the pair interaction thus leading to decrease

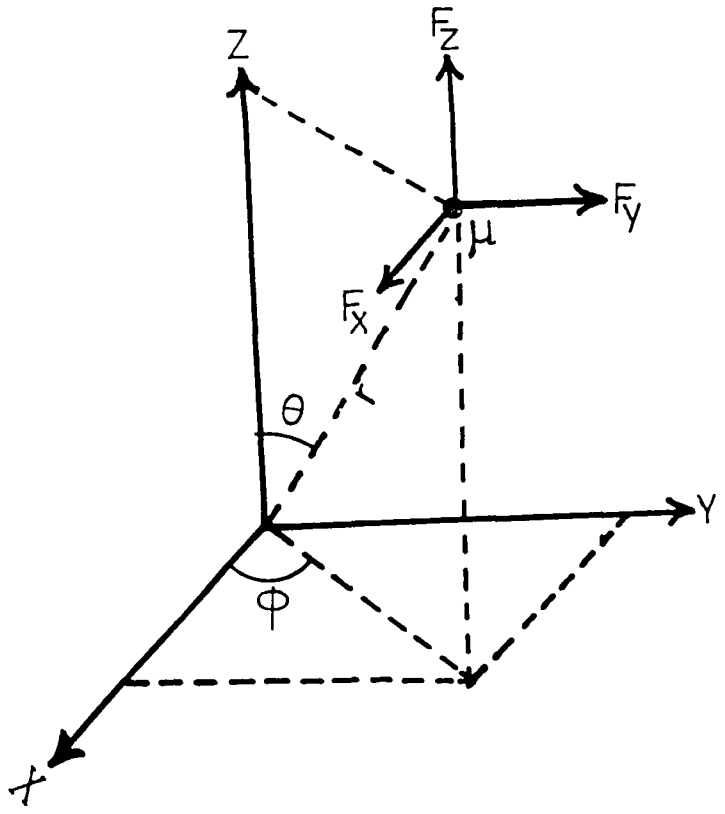

Fig.6.5 Interaction situation between a dipole of acetonitrile and quadrupole of PMA or BH molecule

in anisotropy shift. However, the plate like structure leads to repulsive quadrupole quadrupole interaction[18]. The liquid nature of the system will mainly maintain the plate like structure because hydrodynamic forces may be dominant over electrical forces. The cylindrical shape of CH_3CN molecule may not hinder in the smooth flow of the molecules.

In case of solute-C_6H_6 system the interaction is likely between the dipole moment of the C=O bond and quadrupole moment of C_6H_6 which may be responsible for weakening of the pair interaction between solute molecules. For the molecules containing benzene ring, viz., PMA or BH when dissolved in C_6H_6, after weakening the pair interaction, the benzene rings may also form a plate like structure. The interaction is also likely between the quadrupole moments of solvent C_6H_6 and the benzenoid fragment of the solute.

If we consider the simple shear flow of benzene molecule between two parallel planes constituted by the benzenoid portions of the molecules along Z axis (Fig. 6.6), hydrodynamic properties may now play significant role. The PMA or BH molecule is assumed to be planar. The effective viscosity will depend on the orientation of the dipole moment of the solute molecule, the director. The orientation of the director will not be fixed in the liquid, therefore the equation of motion of the director will come into play in addition to the flow of the liquid. The

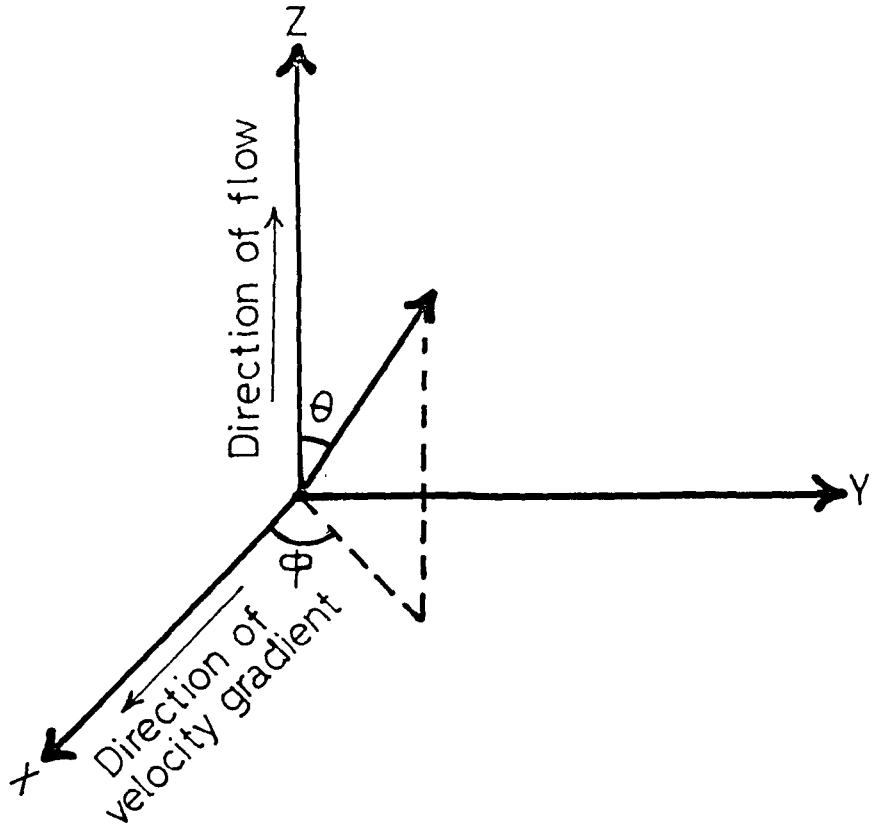

Fig. 6.6 Shear flow of benzene with respect to PMA or BH molecules

equation of motion of the director can be written as

$$I\frac{d\Omega}{dt} = \tau_F + \tau_{visc} \qquad 6.3.10$$

where τ_F is the torque per unit volume on the director due to the electric forces

$$\tau_F = \bar{n}Xh \qquad 6.3.11$$

h being the molecular field. τ_{visc} is a torque on the director due to frictional forces. I is the moment of inertia per unit volume, $\bar{n}$ is the director.

If we consider the benzene ring to be perpendicular to the shear plane, then $\tau_{visc} = 0$, i.e., the shear torque vanishes and a stable orientation exists for $\bar{n}$ which may be compared to the **T** configuration for the quadrupole moments, the minimum energy configuration[18]. For the case when the director is parallel to shear plane (when benzene ring is parallel to benzenoid portion of the solute), one finds a torque which leads to a change in the orientation of the C=O bond due to strong quadrupole-quadrupole repulsive type of interaction. Due to the changed orientation of one of the C=O bonds in the attracting pair, the interaction becomes weaker under the influence of benzene solvent.

These types of interaction though very complicated in nature are

quite significant and are probably responsible for the anisotropy shift as the solutions are further diluted with benzene. These results clearly indicate that the repulsive type of forces are playing significant role in the line broadening mechanism of the Raman bands exhibiting non-coincidence effect.

REFERENCES

1. A. F. Bondarev and A.Mardaeva, *Opt. Spectrosc,* **35,** 167 (1973).

2. T. Fujiyama, M. Kakimoto and T. Suzuki, *Bull. Chem. Soc., Jpn,* **49,** 606 (1976).

3. D. G. Knauss, *Mol.Phys.,* **36,** 413 (1978).

4. R. K. Wartheimer, *Mol. Phys.,* **36,** 1631 (1978).

5. G. Tarjus and S. Bratos, *Mol. Phys,* **42,** 307 (1981).

6. S. Bratos and G. Tarjus, *Phys. RevA,* **24,** 1591 (1981).

7. G. Tarjus and S. Bratos, *Phys. RevA,* **30,** 1087 (1984).

8. S. Bratos and G. Tarjus, *Phys. RevA,* **32,** 2431 (1985).

9. E. W. Knapp and S. Fischer, *J. Chem. Phys.,* **76,** 4730 (1982).

10. J. Yarwood and R. Arndt, *in Molecular Association,* edited by R. Forster, **Vol2, pp.** 287-300, Academic press, London.

11. A. Purkayastha, R. Das and K. Kumar, *J. Raman Spectrosc.,* **21,** 227 (1990).

12. A. Purkayastha and K. Kumar, *J. Raman Spectrosc.,* **22,** 721 (1991).

13. A. Purkayastha, R. Das and K. Kumar, *Spectrochim. Acta,* **47A,** 525 (1991).

14. A. Das and K. Kumar, *Spectrochim. Acta,* **54A,** 743 (1998).

15. K. Tanabe, *Spectrochim. Acta,* **40A,** 437 (1984).

16. D. Levesque, J. J. Weis and D. W. Oxtoby, *J. Chem. Phys.,* **79,** 917 (1983).

17. A. Bondi, *J. Phys. Chem.,* **68,** 441 (1964).

18. C. G. Gray and K. E. Gubbins, *Theory of Molecular Fluids,* **Vol1:***Fundamentals,* International Series of Monographs on Chemistry , Clarendon Press, Oxford, (1984).

CHAPTER 7

Chapter 7

SUMMARY AND CONCLUSION

The laser Raman scattering studies have been carried out on p-methylacetophenone (PMA), benzaldehyde(BH), cyclohexanone (CH), N,N-dimethylacetamide (DMA) and N,N-dimethylformamide (DMF) taking the C=O symmetric stretching vibration as the reference mode in all cases. The carbonyl stretchng vibrations of these aliphatic and aromatic molecules have been studied mainly with regard to the non-coincidence effect, owing to their strong dipolar character. The dipole-dipole interactions are considered mainly to be responsible for the local order of the molecules. The interaction potential between two permanent dipoles has been considered taking care of the orientation dependent term,

The experimental results for both isotropic and anisotropic components of Raman band of pure PMA and BH molecules show non-coincidence with the anisotropic component shifted to higher wavenumber position. That the non-coincidence effect is mainly due to transition dipole-transition dipole (TD-TD) type of interaction is supported by experimental results as the anisotropy shift tends to vanish at high concentration of the solvent.

The non-coincidence effect in PMA and BH molecules was studied by taking into account the screening factor related to the permanent and transition dipoles. The Onsager-Fröhlich dielectric model has been employed to study the behaviour of anisotropy shift at various solvent concentrations. The plot of the term $F = \Delta\tilde{\nu}\left(2\epsilon + n^2\right)^2 \epsilon^{-1}$ with respect to the solvent concentration shows a discontinuity around 50 to 60% concentration of the solvent. This may be due to the structure breaking effect and local fluctuations when the liquid is diluted. However, the plot of the quantity lnF vs. solvent concentration shows a linear relationship for the entire range of dilution in each case.

This study reveals that the model predicted by the TD coupling mechanism may be expected to be valid only for dilute solutions. The effect of dispersion force and various multipolar interactions are likely to vary from solvent to solvent and screening effect may not be as

effective as envisaged by the Onsager-Fröhlich model. Therefore, the methods of statistical mechanics may be used which provide a way of obtaining microscopic quantities when the properties of the molecules and the molecular interactions are known. By treating the molecular interactions with hard sphere interaction model, it has been found that the repulsive potential function of the type $e^{-\alpha R}$ (where R is the appropriate distance of closest approach and α is a constant) is playing a dominant role over the attractive potential function, which is due to the fluctuations of diplole moments and polarizabilities.

The Raman band in liquid shows a more or less broad distribution of frequencies. In case of isotropic part of the Raman band, the reorientational motion of the molecules can be neglected. The excited molecular ensemble sees a somewhat different environment, and the vibrational frequency is, therefore, perturbed by various interaction potentials depending upon geometric relations. The development of the microscopic picture of the processes involved requires the knowledge of dephasing processes. The band shapes of the isotropic components of Raman bands at 80% solvent concentration (v/v) for PMA and at 90% solvent concentration (v/v) for BII were found to be Lorentzian. This is because the perturbation on the solute molecule is for a short time, therefore its phase is retained for longer times.

The isotropic band width at these concentration were measured in different polar and nonpolar solvents to find the dephasing rate (τ_v^{-1}). The theoretical explanation for the dephasing process may be given by correlating the vibrational relaxation rate (τ_v^{-1}) with some molecular parameter which takes into account the effect of solvent electric field on the solute molecule.

The various models proposed for explaining dephasing process takes into account the dynamic viscosity (η) which is a macroscopic property. However, a finer details of the liquid structure requires a microscopic model incorporating the solvent microviscosity (η_m) which may be calculated by estimating the appropriate values of solute and solvent radii. The solute and solvent radii have been estimated keeping in view the orientation of the molecular fragments due to various intermolecular interactions as well as the hydrodynamic properties of the liquid. At sufficiently high concentration of the solvent, the solute molecule may be considered to be in a cage of solvent molecules with an occasional escape to the adjucent position. A parameter f_m which takes into account the solvent microviscosity as well as the distance of closest approach of the solute and solvent molecules was defined and the variation of τ_v^{-1} with respect to f_m was plotted. The graph was found to be linear which indicates that the discreteness of the

medium due to the solvents has a significant influence on dephasing process in complex molecular systems.

The ansiotropic component of the Raman band gives information about the angular dependence of intermolecular potentials. Therefore, the anisotropic band width (FWHM) corresponding to C=O stretching mode of the molecules PMA, BH, CH, DMA and DMF were measured at different solvent concentration ranging from 10 to 90% in the solvents CH_3CN and C_6H_6. The observed data are found to be highly concentration dependent. The graph shows a curvature at lower concentration of the solvent and is linear at higher concentration of the solvent. This indicates a competitive nature of the interactions between similar molecules (within pure solute) and the solute-solvent molecules. To have a detailed information about the intermolecular interactions involved which are responsible for such a complicated behaviour, we have introduced the concept of van der Waals' volume of the sphere of influence in solution. The effective van der Waals' volume (V_w) has been calculated keeping in view the varying solute-solvent distance in a solution. A quantity $ln(\Gamma_{aniso}/V_w)$ has been defined in these systems for taking into consideration the role of van der Waals' volume. The variation of this parameter with solvent concentration is found to the linear for the entire range of dilution

indicating the exponential nature of the repulsive forces which plays role in the line broadening mechanism of the Raman band exhibiting non-coincidence effect. The pair interaction between the solute molecules is responsible for the local order which leads to in-phase and out-of-phase components of vibration. Due to increasing concentration of the solvent the weakening of the pair correlation may occur. This is possible if the interaction between the fragments of the solute and solvent molecules are of comparable nature to the interaction in the neat liquid. However, the orientation of the solute and solvent molecules due to the interaction between different fragments will be such that the hydrodynamic forces may be dominant over electrical forces, thus maintaining the smooth flow of the liquid. The present study indicates that the effect of entire microenvironment should be taken into account in complex molecular systems for determining the different spectral properties of the Raman bands, such as frequency shift and band width of isotropic and anisotropic components.

PARTICULARS OF THE CANDIDATE

Name of the candidate	: **Ms. Arpita Das**
Degree	: Ph.D.
Department	: Physics
Title of Dissertation/Thesis	: **Relaxation studies and intermolecular interactions in some complex molecules**
Date of payment of Admission fee	: 22.03.95
Approval of Research proposal	:
1. BPGS	: 24.4.1996
2. School Board	: 6.5 .1996
Registration No and Date	: 86 of 6.5.1996
Extension (if any)	: No

6/10/96

(Prof. C. S. Shastry)
Head
Department of Physics
NEHU, Shillong

List of Publications

1. Microenvironment dependence of vibrational relaxation in p-methylacetophenone Arpita Das and Kamal Kumar, *Spectrochim. Acta*, **54A** ,793 (1998)

2. Solvent dependent study of anisotropy shift in C=O stretching mode of benzaldehyde, Arpita Das and Kamal Kumar, *J. Raman Spectrosc.*, **30** , 547 (1999)

3. Raman anisotropic line width dependence on the van der Waals' volume of the interacting systems, Arpita Das and Kamal Kumar, *J. Raman Spectrosc.*, **30** , 563 (1999)

4. Vibrational relaxation studies in p-methylacetophenone, Arpita Das and Kamal Kumar, *Proceedings of National Laser Symposium,* CAT Indore, February, 1997

5. Raman line width of the C=O Stretching mode: solvent dependent studies in benzaldehyde, Arpita Das and Kamal Kumar, *Proceedings of National Laser Symposium*, (IIT Kanpur), December, 1998.